2010

Mechanical Properties Of Carbon Nanotube/metal Composites

Ying Sun
University of Central Florida

MECHANICAL PROPERTIES OF CARBON NANOTUBE / METAL COMPOSITES

by

YING SUN
B.S. JILIN UNIVERSITY, 1999
M.S. SHANGHAI INSTITUTE OF CERAMICS, CHINESE ACADEMY OF SCIENCES, 2002

A dissertation submitted in partial fulfillment of the requirements
for the degree of Doctor of Philosophy
in the Department of Mechanical, Materials, and Aerospace Engineering
in the College of Engineering and Computer Science
at the University of Central Florida
Orlando, Florida

Spring Term
2010

Major Professor: Quanfang Chen

ABSTRACT

Carbon nanotubes (CNTs) have captured a great deal of attention worldwide since their discovery in 1991. CNTs are considered to be the stiffest and strongest material due to their perfect atomic arrangement and intrinsic strong in-plane sp^2—sp^2 covalent bonds between carbon atoms. In addition to mechanical properties, CNTs have also shown exceptional chemical, electrical and thermal properties. All these aspects make CNTs promising candidates in the development of novel multi-functional nanocomposites.

Utilizing CNTs as fillers to develop advanced nanocomposites still remains a challenge, due to the lack of fundamental understanding of both material processing at the nanometer scale and the resultant material properties. In this work, a new model was developed to investigate the amount of control specific parameters have on the mechanical properties of CNT composites. The new theory can be used to guide the development of advanced composites using carbon nanotubes, as well as other nano-fibers, with any matrices (ceramic, metal, or polymer). Our study has shown that the varying effect based on changes in CNT dimensions and concentration fit the model predictions very well.

Metallic CNT composites using both single-walled carbon nanotubes (SWNT) and multi-walled carbon nanotubes (MWNT), have been developed through a novel electrochemical co-deposition process. Copper and nickel matrix composites were developed by using pulse-reverse electrochemical co-deposition. Uniaxial tensile test results showed that a more than 300% increase in strength compared to that of the pure metal had been achieved. For example, the ultimate tensile strength of Ni/CNTs composites reached as high as about 2GPa. These are best experimental results ever reported within this field. The mechanical results are mainly attributed

to the good interfacial bonding between the CNTs and the metal matrices and good dispersion of carbon nanotubes within the matrices. Experimental results have also shown that the strength is inversely dependent on the diameter of carbon nanotubes.

In addition to the mechanical strength, carbon nanotube reinforced metallic composites are excellent multifunctional materials in terms of electrical and thermal conduction. The electrical resistivity of carbon nanotube/copper composites produces electrical resistivity of about 1.0~1.2 $x10^{-6}$ohm-cm, which is about 40% less than the pure copper. The reduced electrical resistivity is also attributed to the good interfacial bonding between carbon nanotubes and metal matrices, realized by the electrochemical co-deposition.

To: my parents, Benjun Sun and Guoxiang Li,

my husband, Naigang Wang.

ACKNOWLEDGEMENTS

I would like to express my great gratitude to my advisor Dr. Quanfang Chen. I could not have finished this dissertation without his guidance, support and encouragement. I have been greatly benefited from his insights in research. His erudition guided me all the way through my research.

I also would like to thank the rest of my dissertation committee, Dr. David Nicholson, Dr. Lee Chow, Dr. Kevin Coffey and Dr. Jiyu Fang. Their valuable insights and good questions have helped me to think through research problems from different perspectives.

Thanks a lot to everyone in MCF, Zia, Kirk, Qi Zhang and Karen for their help.

My appreciation also goes to the MMAE staff, Waheeda, Stephanie, Jeanine, and Abdul, for their assistance throughout my study.

Also thanks to my colleagues in the MEMS lab for inspired discussions and contributions to my work. Dr. Bo Li, Dr. Jianwei Gong, Dr. Miao Liu, Dr. Guangyu Chai, Dr. Yitian Peng, Ms. Jenny Sun, Mr. Christopher Bock and Mr. Ke Huang. They made our lab a wonderful working place.

Last, but not least, my gratitude goes to my parents, my husband, my sister and my brother-in-law, for their unconditional encouragement and support.

TABLE OF CONTENTS

LIST OF FIGURES

LIST OF TABLES

CHAPTER 1. INTRODUCTION

1.1 Background

Besides diamond, graphite and C_{60}, the quasi-one-dimensional nanotube is another form of carbons. Since their discovery in 1991 by Iijima[1], carbon nanotubes (CNTs) have captured the attention of researchers worldwide. Due to the perfect atomic arrangement and high intrinsic strength of the sp2—sp2 covalent bonding between carbon atoms, carbon nanotubes possess exceptionally high mechanical properties such as a high Young's modulus (1 TPa), a high tensile strength (200 GPa) and a high fracture strain (10-30%)[2,3,4]. In addition, CNTs have an extremely small size, high aspect ratio, high structural and chemical stability, and remarkable electrical, thermal, and optical properties[5]. A significant amount of work has been done to exploit these properties by incorporating carbon nanotubes into some form of matrix.

Most research has focused on the development of nanotube reinforced polymer composites, including PMMA[6] and various types of epoxy resin,[7,8] and about 20-50% reinforcement has been achieved. These achievements are much lower than the predicated results of most theoretical models. In addition, attempts have also been made to incorporate CNT into ceramic matrices[9,10], but only a slight improvement of mechanical properties has been achieved, or in some cases, even worse properties than those of monolithic ceramic materials resulted. It has been pointed out that the weak bonding between CNTs' and ceramic matrices, and the poor dispersion of CNTs within the matrix are critical issues in the processing of these nanocomposites.

CNT reinforced metallic composites is still a new subject[11,12]. The methods to prepare nanotubes/metal composites include powder sintering and electro and electroless deposition.

Improved anti-wear properties and thermal/ electrical conductivity have been identified with a small addition of CNTs in the matrix. In this research, we report on a simple yet general approach to form Nickel/CNT nanocomposites by electrochemical co-deposition in an attempt to obtain excellent mechanical properties.

Our approach is based on two concepts. First, in the electroplating co-deposition, metallic ions and nano/micro particles are deposited together. This atom/molecular level co-deposition process can lead to strong interfacial strength and homogeneous dispersion. The second key aspect is the fact that Ni particles have been used as catalysts to grow carbon nanotubes. Therefore, good wetting between nickel and CNTs can be expected. These two aspects then present an interesting opportunity to create nickel/CNT nano-composites by electro-deposition. In this project, we will study the physical properties of different metals electrochemically co-deposited with a small amount of carbon nanotubes.

1.2 Problem Statement and Research Objectives

Because of their small size and large surface area, carbon nanotubes tend to aggregate to reduce energy. For carbon nanotube reinforced nano composites, the uniform distribution of carbon nanotubes in the matrix is always a critical problem. In order to realize the uniform distribution of carbon nanotubes in metal matrices, carbon nanotubes must be uniformly suspended in electrolyte solution. In some cases, special additives can be added into the solution working as surfactant to get stable suspension. But the introduced additives will also work as impurities and can greatly affect the properties of the resultant composites. The object of our project is to produce carbon nanotube reinforced metal composites with improved mechanical property.

The theoretical investigation of carbon nanotube reinforced nano composites is also a main purpose of our research. Because of the extremely small size and amazing properties of CNTs, carbon nanotube reinforced composites cannot be evaluated using conventional law of mixtures. In order to understand the relationship between the tensile strength of the composites and main parameters, more sophisticated governing equations need to be developed to account for unique features of nanocomposites.

CHAPTER 2. LITERATURE REVIEW

2.1 Structure and properties of carbon nanotube

Carbon nanotubes are perfectly quasi-one-dimensional straight tubes with diameters on the nanometer scale. A SWNT can be considered as a flat grapheme sheet cylindrically rolled into a seamless tube with a constant radius (Figure1)[13].

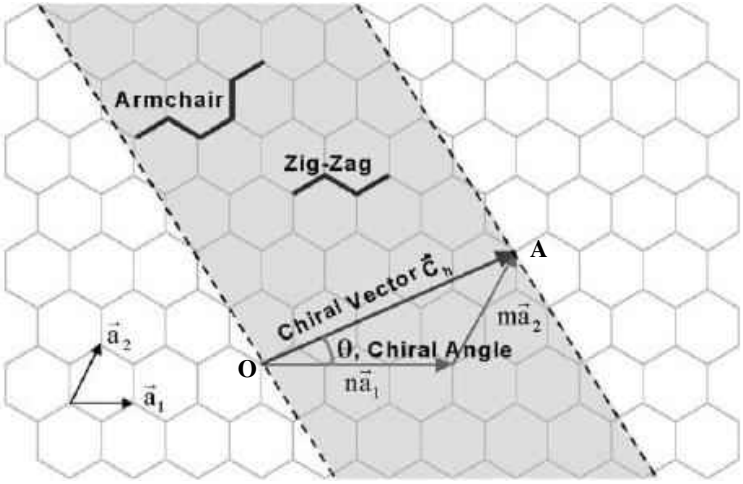

Figure 1. Schematic diagram showing how the sheet of graphite is rolled to form a carbon nanotube[13]

In this case, each carbon atom has three nearest neighbors. Two atoms in the sheet are selected as the origin, and when the sheet is rolled, the two atoms coincide with one another. The vector OA is known as the "rollup" vector, whose length is equal to that of the circumference of the nanotube. The tube is created so that point O touches point A. The tube axis is perpendicular to the rollup vector. The chiral vector of the nanotube, OA, can be defined by

$$OA = n\vec{a}_1 + m\vec{a}_2$$

where $\vec{a}_1$ and $\vec{a}_2$ are unit vectors in the two-dimensional hexagonal lattice, and n and m are integers, which are referred to as chiral indices. The angle (θ) between OA and $\vec{a}_1$ is called the chiral angle and is always less than 30 degree.

As chiral vectors change, nanotube properties change from metallic to semi-conducting. The (n, 0) direction is known as the zigzag structure, while the (n, n) is denoted as the armchair structure (Figure2)[14]. The roll-up vector of the nanotube also defines the nanotube diameter since the inter-atomic spacing of the carbon atoms is known.

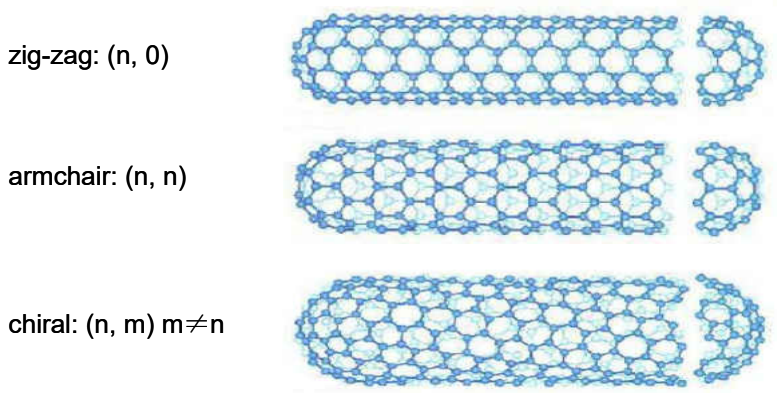

Figure 2. Illustration of the atomic structure of nanotube with different chiralities[14].

It should be noted that all armchair chiralities of CNT display metallic properties. In addition, chiral vectors with n-m=3i where i is an integer, yield metallic properties. All other arrangements of (n, m) in CNT display semiconductor properties. Chirality has a profound impact on the electrical properties of nanotubes, as well as optical activity, and various other properties. The influence of chirality on the mechanical properties has also been reported. The analytical work examined the instability of carbon nanotubes beyond linear response. Their simulations show that carbon nanotubes are remarkably resilient, sustaining extreme strain with no sign of brittleness or plasticity. The chirality has a relatively small influence on the elastic stiffness. According to

Nardelli et al.,[15] the Stone-Wales transformation results in ductile fracture for armchair nanotubes. When a nanotube is stressed in the axial direction, a reversible diatomic interchange happens and the resulting structure is two pentagons and two heptagons in pairs. (Figure 3)

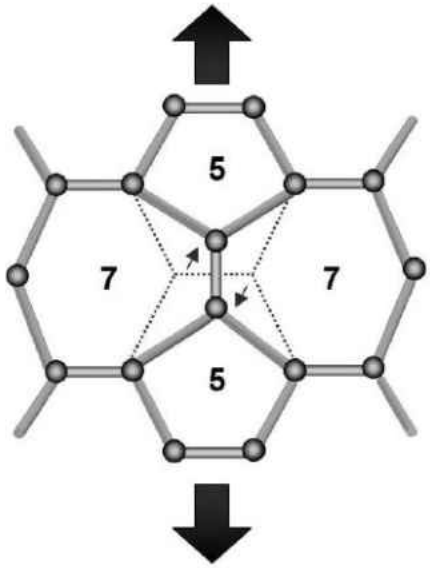

Figure 3. The Stone-Wales transformation in nanotube under axial tension[15]

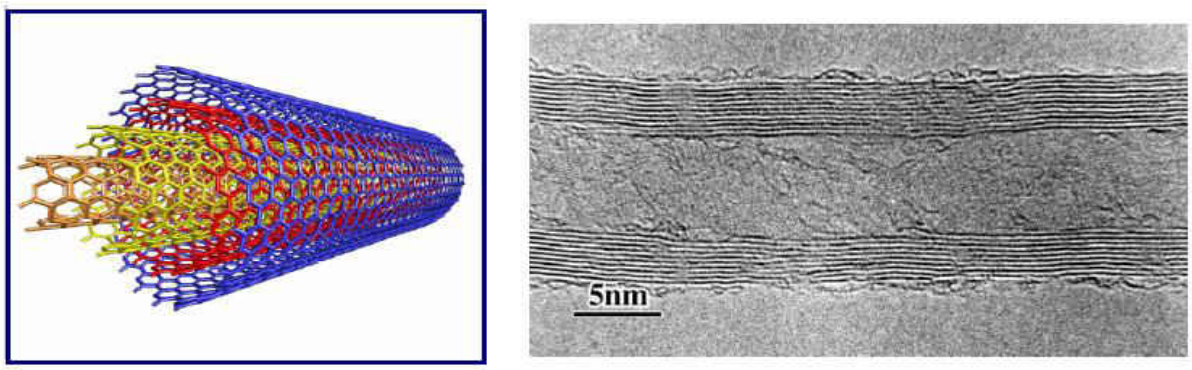

Figure 4. Schematic diagram and TEM micrograph of multi-walled carbon nanotube[16]

Multi-walled carbon nanotubes (MWCNTs) are simply composed of concentric single walled carbon nanotubes. (Figure 4) At high resolution, the individual layers making up the concentric

tubes can be clearly imaged. Multiwall carbon nanotubes can range in length from tens of nanometers to several micrometers, with outer diameter range from 2.5 to 30nm.

The end caps of carbon nanotubes are more often asymmetric conical structures as shown in Figure 5.

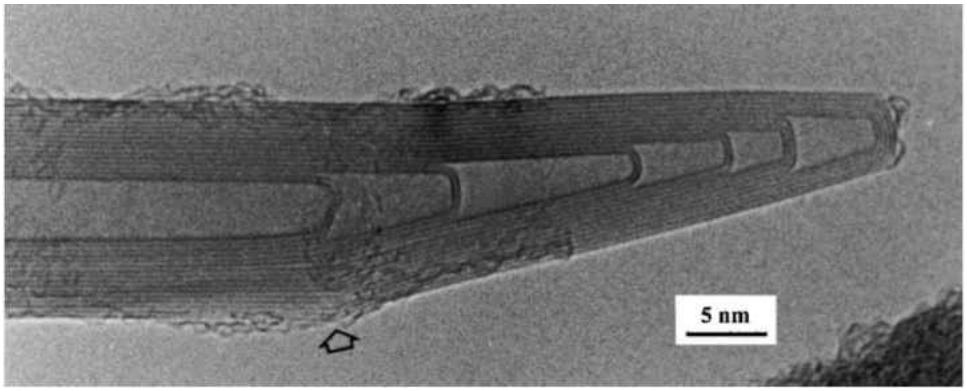

Figure 5. Image of the cap of multiwall carbon nanotube

As a result of their larger diameter compared with single wall nanotubes, multiwall nanotubes are much more inflexible than single wall nanotubes, and therefore can be observed to be straight instead of curled. Single wall nanotubes tend to cluster together to form 'ropes'.

Recently, carbon nanotubes, due to their small dimensions, remarkable strength and physical properties, were proven to be a very unique material for a whole range of promising applications, such as nanotube based field emitters, nano-probes in metrology and biological and chemical investigations, and mechanical reinforcements in high performance composites.

Carbon nanotubes display unique mechanical and electronic properties, which have initiated intensive research on these quasi-one-dimensional structures. There are varying reports in the literature on the exact properties of carbon nanotubes. Theoretical studies have suggested that single walled carbon nanotubes (SWNTs) could have a Young's modulus greater than 1TPa. The

theoretical estimate for the tensile strength of individual SWNTs is up to 200 GPa, or over hundreds of times stronger than steel, which has a tensile strength of 400 MPa.

The experimental study of single nanotubes is still in progress. Measurements were made using a scanning electron microscope (SEM)[17]. The results indicated that the Young's modulus of the outermost layer of MWNTs varies from 270 to 950 GPa and the values of tensile strengths range from 11 to 63 GPa. Measurements of Young's modulus can also be carried out using atomic force microscope (AFM)[18] and the results implied a value of 1280 GPa for the Young's modulus for MWNTs. Determining the mechanical properties of SWNTs presents an even greater challenge. Results showed an average 1TPa for the value of Young's modulus and an average breaking strength of 30 GPa[2].

SWNTs show either a metallic or semiconducting electrical conductivity depending on their chirality. The electric-current-carrying capacity is 1000 times higher than copper wires.[19] The thermal conductivity of CNTs depends on the temperature and their structure[20,21] and they are thermally stable up to 2800℃. Simulation results predicted that (10, 10) SWNTs have thermal conductivity around 30,000W/m·K at temperature of 100K.[22] At room temperature, the thermal conductivity of SWNTs is in the range of 1,750 to 5,850W/m·K.[23]

The potential applications of CNT so far include the use of nanotubes as electron field emitters for vacuum microelectronic devices[24], individual MWNTs and SWNTs attached to the end of an atomic force microscope (AFM) tip for use as a nano-probe[25], MWNTs as efficient supports in heterogeneous catalysis[26] and as microelectrodes in electrochemical reactions, and use of SWNTs as media for lithium and hydrogen storage.[27] Because of their high mechanical strength, CNTs are used as excellent load bearing reinforcement in composites.

2.2 Preparation and Property of Carbon Nanotube/Polymer Composites

The reported exceptional properties of nanotubes have motivated others to investigate the mechanics of nanotube/polymer composite films. Uniform dispersion within the polymer matrix and improved nanotube/matrix wetting and adhesion are critical issues in the processing of these nanocomposites. A commonly used method for preparing nanotube/polymer composites has involved mixing nanotube dispersions with solutions of the polymer and then evaporating the solvents in a controlled way. The nanotubes are often pretreated chemically to facilitate solubilization. Normally, acid treatments enable a stable aqueous solution of carbon nanotubes to be prepared.[28] A nanotube/PVA (polyvinyl alcohol) composite could be prepared simply by mixing one of these aqueous nanotube dispersions with an aqueous solution of the polymer and then casting the mixtures as films and evaporating the water.[29] The Young's modulus of the composite films was characterized in a dynamic mechanical thermal analyzer. The stiffness of the composites at room temperature was relatively low. Using short-fiber composite theory, the calculated nanotube elastic modulus was 150 MPa from the experimental data. This value is well below the values reported for isolated nanotubes. This low value may result from poor stress transfer. Above the glass transition temperature of the polymer (~85°C), the nanotubes had a more significant effect on the properties of the composite. Better results were achieved by Cadek et al. from a PVA/MWNT composite[30]. The addition of 1wt% nanotubes increased the Young's modulus of PVA by factor of 1.8. TEM studies showed evidence of stronger interfacial bonding.

These solution based methods have also been used to produce nanotube/polystyrene composites.[31] This process includes two steps: first nanotubes are treated with acid and then followed by esterification of the surface-bound carboxylic acids. The surface-modified carbon

nanotubes were shown to be soluble in common organic solvents. To prepare composites, polystyrene was dissolved in the nanotube solution, and the wet casting method was used to prepare nanotube/polystyrene composite films. Instead of functionalization of the nanotubes at the first step, Qian et al. used a high energy ultrasonic probe to help the dispersion of MWNTs in toluene.[32] The low viscosity of the polymer solution allowed the nanotubes to move through the matrix, and excellent dispersion would be achieved. The mixture was cast on substrate and after solvent evaporation, MWNT-doped films formed. The solution mixing method can only be used with polymers that can dissolve in common solvents. With only the addition of 1wt% nanotubes, they achieved 36-42% increase in the elastic stiffness and a 25% increase in the tensile strength. Figure 6 is a TEM picture of the film showing the mechanisms of fracture[32].

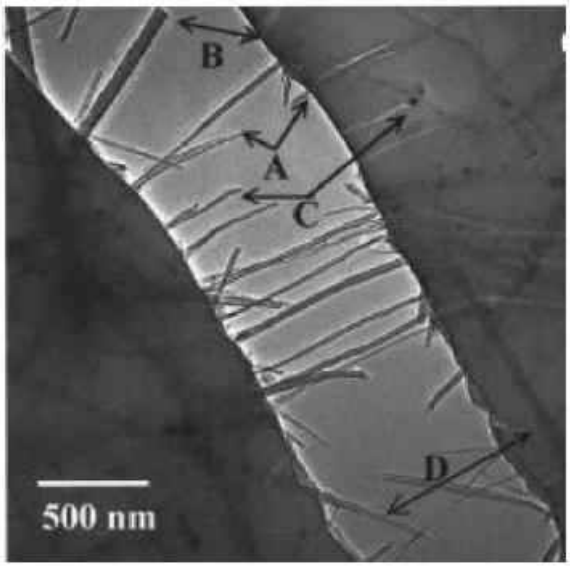

Figure 6. Fracture mechanisms in nanotube/polystyrene composites[32]

As we can see, nanotube pull-out (site B and C), nanotube fracture (site A) and crack bridging (site D) by the nanotubes all happened at the same time. In order to take full advantage of the exceptional stiffness, strength and resilience of carbon nanotubes, strong interfacial bonding is critical.

For thermoplastic polymers, polymers were softened and melted at higher temperatures, and then shear mixing was used to get a homogeneous dispersion of nanotubes. After extrusion or injection moulding, nanotube/polymer composites formed. This method can be used for a range of polymers including high impact polystyrene, [33] acrylonitrile butadiene styrene, polypropylene[34] and polymethylmethacrylate (PMMA).[35,36] For MWNT/polystyrene composites containing from 2.5 to 25 vol% nanotubes, Young's modulus increased progressively from 1.9 to 4.5 GPa, with the major increases occurring when the MWNT content was at or above about 10 vol%. Composite fibers with a high degree of nanotube orientation were produced by melt spinning. Sennet et al. have used melt processing techniques to disperse and align carbon nanotubes in polycarbonate.[37] Dispersion was achieved by mixing the catalytically produced MWNTs and SWNTs with polycarbonate resin in a conical twin-screw extruder and alignment was carried out using a fiber spinning apparatus. By optimizing mixing time and fiber draw rates, excellent dispersion and alignment were accomplished.

Nanotube/epoxy composites have also been prepared by a number of groups and their mechanical behaviors were studied. The results from epoxy/MWNTs showed that the compression modulus was higher than the tensile modulus[38]. This indicated that load transfer to the nanotubes in the composite was much higher in compression. A possible reason is during the load transfer process for MWNT, only the outer layers are stressed in tension, whereas all the layers respond in compression. Nanotube/epoxy composites prepared by Xu et al. showed good mechanical properties.[39]

A 20% increase in Young's modulus was seen when 0.1 wt% MWNTs were added. Fracture behavior of the films was investigated by SEM, and the results showed that pulled-out tubes were often covered with polymer, suggesting strong interfacial adhesion. (Figure 7)

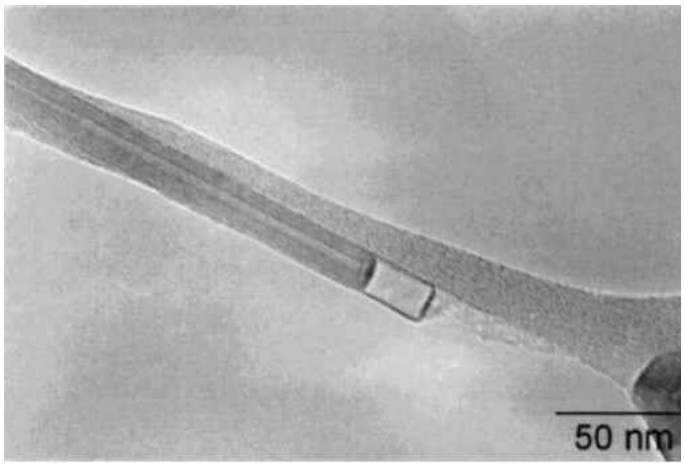

Figure 7. Pull-out nanotube covered with epoxy[39]

Single-walled nanotube/epoxy composites have also been prepared by Biercuk et al.[40] The Vickers hardness of the polymer composite was found to increase monotonically with addition of SWNTs, up to a factor of 3.5 at 2 wt% nanotubes loading. Greatly enhanced thermal conductivities were also observed. Thus, samples loaded with 1 wt% unpurified SWNT material showed a 70% increase in thermal conductivity at 40 K, rising to 125% at room temperature.[32]

Another approach called in situ polymerization has also been used to prepare nanotube /polymer composites. Here monomers instead of the polymer are used as a starting material. Cochet et al. were among the first to use this method, to prepare a MWNT/polyaniline composite.[41] Nanotubes prepared by arc evaporation were used, and were sonicated in a solution of HCl to achieve dispersion. The aniline monomer, again in HCl, was added to the suspension and a solution of an oxidant was slowly added with constant sonication and cooling. Sonication was continued in an ice bath for 2 h, and the composite was then obtained by filtering, rinsing, and

drying. In this way, it was possible to prepare composites with high MWNT loadings (up to 50 wt %). Transport measurements on the composite revealed major changes in the electronic behavior, confirming strong interaction between nanotubes and polymer. A number of other nanotube/polymer composites have been prepared using in situ polymerisation, including MWNT/polystyrene [42] and SWNT/ polyimide. [43] Several groups have used electrochemical polymerisation to grow porous composite films of MWNT and polypyrrole for use as super-capacitors.[44,45]

For some special applications, such as photo-voltaic devices, multilayer SWNT/polymer composites are required. The method involved the layer-by-layer deposition of SWNTs and polymer onto a substrate, followed by cross-linking. In this way, composites with SWNT loadings as high as 50 wt% could be obtained. The coating was carried out by the alternate dipping of a glass slide or silicon wafer into dispersions of SWNTs (stabilized by acid treatment) and polymer solutions. The layers were held together by van der Waals forces and by electrostatic attraction between the negatively charged SWNTs and a positively charged polyelectrolyte, such as branched polyethyleneimine (PEI). Coatings containing up to 50 SWNT/PEI bilayers could be built up in this way. When the procedure was complete, the multilayer films were heated to 120°C to promote crosslinking. The films could then be lifted off the substrate to obtain uniform free-standing membranes. The films produced in this way were shown to have exceptional mechanical properties. Thus, the average ultimate tensile strength of the films was found to be 220 MPa, with some measurements as high as 325 MPa.[46]

Fig. 8 shows the exceptional flexibility of the as-spun nanotube composite fiber produced by Vigolo and coworkers.[47] Their technique for spinning nanotubebased fibers involves dispersing

the nanotubes in surfactant solutions followed by re-condensing the nanotubes in the stream of a polymer solution to form macroscopic fibers and ribbons. Although the elastic modulus of the nanotube fibers (9–15 GPa) is far below the values for individual nanotubes or conventional carbon fibers, the demonstrated resilience of the fibers gives hope for future improvements.

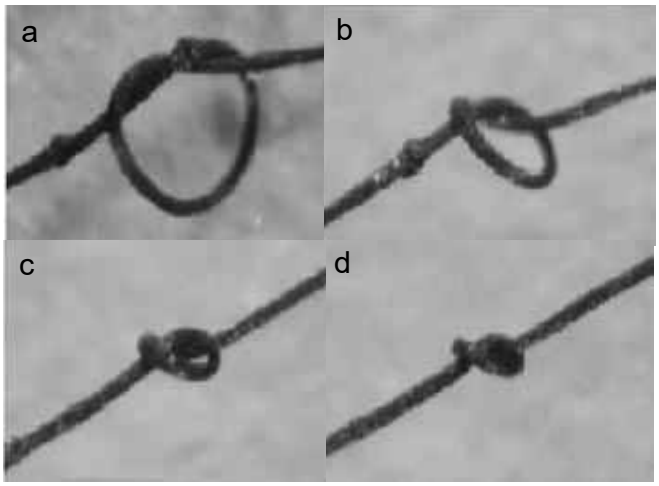

Figure 8. Micrographs showing the exceptional flexibility of carbon nanotube/ fiber[47]

Strong and versatile carbon nanotubes are finding new applications in improving conventional polymer-based fibers and films. For example, composite fibers made from single-walled carbon nanotubes (SWNTs) and polyacrylonitrile – a carbon fiber precursor – are stronger, stiffer and shrink less than standard fibers. Nanotube-reinforced composites could ultimately provide the foundation for a new class of strong and lightweight fibers with properties such as electrical and thermal conductivity unavailable in current textile fibers.

2.3 Preparation and Property of Carbon Nanotube/Ceramic Composites

Although ceramics have high stiffness and excellent thermal stability with relatively low density, their brittleness impedes their use as structural materials. Because of their exceptional resilience, carbon nanotubes might be particularly desirable as reinforcement for ceramics. Incorporation of nanotubes into a ceramic matrix could potentially create composites that have high temperature

stability as well as exceptional toughness and creep resistance. However, achieving a homogeneous dispersion of nanotubes in ceramics, with strong bonding between nanotubes and matrix presents greater challenges than incorporating tubes into a polymer.

Ma et al. formed MWNT/silicon-carbide (SiC) composites via mixing nano-particles of SiC with 10 wt% carbon nanotubes and hot pressing at 2000°C.[48] They reported a 10% improvement in the both bending strength and fracture toughness as compared to the monolithic ceramic. These modest improvements were attributed to nanotube/matrix debonding and crack deflection.

Other researchers have developed techniques to synthesize carbon nanotubes in situ to form carbon-nanotube/metal-oxide composite powders. Peigney et al.[49] used iron-containing α-alumina as catalysts and CH_4 as the carbon source for in situ growth of carbon nanotubes on iron particles. These powders were then hot pressed to form macroscopic composites. But despite the high homogeneity of this dispersion, which provides high electrical conductivity, the toughness is lower than that of carbon free Fe-Al_2O_3 nanocomposites. There are two main reasons for this. The carbon nanotubes greatly inhibit the matrix grain growth during hot pressing, preventing full densification of the material. And hot pressing at higher temperatures does not increase the densification, but damages the nanotubes. This work was expanded by using different catalyst such as Mg- containing alumina and different carbon source such as C_2H_2. Some of them showed reinforcement effect.

Zhan et al. reported a very large toughness gain in a SWNT/Al_2O_3 composite.[50] The fracture toughness of the composite was increased from 3.7 to 9.7 MPa $m^{½}$ by adding 10 vol.-% SWNTs into Al_2O_3 power. In this research, high quality SWCN bundles were used, and the alumina powder particles are very small (50 nm). The powders were mixed first by ball-milling, which

produced a reasonably homogeneous dispersion without damaging the nanotubes. A new technique of spark plasma sintering (SPS) was used to prepare the composites. The advantage of spark plasma sintering is that it allows ceramic powders to be annealed at lower temperatures and for much shorter times than other sintering processes, leading to the fabrication of fully dense ceramics or composites with nanocrystalline microstructures under mild conditions. Unlike other sintering processes, spark plasma sintering does not damage the nanotubes and the nanotube bundles could be seen to be located mainly at the boundaries of the Al_2O_3 grains, in good contact with the Al_2O_3 matrix (figure 9).

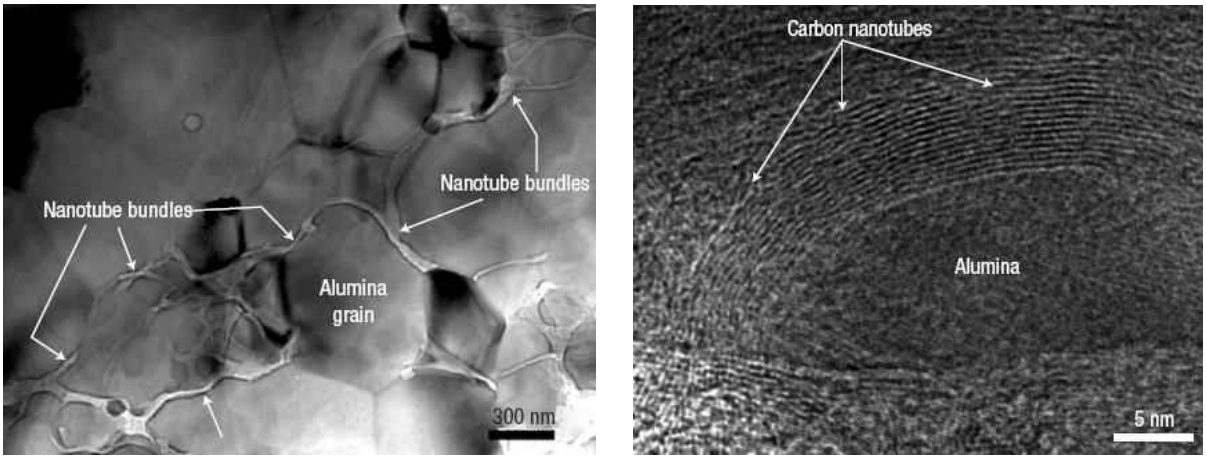

Figure 9. TEM images show that the nanotube bundles are well distributed at the matrix grain boundaries, and have good contact with the matrix grains[36]

In contrast to previous work on nanotube/ceramic composites, the fracture toughness was found to increase with nanotube density. This is thought to be due to the formation of entangled networks of single-walled carbon nanotubes, which may inhibit crack propagation.

Various techniques have been used to prepare carbon nanotube/silica composites. Seeger et al. described a method which involved preparing a composite gel of MWNTs with tetraethoxysilane (TEOS) and then sintering this at 1150°C in argon. In order to prevent the partial crystallization of the SiO_2 during the sintering, an alternative Nd :YAG laser method can be used to rapidly heat the TEOS/nanotube mixture. This produced an amorphous silica matrix, with no crystallization.[51]

There have been a few studies on preparing nanotube composites using oxides other than alumina and silica. Vincent et al. reported the production of nanotube/TiO_2 composites using sol–gel methods.[52] Possible applications of the composites included optical non-linear wave guides and unidimensional conductive films. Sol–gel methods were also used by Sakamoto and Dunn to prepare SWNT/V_2O_5 composites for use as electrodes in secondary lithium batteries.[53]

2.4 Preparation and Property of Carbon Nanotube/Metal Composites

There is growing interest in the addition of carbon nanotubes to metal matrices. Materials fabrication difficulties have limited research on nanotube-reinforced metal composites. One of the key issues is obtaining a uniform dispersion of nanotubes in the matrix. Damage or destruction of the nanotubes is often a problem because of the high temperatures and highly reactive environments associated with many methods of forming metal matrices.[54]

Kuzumaki et al. described the preparation of a nanotube/aluminum composite in 1998.[55] In their experiment, nanotube were mixed with a fine aluminum powder, followed by a hot-press and a hot-extrusion process at 700°C in a vacuum furnace. The result was a composite wire in which the nanotubes were partially aligned along the axial direction. The tensile strengths of the composite wires were comparable to that of pure aluminum, but the composite wires retained

this strength after prolonged annealing at 600°C, while that of the pure Al produced in a similar powder metallurgy process significantly decreases with time. They also prepared nanotube/titanium composites which showed a large increase in hardness and modulus compared to pure titanium.[56]

Because of the difficulty of using traditional powder-metallurgy processes to achieve homogeneous dispersion of nanotubes in the matrix, a novel fabrication process called "molecular-level mixing" was introduced.[57] After mixing a Cu ion solution with a well dispersed CNT suspension, the admixture was dried, calcined and then reduced. Then the resulting composite powder was consolidated by spark plasma sintering. This process provided a relative high interfacial strength between the CNTs and Cu and the CNTs were located within the powders rather than on the powder surface. (Figure 10)

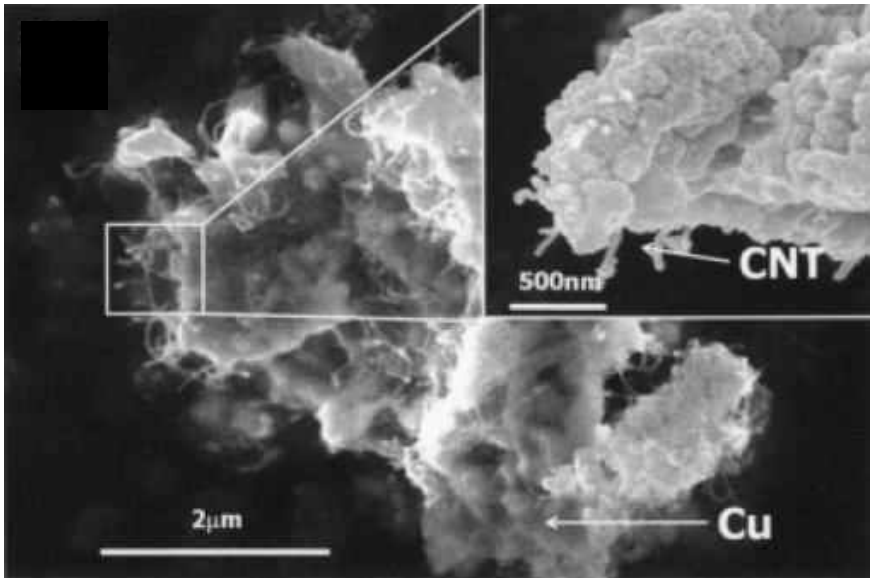

Figure 10. SEM micrographs of CNT/Cu composite powder[57]

The resulted nanocomposite is shown to possess three times the strength of the Cu matrix and to have twice the Young's modulus. As shown in figure 11, a 5 vol% CNT reinforced composite

showed yield strength of 360MPa, which is 2.3 times higher than that of Cu. When the addition of CNTs was increased to 10 vol%, the yield strength was 455 MPa, which is more than 3 times higher than that of Cu.

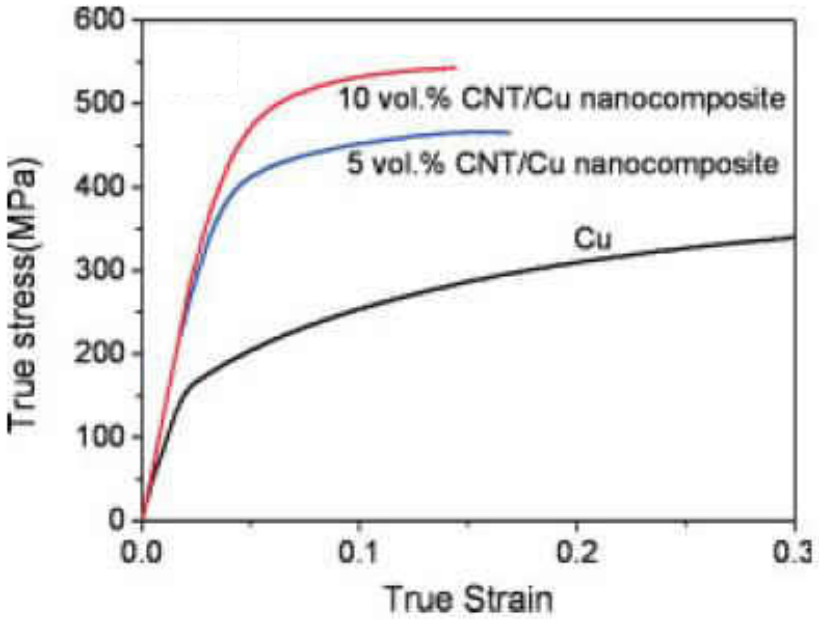

Figure 11. Stress-strain curves of CNT/Cu nanocomposites obtained by compressive testing[57]

Several other efforts were made to obtain "atomic-level mixing" of nanotubes and metal.[58] Chen et al.[59] fabricated CNT-Ni/P materials and tested them under lubricated wear conditions. Decreased friction coefficient and wear rates were measured, relative to similar materials with SiC or graphite additions and to virgin Ni/P itself. The potential for CNT-enhanced lubricity and/or the potential enhancement of hardness or damage tolerance make these types of systems attractive for further investigation[60]. CNT-Mg materials have been fabricated and their damping characteristics have been investigated but with little notable effects over other metal matrix

materials.[61] Xu et al.[62] also deposited copper nano-particles on the acid pretreated CNT surface using electroless plating. (Figure 12)

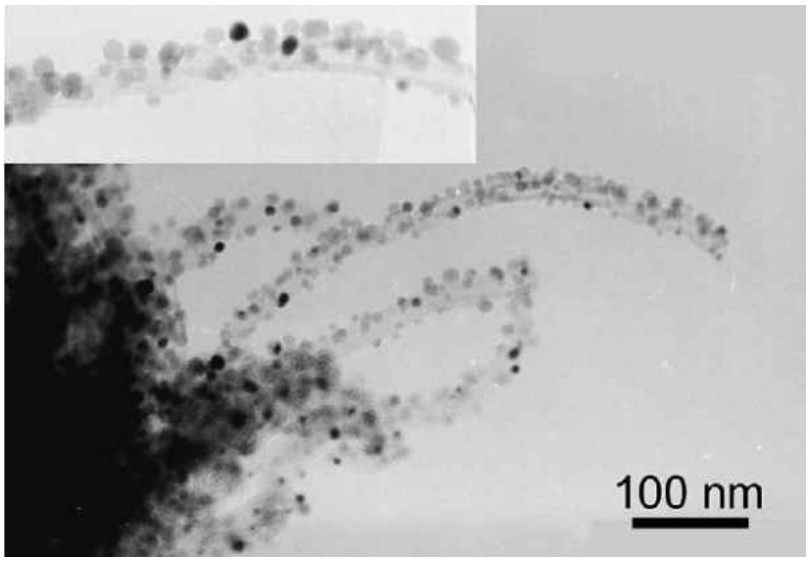

Figure 12. TEM images of copper nanoparticles deposited on the carbon nanotubes[62]

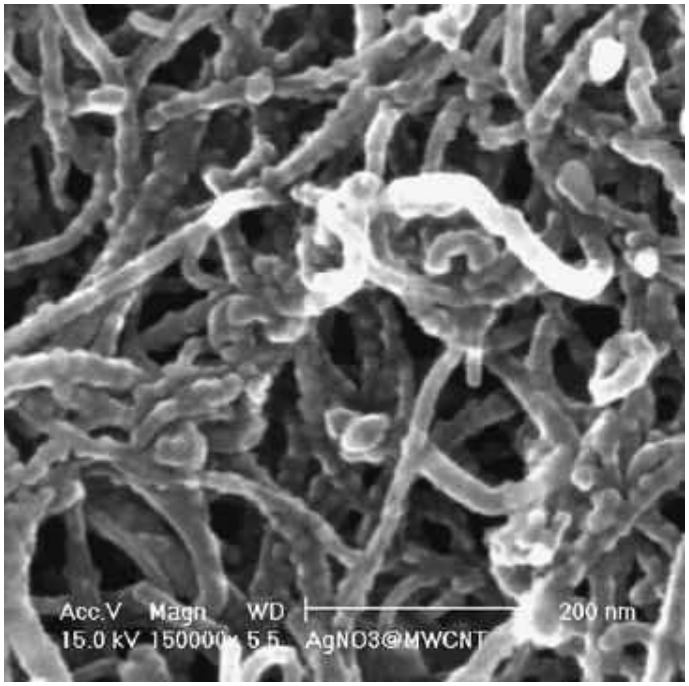

Figure 13. SEM image of the Ag nanoparticles/MWNTs composite[63]

A new solution phase method was described to prepare carbon nanotubes/metal composites. By injection of CNT solution into a diethyl ether/aqueous solution of metal salt biphasic mixture, metal (Ag, Au, Pd, and Pt) nanoparticles decorated CNTs composite materials can be prepared by spontaneous reduction of metal ions on the sidewalls of multiwall carbon nanotubes.[63] (Figure 13)

The driving force of this reaction is the difference in reduction potential between metal cations and CNTs. The deposition of particles proceeds without the aid of reducing agents or catalysts. Because no substrate was required in this process, non-specific formation of nanoparticles can be avoided. Based on the resulting composite, further bulk synthesis can be processed. Using similar process, Hu et al. fabricated a multilayered film of carbon nanotube/metal nanoparticle composite recently.[64] Additionally, the brush plating[65] and the sol-gel[66] method has been also used to prepare CNT/metal composites.

Electroplated microstructures of several different element metals and metal alloys have been demonstrated, including gold, silver, copper, nickel, and nickel alloys. (As shown in figure14) The films can be made in any thickness from ~1um to 1cm. Electroplating co-deposition, in which both metallic ions and nano/micro particles are deposited together on to the cathode, has been successfully used to fabricate metallic composites reinforced with nano-particles of materials such as SiC, Al_2O_3, graphite and ZrO_2. Electroplating has been proved to be a low cost and easy to apply method for fabrication of CNT reinforced composites. Better interfacial bonding between CNTs and the matrix could be achieved via electroplating because the solution phase allowed “atomic/molecular level of mixing” of metal and CNTs. Chen et al. prepared

nickel/CNT composite on carbon steel substrate by means of an electrodeposition process and studied several parameters influencing the content of CNTs in the deposit.[67]

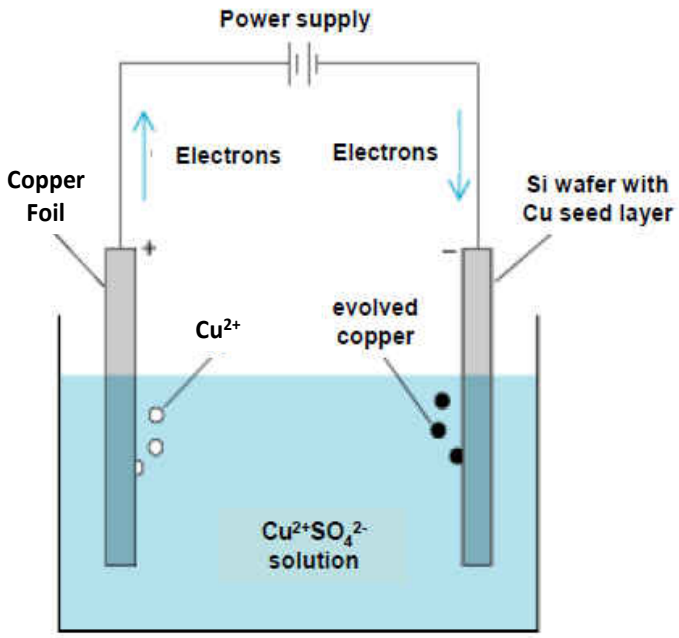

Figure 14. Schematic figure for electrodeposition of copper on silicon wafer

The electrodeposition process was also used to fabricate a carbon nanotube field emission structure.[68] The emitter structure is a composite of single-wall carbon nanotubes (SWNTs) and Ni. The carbon nanotubes distributed in the Ni matrix showed a strong contact with the substrate. To enable good dispersion of the SWNTs in the conventional Ni Watt bath solution which is required for uniform codeposition, several techniques are successfully employed, i.e., oxidation and heat-treatment of the carbon nanotubes, surfactant coating, ultrasonic agitation, etc.

Arai et al. obtained the powders of CNT/copper [69] and CNT/nickel [70] composite by electrodeposition techniques. These powders can be used as promising precursors for further development. A homogeneous dispersion of MWNTs was achieved by the addition of

polyacrylic acid to the basic bath with stirring. Their study showed that because the MWNTs possess high electrical conductivity, Ni is electrodeposited both on the substrate and on the MWNTs when they are incorporated into the deposited Ni film, and resulting in a "skewered dumpling" structure as shown in figure 15a. Ni did not deposit uniformly on the MWNTs, but selectively electrodeposited on the end and locally on the outer MWNT surfaces. (Figure 15b)

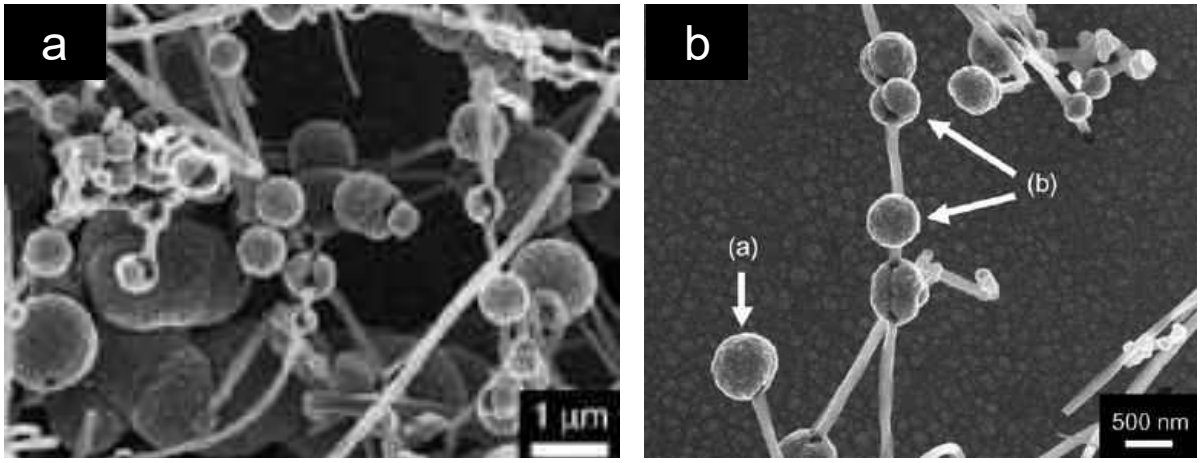

Figure 15. Skewered dumpling structure of nickel on MWNTs[70]

The selective deposition is because MWNTs possess high electrical conductivity in the axis direction due to their structure, the protruding ends of the MWNTs incorporated into electrodeposited Ni have lower resistance than other sites. Therefore, nickel ions easily accept electrons on the ends. However, it is also well known that CNTs contain defects, such as vacancies, on the outer surface. The defect sites on the outer surface are active and may also have lower resistance than other sites.

Carbon nanotubes were also used to improve the mechanical and tribological properties of electrodeposited Ni-Co magnetic alloy coatings.[71] In this case, nanotubes are introduced because of their high strength, good flexibility and unique conductivity. Shi's experimental results showed that the introduction of the carbon nanotubes in the electrolyte has caused a negative

shift towards of the reduction potential of the Ni–Co alloy coating, and the co-deposited CNTs had no significant effect on the electrodeposition process of the Ni–Co alloy coating. Their AFM study showed that the Ni-Co-CNTs composite coating has smaller particle size than Ni-Co coating. (Figure 16)

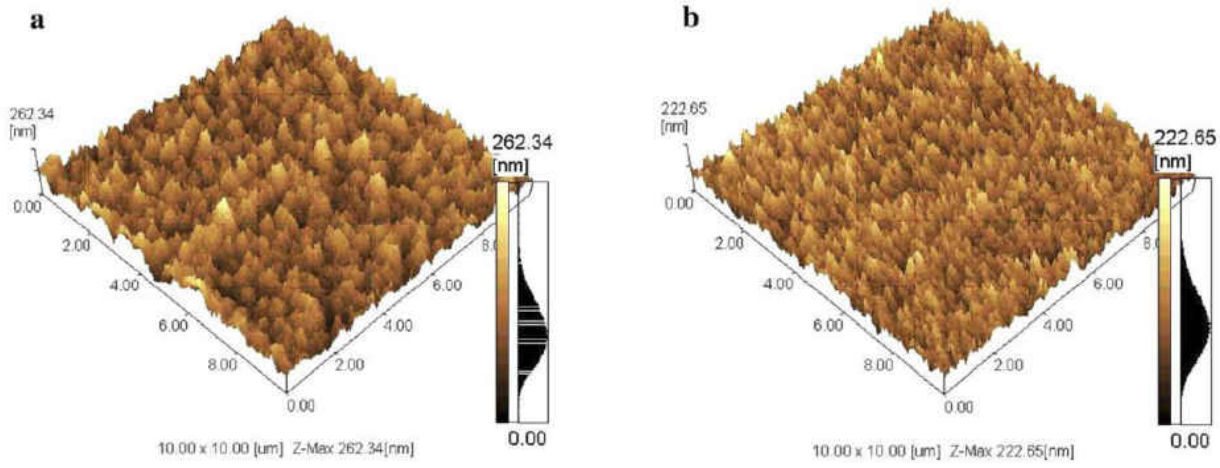

Figure 16. AFM images of (a) Ni-Co and (b) Ni-Co-CNTs composite coating[71]

X-ray diffraction (XRD) pattern of the composite revealed lower and broaden peaks for Ni-Co solid solution which was also attributed to the decrease in the grain size. Mechanical properties of the film were studied using nano-indentation measurement. Its nano-indentation hardness increased from 4.41 GPa to 5.87 GPa and elastic modulus increased from 202 GPa to 236 GPa.

2.5 Some Applications

Carbon Nanotube sheets can be made so thin that they will be transparent and you can see through them. Base on this property, carbon nanotube windshields can be produced. (Figure 17) They will be somewhat flexible allowing for impact without major injury. These windshields will be 50 times stronger than steel and harder than glass, but they will not be brittle and will not break.

Additionally, carbon nanotube windshields will be light-weight and the average car has up to 400 pounds of glass on it. By lowering the cars weight you increase its performance and gas mileage and can even put a smaller motor in the car and thus use even less fuel still.

Figure 17. Carbon nanotube windshields

Nanotube sheets are light, flexible, strong and transparent. They can also be electrical conductive. All these properties are ideal for use in pipelines. Carbon nanotubes are proposed to be looked at for such applications as military cockpit canopies, bulletproof glass, et al. The nanotubes sare good conductors of electricity and will work well as flat panel displays.

CHAPTER 3. THEORETIC BASE OF CARBON NANOTUBE/METAL COMPOSITES

3.1 Introduction

The subject of carbon nanotube composites has grown rapidly over the past 8 years. A lot of outstanding properties can be exploited by incorporating the nanotubes into some form of matrix, and the preparation of CNT composite materials is now a rapidly growing subject. In most cases, these composites have employed polymer matrices. Limited efforts have been made to utilize metal/carbon nanotube composites. Besides their mechanical properties, the electrical and thermal properties of the CNT-composite system are also studied. Further research will certainly lead to better materials, but significant challenges to real success still remain.

Given the amazing properties of carbon nanotubes, the improvements in the properties of nanotube reinforced polymer composite are not sufficient, although significant efforts have been made. For example, it has been indicated that carbon nanotubes have a mechanical strength of about 60GPa. If 1% of such carbon nanotubes are added into a polymer matrix which has a strength of 50MPa, the resultant mechanical strength of the nanocomposite should be about 680MPa, or more than 13 times stronger than the matrix, based on the law of mixture: $\sigma_c = V_f\sigma_f + (1-V_f)\sigma_M$, where V_f is the fiber's volume fraction in percentage, σ_f and σ_M are strength of fiber and matrix, respectively. However, so far the strengthening achieved is much smaller, in a range of 30~60%, as described in previous sections.[72, 73, 74] It has also been indicated that although a much higher volume fraction of nanotubes has been tried, the strength increase is much lower than that predicted by the law of mixture. These discrepancies imply that the law of mixture, which has been widely used in conventional fiber composites, may not be valid for

nanocomposites. New and more sophisticated governing equations (formula) need to be developed to account for unique features of nanocomposites.

3.2 Theoretical Basis

In comparison to conventional fibers, the primary differences in nanofibers are their dimensions. First, conventional carbon fibers have a larger diameter, in the range of a few micrometers to a few tens micrometers. In contrast, nanofibers have a much smaller diameter, in the range of one to tens of nanometers. Second, conventional carbon fibers can be made infinitely long, while nanofibers are normally much shorter, in the range of a few micrometers or even down to sub-micrometers.

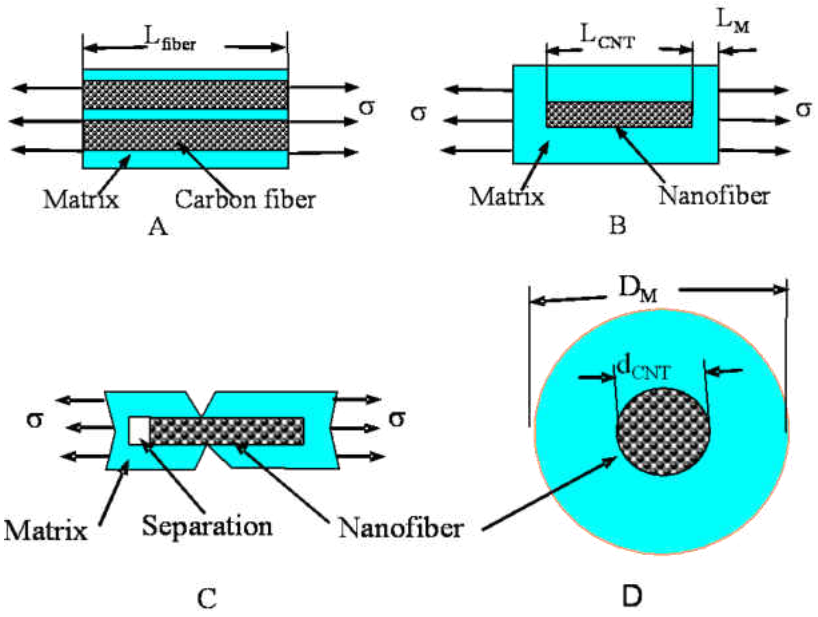

Figure 18. Sketch of long carbon fiber reinforced composite (A) and initial state of short nanofiber reinforced composite under tensile pressure (B), (C) shows potential outcomes, (D) sketches a cross section of a fiber contained in a matrix (not in scale)

As a result, conventional carbon fibers are normally continuous within a matrix meaning that each fiber can fully support the load applied (Fig. 18A). In other words, conventional fibers can be used to bear most portion of the applied load. In addition, due to the fact that large volume fraction of fibers is normally used in conventional composites[75], the matrix behaves more like an adhesive that binds fibers together, or the requirement of interfacial bonding is not very critical. Therefore, the deformation of the matrix is constrained within the deformation limit of fibers. In contrary, nanotubes are kind of tiny short fibers (about one to a few micrometers in length) that are trapped discontinuously within a matrix (Fig. 18B), and the applied load is normally transferred indirectly to the nanofibers via the matrix, as sketched in Fig.18B.

For simplicity, a small cylinder shaped cell that consists of only one nanofiber and a portion of matrix around it is selected for analysis. The averaged stress applied in the axial direction to the cell is denoted as σ (Fig. 18B). The resultant displacements between nanofiber and the matrix within the same length of L_{NF} (Fig. 18B) can be expressed as

$$\Delta L_{NF} = \varepsilon_{NF} L_{NF} = \frac{\sigma}{E_M} L_{NF}, \quad \Delta L_M = \varepsilon_M L_{NF} = \frac{\sigma}{E_M} L_{NF} \qquad (1)$$

Therefore, the relative displacement ratio between the matrix and the nanofiber is

$$\gamma = \frac{\Delta L_M}{\Delta L_{NF}} = \frac{E_{NF}}{E_M} >> 1 \qquad (2)$$

Since Young's modulus of polymer matrix is much smaller (about a few GPa or less) than that of the nanofiber's Young's modulus (up to 1TPa, carbon nanotube, e.g.), the deformation difference between a matrix and a nanotube from equation 2 could be up to a few hundred to a thousand times. For example, if the E_M is 1.2 GPa (polystyrene[32]) and E_{CNT} is 1,000 GPa, then the deformation difference between CNT and polystyrene is about *833* times larger! The

consequence of this large deformation difference is that the matrix surrounding the nanotube may experience extremely large distortion thus large strain energy would be produced within the matrix. If this distortion is larger than that of the elongation at the break of the matrix material, then a fracture is likely to occur within the matrix (Fig. 18C). On the other hand, if the relative distortion associated strain energy is larger than the interfacial bonding energy between the nanotube and the matrix then the nanotube will be partially separated from the matrix. The separation of the nanotube from the matrix will largely reduce the load support capability which is proportional to the bonded nanotube length, and the nanotube withdrawing out of the matrix is inevitable. At this point, adding more nanotubes may not produce expected proportional reinforcement, since both the interfacial bonding of nanotube/matrix and matrix's mechanical properties are accountable for the reinforcement efficiency. Therefore, it is important to identify the main factors which will affect mechanical properties of nanofiber reinforced nanocomposites.

From Fig. 18B, the strain energy of a nanofiber within a composite under stress σ can be expressed as stress x strain x half volume:

$$U_{NF} = \frac{\sigma^2}{2E_{NF}} \frac{\pi}{4} d_{NF}^2 L_{NF} \qquad (3)$$

Similarly, the strain energy of a matrix cylinder surrounding the nanofiber within the same length L_{NF} is

$$U_M^{'} = \frac{\sigma^2}{2E_M} \frac{\pi}{4} (D_M^2 - d_{NF}^2) L_{NF} \qquad (4)$$

As indicated in Fig 18B, when counts the strain energy associated with the matrix portion where no nanofiber is trapped inside (length L_M in which no nanofiber is trapped), then the total strain energy of the matrix is

$$U_M = \frac{\sigma^2}{2E_M}\frac{\pi}{4}(D_M^2 - d_{NF}^2)L_{NF} + \frac{\sigma^2}{2E_M}\frac{\pi}{4}D_M^2 L_M \qquad (5)$$

Since the interfacial-bonding energy between nanofiber and the matrix has to bear the strain energy difference produced between the matrix (UM) and the trapped nanofiber (UNF), thus at equilibrium

$$U_M - U_{NF} = \frac{1}{2}S \qquad (6)$$

where S stands for the total bonding energy associated with the interface formed between the nanofiber and the matrix, then equation 6 can be expressed as

$$\sigma^2[D_M^2(1+2\frac{L_M}{L_{NF}}) - d_{NF}^2 - \frac{E_M}{E_{NF}}d_{NF}^2] = \frac{4E_M S}{\pi L_{NF}} \qquad (7)$$

From Fig. 16B and Fig. 16D, the volume fraction of nanofiber is

$$V_f = \frac{d_{NF}^2}{D_M^2(1+2\frac{L_M}{L_{NF}}) - d_{NF}^2} \qquad (8)$$

Then eq.7 can be expressed as

$$\sigma^2 = \frac{4E_M V_f S}{\pi L_{NF} d_{NF}^2 (1 - \frac{E_M}{E_{NF}}V_f)} \qquad (9)$$

If the bonding energy density is denoted as s*: $$s^* = \frac{S}{\pi d_{NF} L_{NF}} \quad (10)$$

then the strength * of a nanofiber reinforced composite can be described as

$$\sigma = 2\sqrt{\frac{E_M V_f s^*}{d_{NF}(1-\frac{E_M}{E_{NF}}V_f)}} \quad (11)$$

Strength from continuous matrix portion can be expressed as

$$\frac{D_M^2 - d_{NF}^2}{D_M^2}\sigma_M = (1-V_f)\sigma_M \quad (12)$$

So the total strength of nano-fiber/nano-tube reinforced nano-composite is:

$$\sigma_C = 2\sqrt{\frac{E_M V_f s^*}{d_{NF}(1-\frac{E_M}{E_{NF}}V_f)}} + \sigma_M(1-V_f) \quad (13)$$

Therefore the resultant mechanical strength of a nano-fiber filled nano-composite is mainly determined by the following factors: 1) the Young's modulus of the matrix (E_M), or the stiffness ratio between matrix and nano-fiber (EM/ENF), 2) the volume fraction of nano-fiber (V_f), 3) the interfacial bonding energy density (s*) and 4) the dimension of nano-fiber (d_{NF}).

Following are expanded discussions on relationships between these factors and the resultant mechanical strength of nano-fiber reinforced nano-composites.

3.3 Effect of carbon nanotube dimension

Equation 13 suggests that under the same bonding energy density s*, the tensile strength of nanotubes reinforced nano-composites largely depends on nanotube diameter, i.e. the smaller the diameter the greater the tensile strength. Fig. 19 indicates that when a nanotube's diameter is smaller than about 5nm, a reduction in diameter would result in a rapidly increased strength. For example, if carbon nanotube can be made with 1nm in diameter that is about 10,000 times smaller than the diameter of conventional fibers, the resultant strength of nanocomposites could be 100 times stronger than the conventional composites, if the volume fraction and Young's modulus are the same. For nanotubes with diameters between 5nm to 20nm, the change in diameter produces much less effects on resultant strength.

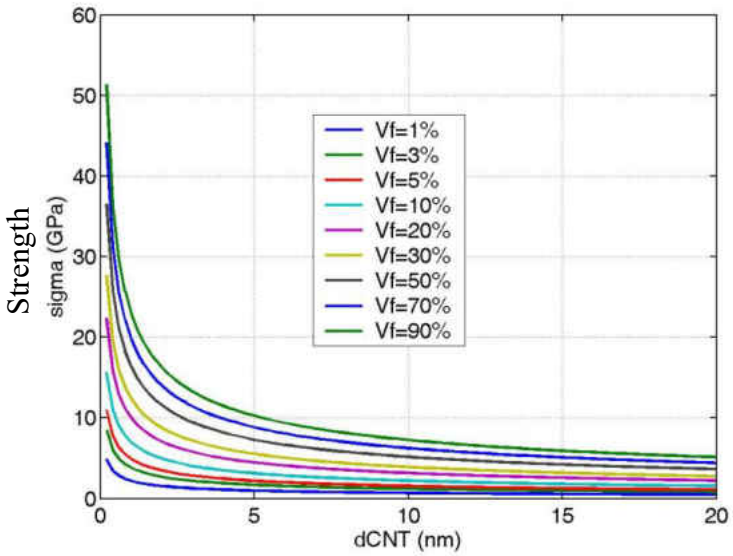

Figure 19. Strength of carbon nanotube reinforced nanocomposites versus diameter, based on equation 13. Conditions: stiffness of matrix is 200GPa, bonding energy density (s*) is 0.7J/m^2, and stiffness of nanofiber is 1,000GPa.

Fig. 19 also indicates that the manipulation of the nanotubes' diameter produces much greater effect than volume fractions in achieving a desired mechanical strength. For example, only 3% of nanotubes with 1nm in diameter would produce the same resultant strength as that produced by 90% (volume fraction) nanotubes with 10nm in diameter. This means that much stronger nanocomposites can be produced by the addition of a few percentages of nanotubes addition, if their diameter can be produced small enough. The largely reduced need on volume fraction means more cost effective. Therefore, stronger and cheaper nanocomposites can be developed.

3.4 Effect of Matrices' Young's Modulus

Equation 13 suggests that the stiffness of the matrix is also important in determining the mechanical strength of nanocomposites. Fig. 20 is a sketch showing that the higher the matrix stiffness the greater the mechanical strength of the nanocomposite. For example, when the Young's modulus of a matrix is less than 200GPa, any increase in the matrix's stiffness would result in a significant increase in the resultant strength. For typical polymers the Young's modulus is about 50GPa or less. Therefore, a stiffer polymer matrix would produce greater mechanical strength if other factors remained the same. However, when the matrix stiffness is greater than about 200GPa, the resultant strength is almost linearly proportional to the stiffness (Fig. 20). The trend is similar for different volume fractions. Stiffer matrices such as some polymers, most metals and ceramics are capable as matrices in developing stronger nanocomposites.

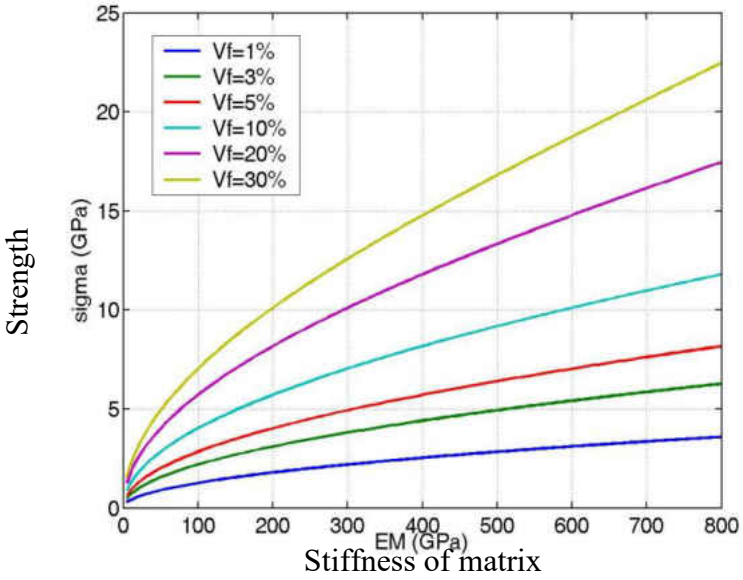

Figure 20. Sketch of nanocomposite's strength versus stiffness of matrices, based on equation 13. Conditions: diameter of carbon nanotube is 1.5nm, volume fraction (Vf) of CNT is 1%~30%, bonding energy density (s*) is 7J/m^2, and stiffness of CNT is 1000GPa.

3.5 Interfacial Bonding Between Nanotubes and Matrix

The dependence of resultant strength on interfacial bonding energy (strength) is plotted in Fig. 21. It indicates that the interfacial bonding between nanotubes and a matrix is very critical. For example, any increase in the interfacial bonding would result in a rapidly increase in strength, especially when the interfacial bonding energy is less than about 0.2J/m^2. After that, the resultant strength is almost linear proportional to the interfacial bonding strength. Therefore, it is important to enhance the bonding between nanotubes and matrix.

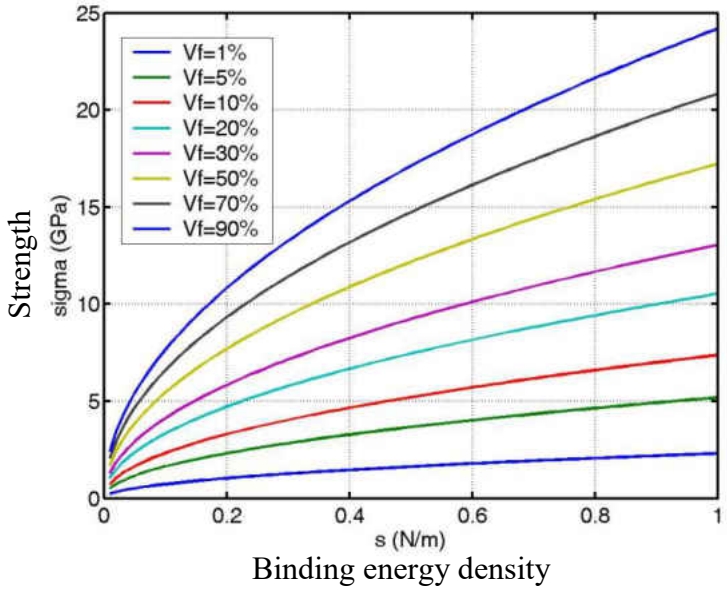

Figure 21. Strength of nanofiber reinforced nanocomposites versus binding energy density s*, based on equation 13. Conditions: diameter of nanofiber is 1.5nm, stiffness of matrix is 200GPa, and stiffness of nanofiber is 1000GPa.

CHAPTER 4. DISPERSION OF CARBON NANOTUBES

Uniform distribution of carbon nanotubes in matrix is one of the most important parameters in determining the properties of carbon nanotubes and metal nanocomposites.

Carbon nanotubes tend to bundle together because of their large specific surface areas which create strong inter-tube non-covalent interactions and make them intractable and insoluble in common solvents. This has lead much of the recent research to focus on the preparation of processible carbon nanotubes. [76, 77] The dispersion of CNTs in solution can be studied by cryogenic transmission electron microscopy (cryo-TEM)[78], atomic force microscopy (AFM)[79], scanning electron microscopy[80], Raman spectroscopy[81], and optical microscopy[82]. Moreover, the discovery of nanotube fluorescence[93] offers a more precise method for detecting the dispersion of individual nanotubes, and UV–visible spectroscopy has been successfully used to monitor the exfoliation dynamics of SWCNTs in aqueous solution [83]. That being said, systematic investigations on parameters determining the dispersion behavior of CNTs, such as sonication energy, applied concentration of CNTs, ratio of CNTs to surfactant and so on have not yet been performed.[84]

4.1 Surfactant assisted carbon nanotube dispersion

Several methods have been developed for carbon nanotube dispersion. One of the common methods for improving processibility is the covalent attachment of organic groups onto the graphene surface.

Because the as-produced CNTs exist as aggregates or bundles that are tightly bound by an estimated interaction of 500 eV/um of tube length for SWCNT, [85,86] one of the key challenges is processing or engineering CNTs for further potential applications. Significant efforts have

already been devoted over the last couple of years to achieve this goal. [87, 88, 89, 90] The most used technique available for processing CNTs is solution based processing[91]. In particular, surfactants such as sodium dodecyl sulphate (SDS) have been studied for their excellent nanotube stabilization and separation capabilities. [92, 93, 94] The SDS molecules can be adsorbed on the surface of SWCNTs and MWCNTs, and prevent re-aggregation after sonication-driven dispersion. The colloidal stability of aqueous MWCNT dispersions can be maintained for several months.

SDS covered carbon nanotubes are negatively charged. In our study, we need the carbon nanotube to be co-deposited onto cathode with metal ions. So we used Octadecyl Trimethyl Ammonium Bromide (OTAB) and Hexadecyl Trimethyl Ammonium Bromide (CTAB) instead as surfactant to help the dispersion of carbon nanotubes in the electrolyte. The chemical formulas of SDS and CTAB are showed below.

SDS: $CH_3(CH_2)_{11}SO_3^- \quad N_a^+$

CTAB: $CH_3(CH_2)_{14}CH_2N^+(CH_3)_3 \quad B_r^-$

Carbon nanotubes covered with CTAB or OTAB will be positively charged. During the electro-deposition process, positively charged carbon will migrate towards the cathode under electrical field. This process has been verified by our results. As shown in figure 22. 10mg purified MWCNTs (with OD about 20~30 nanometer) were added into 200ml DI water. An ultrasonic bath was then used to disperse carbon nanotubes. In the mean time, 5 grams of OTAB was dissolved into 100ml DI water. The surfactant solution was slowly added into the carbon nanotube solution until we achieved a stable carbon nanotube suspension. Copper foil was used for both the cathode and the anode, and the applied current was 5mA. After applying DC current

for 10min, the cathode was covered with carbon nanotubes. Using SEM, we can observe CNTs clearly.

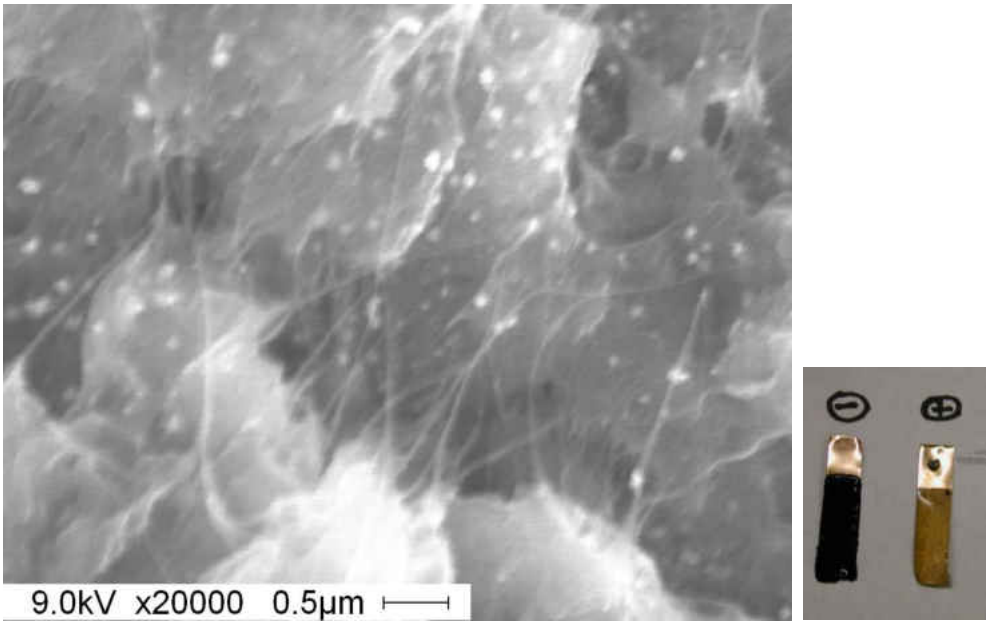

Figure 22. SEM image of CTAB covered CNT

Adding a well dispersed CNT solution into either copper or nickel electrolyte, the carbon nanotubes and the metal ions will be co-deposited on to the substrates. Figure 23 shows the SEM image of the co-deposited carbon nanotube and metal composites. Here, OTAB was used as surfactant.

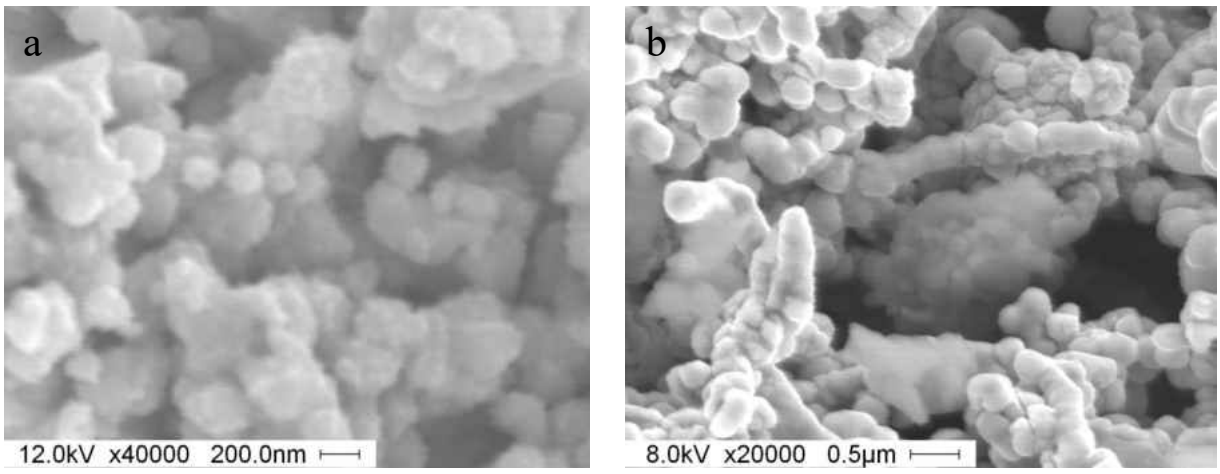

Figure 23. SEM pictures of a) CNT/Copper and b) CNT/Nickel nanocomposites when using OTAB as CNT dispersion agent.

The images indicated that the sample surfaces were not as dense as the normal electroplated copper or nickel surface. High porosity was observed.

In our project, we mainly focus on the mechanical properties of carbon nanotube/metal nanocomposites. Preparing samples with high purity, low porosity is the first step in producing nanocomposites with optimized mechanical properties. Also, when the surfactant was applied, the carbon nanotube surface was covered with organic molecule chains first. The bonding between carbon nanotubes and metal ions are indirect which will lead to the weak bonding between them. In order to realize the reinforcement proposed by adding carbon nanotubes into metal matrices, we need find other methods of dispersing carbon nanotubes.

4.2 Effect of different acid treatment on carbon nanotube dispersion

Covalent functionalization represents an efficient way to render the CNTs soluble either in aqueous or organic phase, by attaching different functional groups directly to the CNTs.[95] Nitric acid is extensively used to oxidize CNTs. Acid washed CNTs showed better dispersibility. This may be due to the OH groups formed in the acid washed case that make hydrogen bonding with water molecules. Nitric acid treatment produces mainly carboxylic groups[96, 97, 98] which contribute to the solubilization of the nanotubes.[99, 100] C-O, C=O and O=H bonds are identified in chemically modified nanotubes. Acidic groups like carboxyl, phenol and lactol were formed on the carbon nanotube surface. The acid concentration varies in the range of 15–70 wt%, the initial concentration of the CNTs varies from 0.1 to 10 mg/ml, and the treatment duration from 1 to 48 h.

In our study, besides nitric acid, hydrochloric acid and sulfuric acid are also used to do the surface treatment of carbon nanotubes. The solubility of the CNTs is assessed qualitatively, based on visual appearance. Predetermined quantities of MWNTs (10 mg) and various acids (20 ml) were added into centrifuge tubes, and the MWNTs were dispersed for 60 min in an ultrasonic bath. After ultrasonic treatment, carbon nanotubes were separated from the acids using a centrifuge. The carbon nanotubes were rinsed 3~5 times using DI water. Then, the carbon nanotubes were dispersed in DI water through the use of an ultrasonic bath. Figure 24 shows our experimental results. The suspensions in tubes No. 8, 9 and 10 are carbon nanotubes treated with HCl, HNO_3 and HSO_4 respectively. From the results we can see that carbon nanotubes treated with both HCl and HNO_3 can achieve stable dispersion for more than 1 day. In our following experiments, HNO_3 acid was used to do the surface treatment for carbon nanotubes.

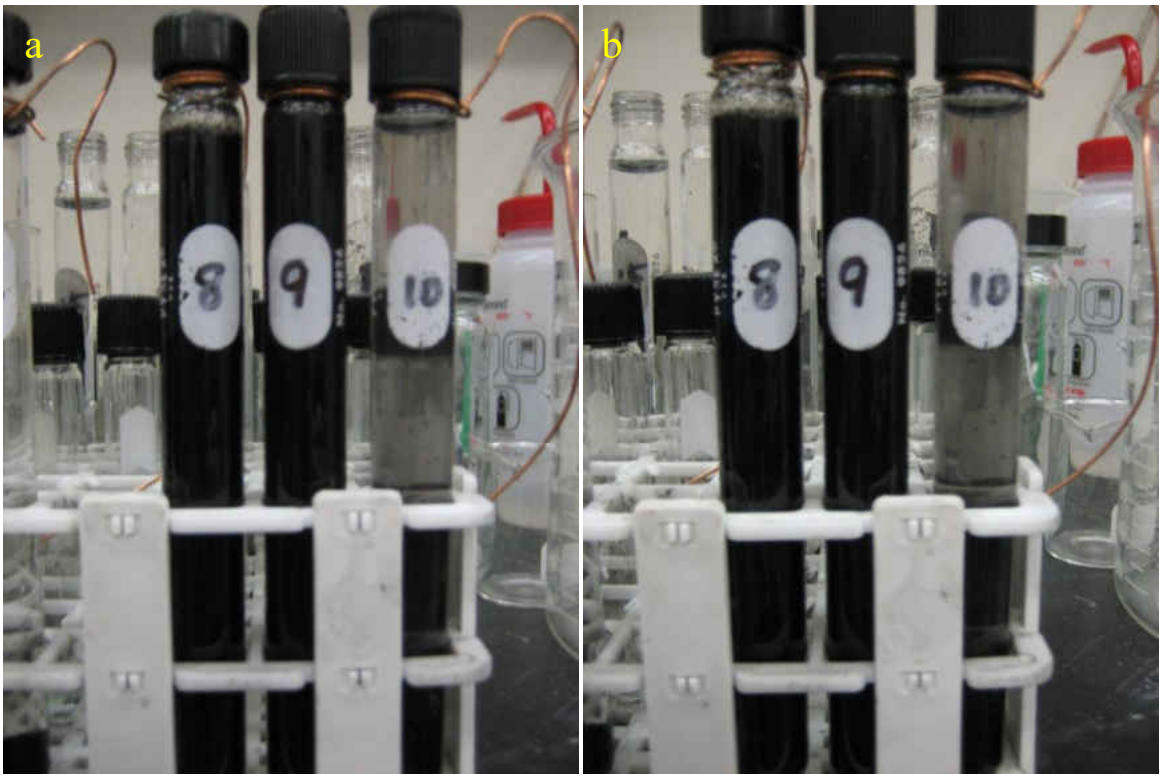

Figure 24. CNT dispersion after treated with HCl, HNO_3 and HSO_4. (a) 1h after ultrasonic bath; (b) 1day after ultrasonic bath

4.3 Ultrasound assisted carbon nanotube dispersion

Carbon nanotubes are strong and flexible but very cohesive. They are difficult to disperse into liquids, such as water, ethanol, oil, polymer or epoxy resin. Ultrasound is an effective method to obtain discrete - single-dispersed carbon nanotubes.

Carbon nanotubes are generally available as dry material. A simple, reliable and scalable process for de-agglomeration is needed, in order to utilize the nanotubes to their maximum potential. For liquids up to 100,000cP, ultrasound is a very effective technology for the dispersing of nanotubes in water, oil or polymers at low or high concentrations. The liquid jet streams resulting from ultrasonic cavitations, overcome the bonding forces between the nanotubes, and separate the tubes. Because of the ultrasonically generated shear forces and micro turbulences ultrasound can assist in the surface coating and chemical reaction of nanotubes with other materials, too.

Ultrasound machine was used in our research to help the dispersion of pre-treated carbon nanotubes in the electrolyte. The pre treated carbon nanotubes can form a stable suspension in DI water for several days. But once the electrolyte was added, carbon nanotubes tend to precipitate from the suspension. This was due to the bonding between the functional groups on the carbon nanotube surface and the metal ions in the electrolyte. As shown in the TEM image below. After the ultrasonic dispersion of carbon nanotubes, we observed the CNTs using TEM (figure 25). Several particles were found attached to the surface of MWNT. (Figure 25 a) Using the tools in TEM, we can calculate the lattice parameter of these two particles (figure 25b and 25c). The calculation results showed that the lattice parameter of particle 1 was 0.348nm which was similar to the inter-layer spacing of zigzag carbon nanotubes (0.341nm). And the lattice parameter of particle 2 was 0.384nm which was comparable with the publication date of copper (0.3615nm).

We can conclude that even before the electrodeposition process, some of the metal ions will form bonds with the pretreated carbon nanotubes or deposit onto the surface of carbon nanotubes in electrolyte. The defects formed during acid treatment will create some active sites for this automatic deposition.

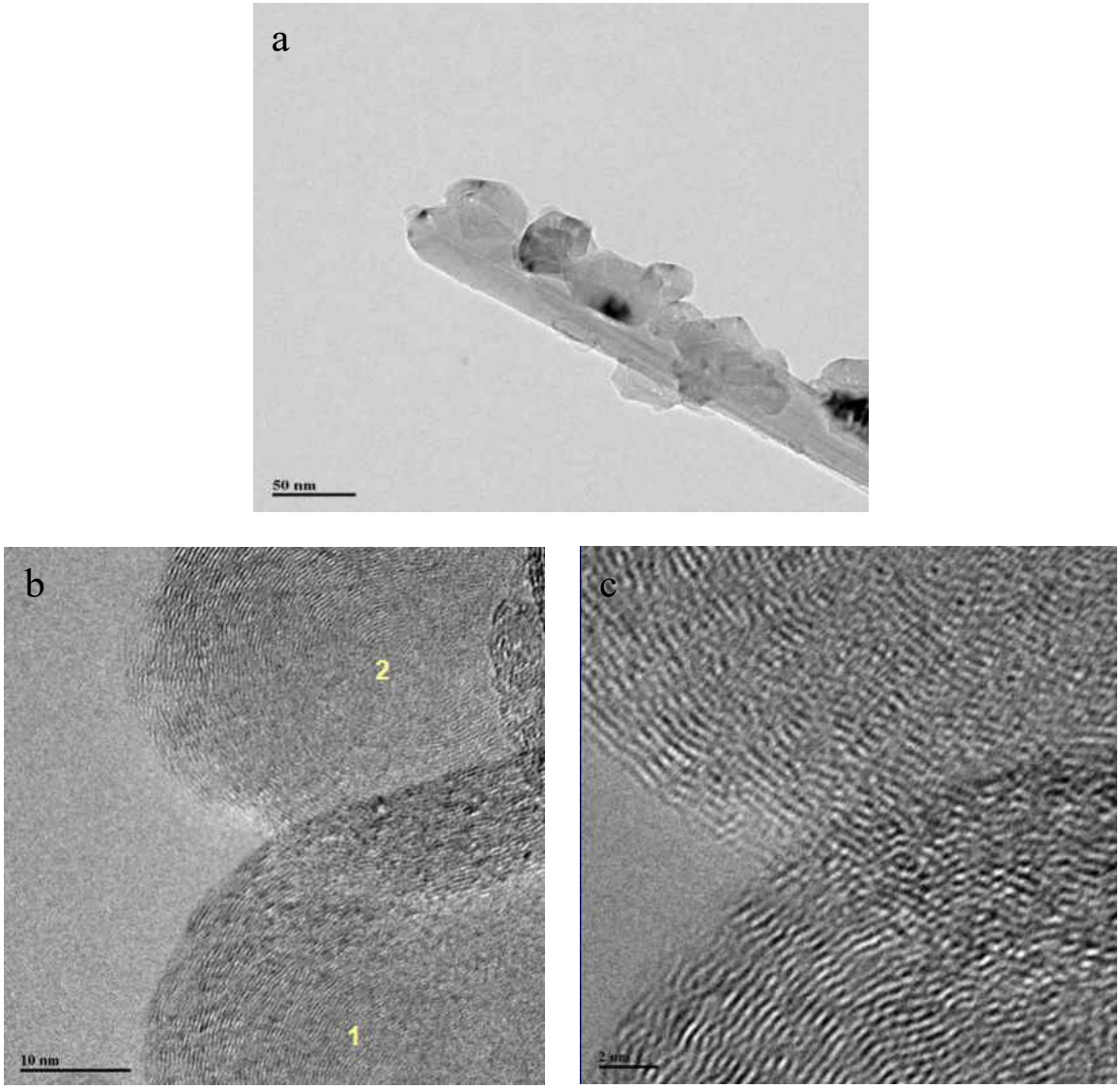

Figure 25. TEM images of carbon nanotube after ultrasonic dispersed in copper electrolyte

Because of the addition of the electrolyte, the suspension of carbon nanotubes was unstable. As shown in figure 26, precipitation happened after 1 hour of the electrodeposition process. When the ion concentration of the electrolyte increased, a shorter stable time was observed.

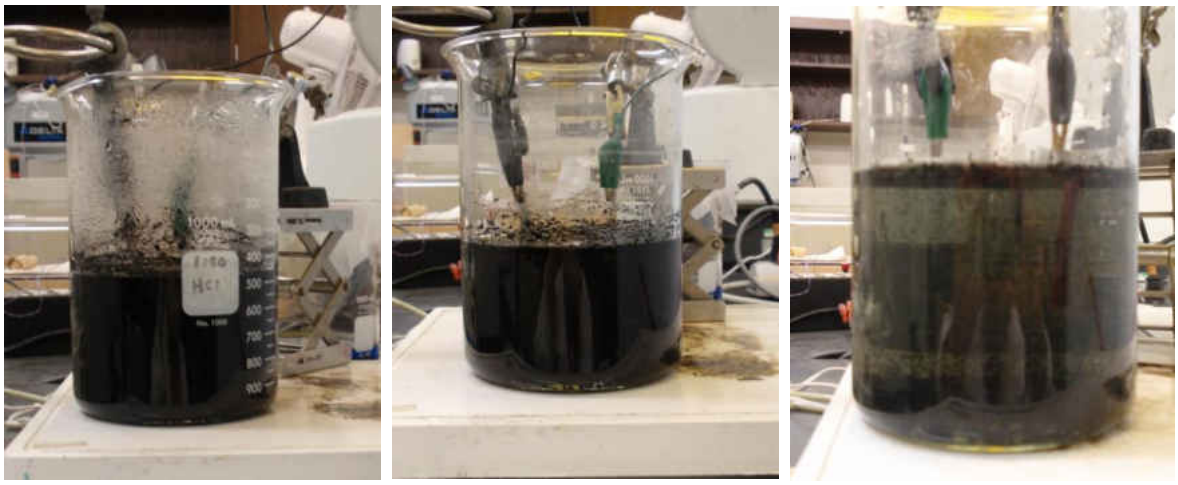

Figure 26. Precipitation of CNT in diluted copper electrolyte. (a) after sonication; (b) after 1h and (c) after 2h

4.4 Temperature effect on carbon nanotube dispersion

In the electrolyte, particles randomly collide with each other at a rate determined by their Brownian motion. The rate of particle collision in a suspension is diffusion limited and is proportional to the suspension concentration and temperature. In order to study the effect of temperature, three temperature points were selected: 1) 63 Celsius, controlled using a hotplate; 2) 40 Celsius, also hotplate controlled; and 3) 0 Celsius, controlled by a mixture of water and ice.

10mg MWNTs (with OD 20~30nm) and 20ml of nitric acid were added into centrifuge tubes, and put into an ultrasonic bath for 1h. After the ultrasonic treatment, carbon nanotubes were separated from the acids using a centrifuge and rinsed 3~5 times using DI water. Carbon nanotubes were then dispersed into the diluted copper electrolyte using an ultrasonic bath under different temperatures. See figure 27.

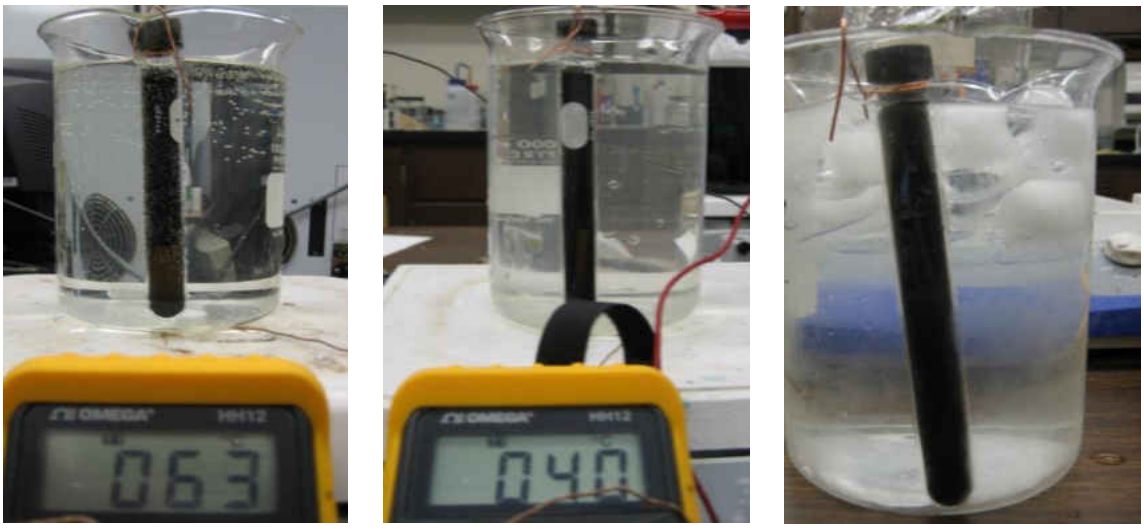

Figure 27. Study the dispersion of carbon nanotubes under different temperature

The temperature was controlled during sonication by adding ice into the bath or heating up the bath. Because of the low ion concentration, these suspensions can be stable for at least 1 hour.

Figure 28. Dispersion of carbon nanotubes under different temperature 2 hours after ultrasonic bath

When the suspension was kept at zero degrees, no visible precipitation was observed 2 hours after the ultrasonic bath. When the temperature increased, nanotubes tended to aggregate. This was because that temperature provided the energy to enhance the Brownian motion of the carbon nanotube particles and overcome the repulsion between particles.

CHAPTER 5. MECHANICAL PROPERTY OF CARBON NANOTUBE / METAL COMPOSITES

5.1 Electrochemical Co-deposition

The pulsed electrodeposition technique (PED) is a versatile method for the preparation of nanocrystallized and nanostructured metals/alloys using pulsed current electrolysis. In the past three decades, PED has found much attention worldwide[101, 102]. Electroplating is an important technique for the production of micro-systems due to its advantages, such as high rate of deposition, high resolution, high shape fidelity, simple scalability and good compatibility with existing processes in microelectronics. This is a technique that allows the preparation of large bulk samples with high purity, low porosity[103] and enhanced thermal stability. Furthermore, like other electrochemical procedures, the PED technique enables us to control the microstructure such as grain size, grain size distribution, and micro-stress and crystallite shape. The microstructure of the resultant materials determines the physical and chemical properties, e.g., hardness[104], conductivity, or chemical stability[105]. Also, atomic level co-deposition of CNTs and metal in the aqueous electrolyte can provide better interfacial bonding between the CNTs and the metal matrix.

The parameters of PED are the pulse length (t_{on}), the time between two pulses (t_{off}), the peak height (I_{pulse}), and the average current density (I_a).

$$I_a = \frac{I_{pulse}\ t_{on}}{t_{on} + t_{off}} \qquad (14)$$

The change of these parameters primarily modifies the cathodic over-potential, which influences the nucleation rate and activation energy of the nucleation.

In electrodeposition processes, the surface profile of a deposit will be rougher than the original surface profile of the cathode. Protrusions on a surface grow more rapidly than the surrounding surfaces because their current density is higher. During the nickel/copper and CNT co-deposition process, CNT became embedded in the substrate creating numerous protrusions which caused the surface roughness. During the electrodeposition process, the surface roughness could be amplified. When the thickness of the deposited layer increases, the surface becomes rougher. In electrodeposition, pulse current is one of the commonly used methods for the improvement of the surface finish of a deposit.

In our project, pulse-reverse electrodeposition technique was used to produce Ni/CNTs and Cu/CNTs composites from electrolyte baths. The recipe for the nickel electrolyte bath and copper electrolyte bath are shown in Table 1 and Table 2 respectively. Purified single-walled, double-walled and multi-walled carbon nanotubes were obtained commercially from different sources. The diameters of carbon nanotubes varied from less than 1nm to up to 60nm, and the length of carbon nanotubes also varied from ~500nm to around 50μm. All carbon nanotubes were treated with nitric acid and then dispersed in DI water first; ultrasonic agitation is used to break up nanotube aggregates. Then the uniformly dispersed solutions were added into the electrolyte. The solution is stable for at least 1 hour without visible aggregation.

Table1. Receipt of nickel electrolyte bath

Nickel Sulfate	Boric Acid	Nickel Chloride	SDS	CNTs	Saccharine
315g/L	35g/L	25g/L	0.1g/L	30~150mg/L	0.1g/L

Table2. Receipt of copper electrolyte bath

Copper Sulfate	Sulfuric Acid (98%)	Hydrochloric acid	CNTs
150g/L	100ml/L	0.13ml/L	150mg/L

The pulse-reverse plating was carried out using cathodic square wave pulses by reversing the current periodically (switched from cathodic to anodic polarization). The current density of electro-deposition was determined by evaluating the resistivity of the as-prepared nickel/carbon nanotubes composite samples. A high cathodic current density is responsible for low activation energy for nucleation, resulting in an increased formation of nuclei. High current density will also strongly decrease the ion concentration near the cathode and will not leave enough time for Ni^{2+} ions to migrate toward the electrode. As a result, higher current density led to poor quality of the produced composite samples. Figure 29 shows the relation between current density and resistivity of produced samples. Each point was the average value of 8~10 samples. We can see that when current density was increased, the resistivity of the as-prepared samples increased as well. During our study, we chose a current density of 10~20mA/cm^2 for the electro-deposition of nickel/carbon nanotube composites.

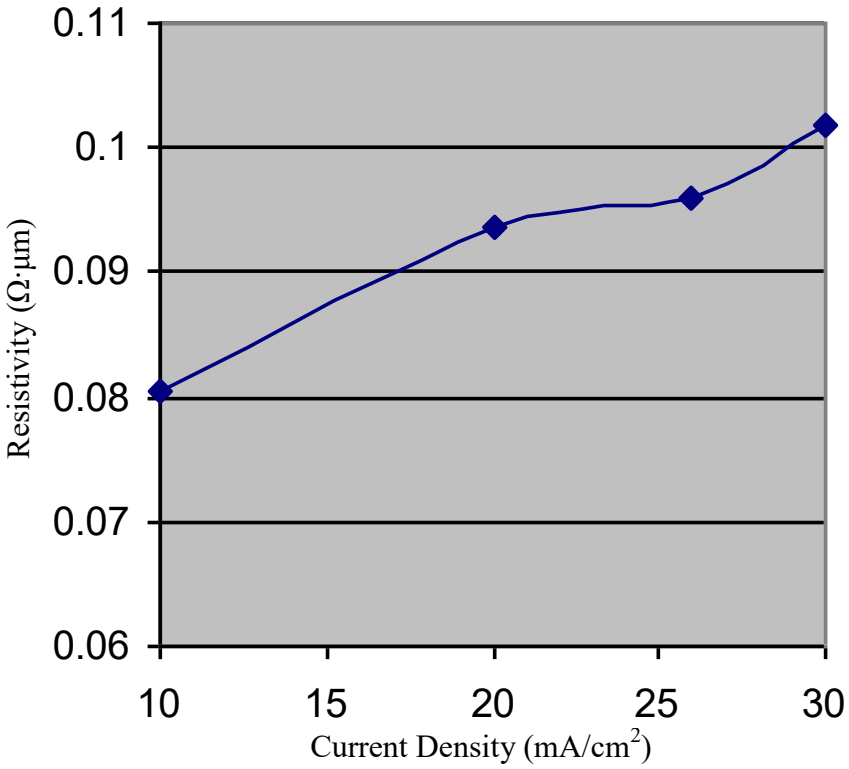

Figure 29. Relation between current density and resistivity of produced Ni/CNT composites

The frequency of pulse and pulse-reverse current was studied by adjusting the on, off and reverse time. The results were evaluated using resistivity and SEM observation. The current densities used here were 10mA/cm^2 and 20mA/cm^2. We need to balance the deposition efficiency and finishing quality. Table 3 shows the size of the substrate, electrolyte, electro-deposition setting, measured sheet resistance, samples thickness and calculation results of resistivity after sample size correction. By adjusting the forward and reverse current on time, we chose different forward/reverse current ratio. The ratios we used were 2:1, 4:1, 5:1, 8:1 and 10:1. Figure 30 shows the surface morphology of samples under different current ratios. When there was no reverse current (figure 30a), the sample surface was rougher even though a relatively longer pulse was applied. The best surface finishing was found when the current ratio was 4:1 (figure 30b) or 5:1(figure 30c). No obvious differences were observed between them. The surface

roughness was clearly observed when the current ratio was increased to 8:1 (figure 30d). Figure 30e shows the surface of the prepared sample when current density was 20mA/cm^2. The current ratio here was 5:1. A relatively rough surface was found.

The sheet resistance was tested using a four point probe. And the thickness of the samples was measured using SEM observation. A correcting factor was applied according to the sample size.

Table3. Study the effect of different forward and reverse current ratio

Size	Solution	Setting	Sheet resistivity(Ω)	Thickness (μm)	Resistivity after Correction(Ω·μm)
10*20mm	Nickel+SWNT	Fwd Amp: 20mA Time: 60ms On Time: 40ms Off Time: 20ms	0.0333	3.08	0.0851
10*20mm	Nickel+SWNT	Fwd Amp: 20mA Time: 40ms Rev Amp: 20mA Time: 10ms	0.0401	2.67	0.0889
10*20mm	Nickel+SWNT	Fwd Amp: 20mA Time: 50ms Rev Amp: 20mA Time: 10ms	0.0271	3.08	0.0693
10*20mm	Nickel+SWNT	Fwd Amp: 20mA Time: 40ms Rev Amp: 10mA Time: 10ms	0.0431	2.33	0.0834
10*20mm	Nickel+SWNT	Fwd Amp: 40mA Time: 50ms Rev Amp: 20mA Time: 10ms	0.0441	2.39	0.0875

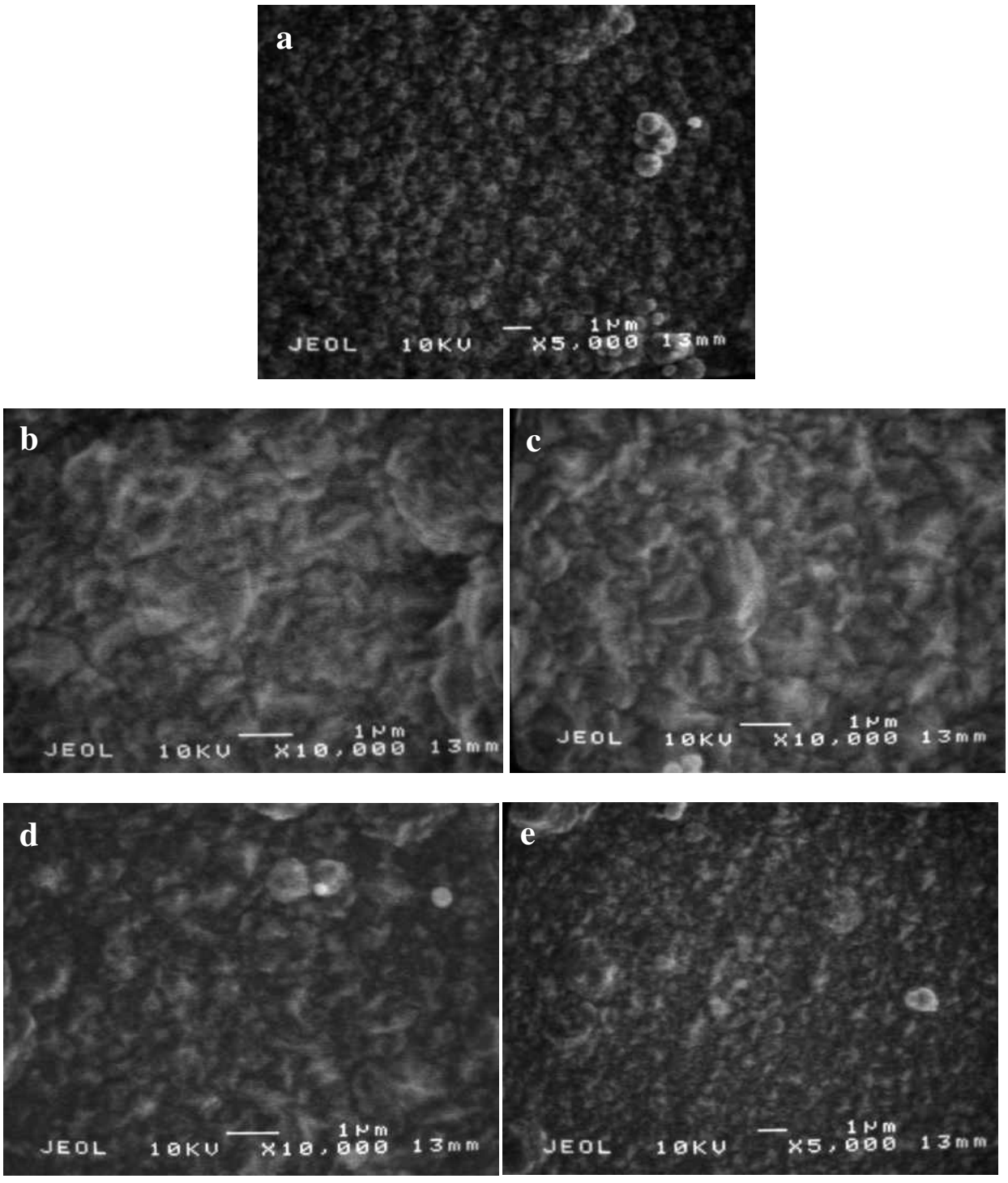

Figure 30. SEM images of samples under different current ratio. a) no reverse current; b) 1:4; c) 1:5, current density 10mA/cm^2 ; d) 1:8 and e) 1:5, current density 20mA/cm^2

According to the above results, the best forward/reverse current ratio was 5:1 considering both the electro-chemical-deposition efficiency and the quality of the sample's finish. High current frequency assisted the electrophoretic deposition of charged carbon nanotubes in the electrolyte. So, in the following study regarding nickel/carbon nanotubes deposition, a forward time period of 5ms and a reverse time of 1ms were applied. Both the forward and reverse peak current density is about 10~15mA/cm^2.

The same investigation was performed on electro-deposition of copper/carbon nanotubes nanocomposites by Dr. Guangyu Chai. A similar conclusion was reached, that the optimized current ratio should be 5:1. Both the forward and reverse peak current density is around 30mA/cm^2 for copper.

For comparison purposes, pure nickel and copper without CNT were also deposited under the same condition.

In the solution phase, the nickel and copper was in the form of ions. Then, these metal ions started to nucleate on or around the nanotubes. The nanotubes fell down on the substrate through gravity and flows caused by the potential, and increased the local resistance which increased the current density in/around nanotubes, thereby promoting the deposition of nickel on the nanotubes. Figure 31 shows the SEM image of the as-deposited Ni/CNTs surfaces after an hour of electrodeposition. It is clear that the nanotubes co-deposited with the nickel. Most CNTs have one end embedded deeply in the nickel matrix. Some nanotubes not in the matrix have already been coated by nickel. We can clearly see the nucleation and growth of nickel on the surface of CNTs. It also seems that the CNTs tend to attach end to end through nucleation and growth of nickel. This phenomenon has also been verified by S. Arai, et al.,[51] who found that, during

deposition, the nickel prefers to nucleate on the end of nanotubes or defects sites on the outer surface, where a low resistivity is expected and Ni (II) ions easily accept electrons.

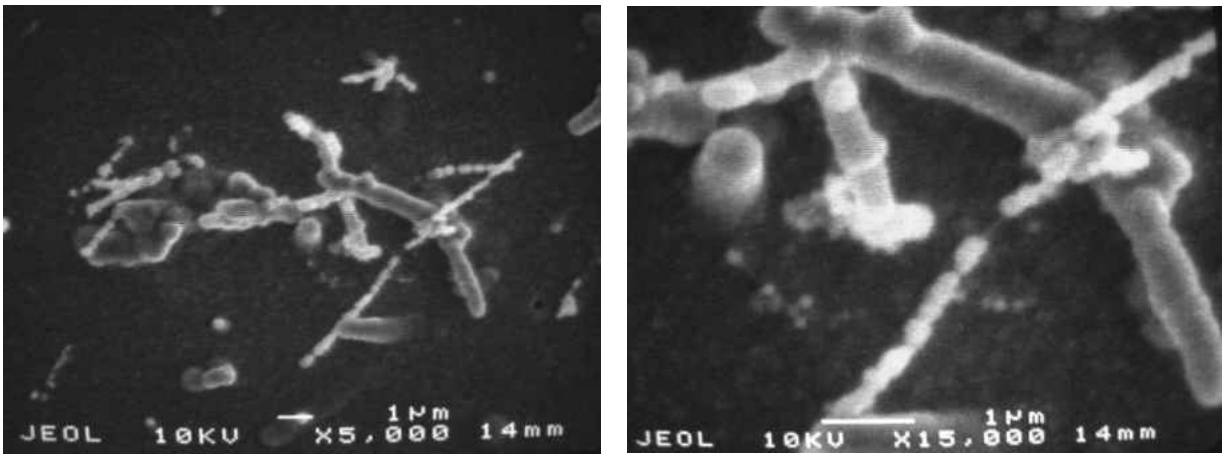

Figure 31. SEM image of the Ni/CNTs surfaces after electrodeposition for an hour.

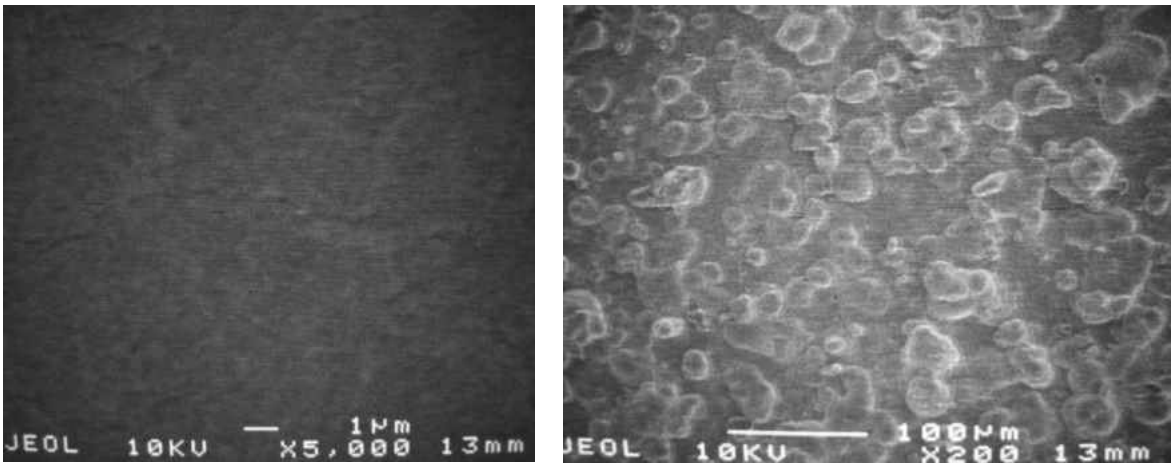

Figure 32. SEM image of the as-deposited pure nickel and composite

Figure 32 shows the SEM image of the pure nickel and composite. The surface of the nickel is smooth and dense, while on the surface of the composite, dispersed bulges, which show the ends of nanotubes covered by nickel, can also be seen.

5.2 Test Sample Preparation

In order to test the tensile strength of the composite, Dog-bone shape micro-samples were used. The samples were prepared using the standard LIGA process as shown in figure 33. Here we use SU8 (MicroChem inc.) to fabricate molds for the test sample. SU8 is a negative thick photoresist, good for fabricating fine and stable patterns because of its good physical and optical properties as well as its stability in most chemicals. After evaporating a thin layer of copper onto silicon wafer as a seed layer, SU8 molds were fabricated on the surface using surface micro-fabrication. The thickness of the SU8 molds are 50~100um. Then nickel/copper and carbon nanotubes were co-deposited into SU8 molds using a pulse-reverse electrodeposition technique in an electrolyte bath, following the process described in the above section. After deposition, the SU8 molds were removed using SU8 remover. The samples were then released from the substrate and ready for testing.

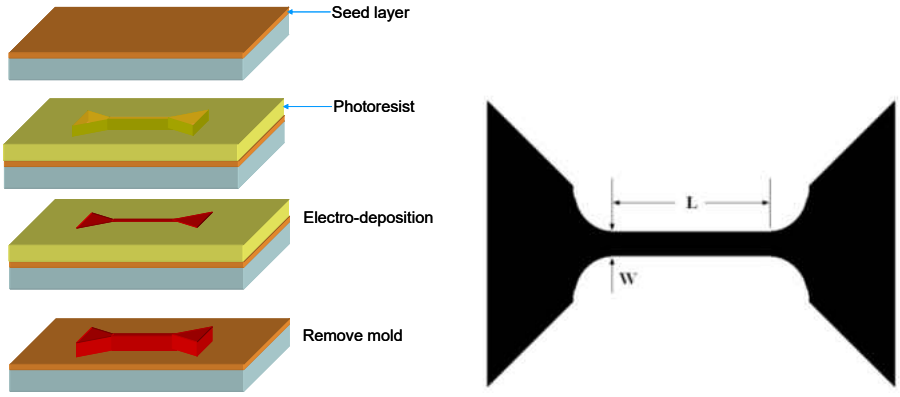

Figure 33. Schematic flows chat of LIGA process and the shape of the tensile test sample

The microsamples used in the present study were 25~50 micrometers thick and 200, 400, 600 micrometers wide in the gauge section. The length of the gauge (L) is 4mm. The sample thickness was determined by using scanning electron microscopy observations.

5.3 Micro Tensile Test of Composite Samples

Uniaxial tensile tests were performed in a Tytron 250 Microforce Testing System (MTS, USA) at a force loading rate of 10 N/min.

When testing, the specimen is held on the tester with gripers (figure 34), which are aligned using the alignment guider. An axial force is used to stretch the specimen which is controlled by software. The deformations and the axial forces are recorded automatically in a data file.

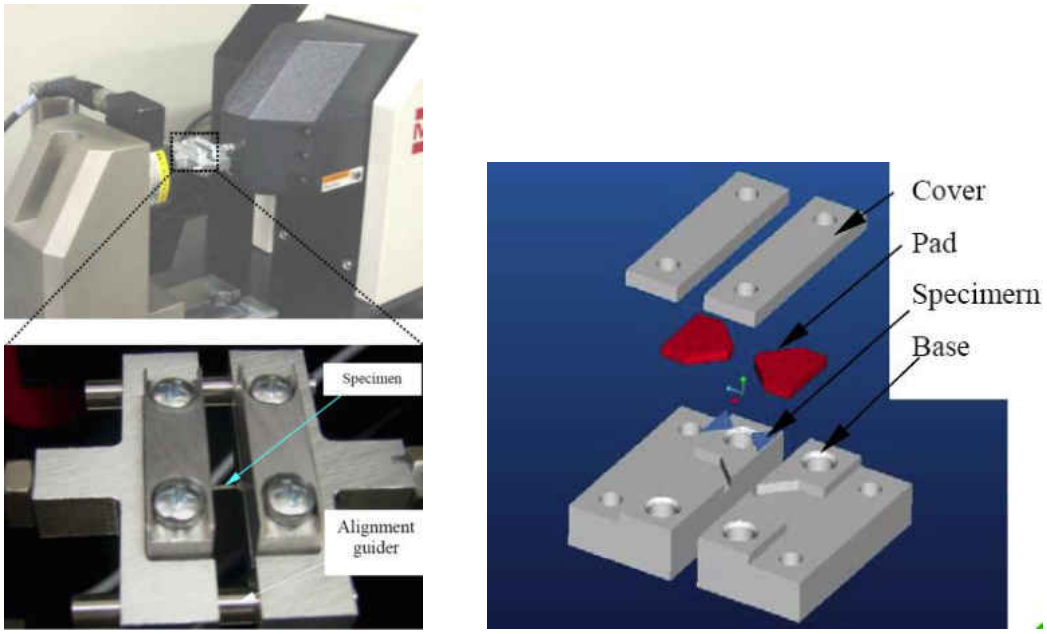

Figure 34. Testing system

Figure 35 shows the tensile stress-strain response of the as-deposited pure nickel and Nickel/CNTs composite samples which were deposited under the same conditions. Obviously, the composite exhibits significantly higher strengths than that of pure nickel. The 2% yield strength and ultimate strength of the as-deposited pure nickel were found to be 506MPa and 625MPa respectively, which are comparable to the values that have been reported previously. The yield strength and ultimate strength of Ni/CNTs composites reaches as high as 1290MPa

and 1715MPa in Ni/MWNT, 1692MPa and 1997MPa in Ni/SWNT. These values were at least 2.5 times larger than those of pure nickel. More interestingly, as shown in the figure, the Ni/MWNT composite has a larger elongation than that of pure nickel, while the Ni/SWNT has a smaller one.

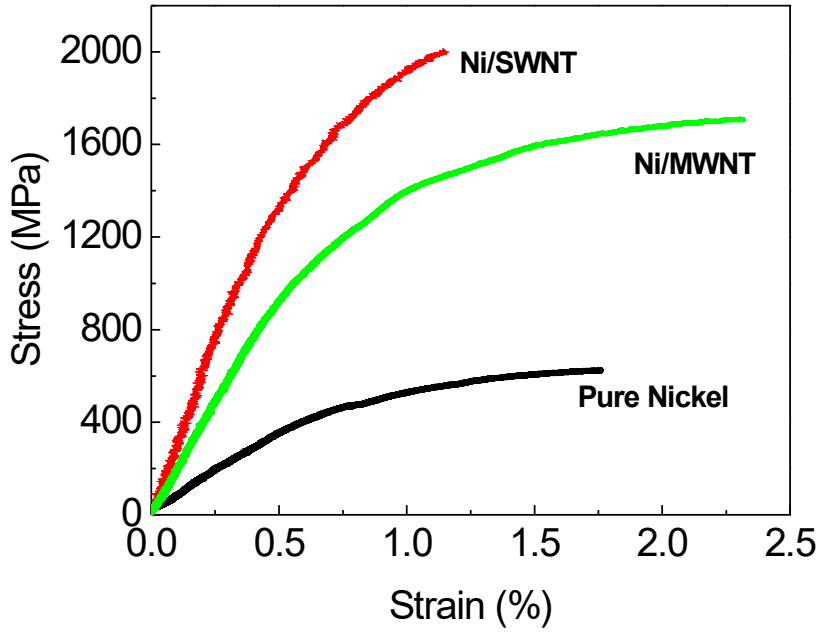

Figure 35. Tensile stress-strain response of the pure nickel and Nickel/CNTs composite samples

As in the case of copper, the yield tensile strength reaches 422 MPa, and the ultimate tensile strength is as high as 714 MPa (Figure 36). These values are at least three times larger than those of the pure copper samples (75 MPa and 230 MPa respectively) prepared under the same condition. The CNT-Cu nanocomposite samples also show considerable tensile ductility, with an elongation-to-failure value up to 5%.

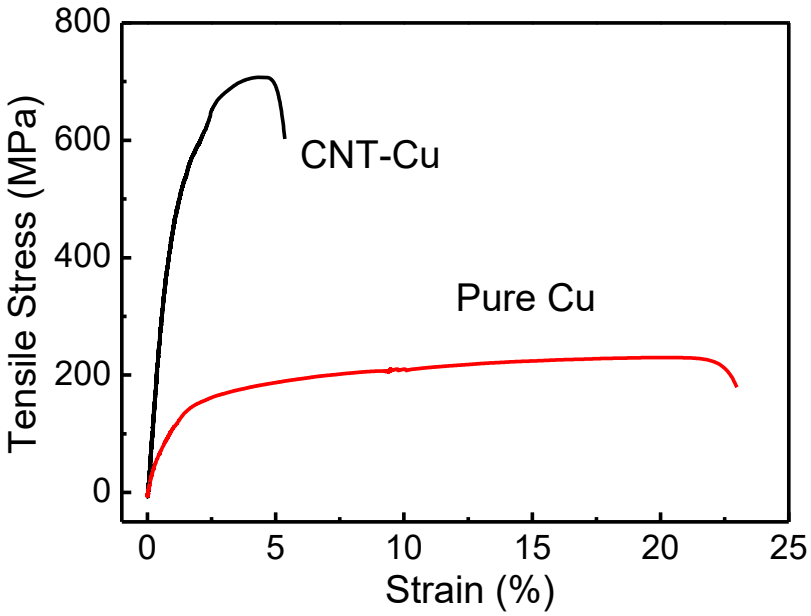

Figure 36. Tensile stress-strain curve of the CNT-Cu sample in comparison with that for a pure Cu sample

Such remarkable strengthening by CNT reinforcement was due to the strong interface bonding between carbon nanotubes and the metal matrix.

In addition, the metallic matrices are stiff enough to prevent an enlarging deformation from occurring when nanotubes are withdrawn, which can often be seen in the CNT/polymer composite. Consequently high load transfer efficiency can be obtained. This is further proved by the SEM characterization of the sample fracture after the tensile test. As for the CNT-Cu nanocomposite, after separation, the copper at the fracture is stretched and forms a "horn" shape surrounding the CNTs (Figure 37). Yet the "horn" structures are not observed from the pure copper tensile test samples. More interestingly, the maximum tensile strain obtained from the CNT-Cu nanocomposite is around 5%, which is close to the limitation of previous theoretical prediction and experimental results for the elongation of CNTs themselves. [106,107] It clearly

clarifies that the remarkable strengthening of the CNT-Cu nanocomposite is due to the reinforcement of the CNTs.

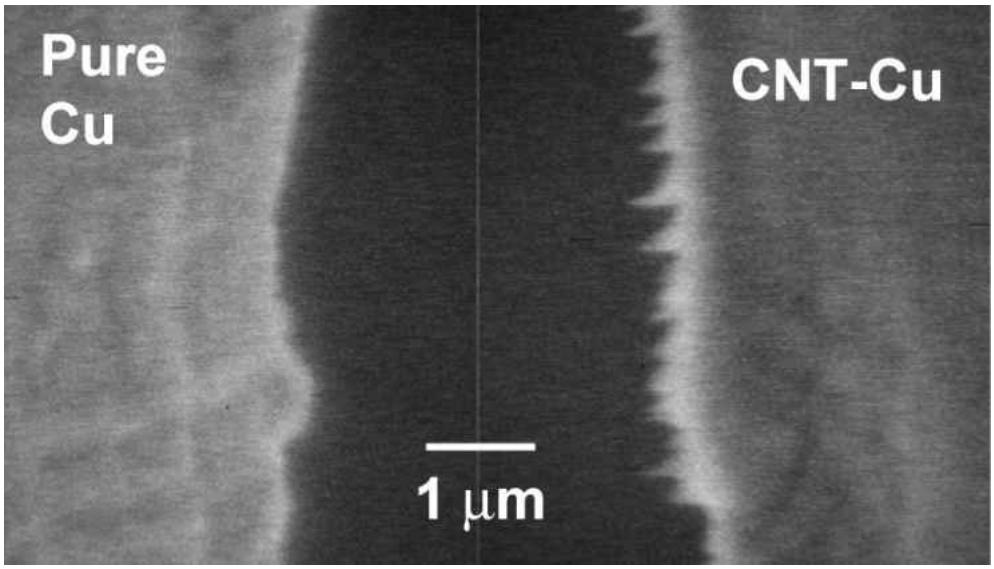

Figure 37. SEM characterization of the tensile test fractures for the CNT-Cu nanocomposite and the pure Cu sample prepared under the same condition.

In a CNT-reinforced material, interface behavior is expected to be significantly different from conventional carbon fibers because of the unique chemical bonding inherent in CNTs. Experiments have shown that high-quality, multiwall CNTs exhibit very easy interwall sliding, with inner graphitic walls able to be extracted from outer walls in a 'sword and sheath' mechanism at low applied forces.[108] Our experimental results also show that Ni/SWNT has much higher strength but slightly lower elongation, while the MWNT have a slightly lower strength but higher elongation. Molecular dynamics simulations have shown that the pull-out forces in MWNT are increased when the inner walls have a fractured end.[109] The fractured end of the inner wall(s) would naturally deform outward but is constrained by the outer wall(s), generating high local stress (Fig. 38).

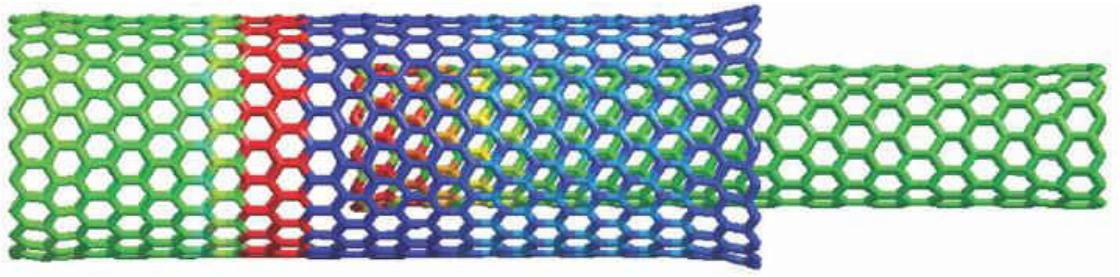

Figure 38. Forces in a double-walled nanotube during pull-out of the inner tube (red=high; blue=low). Forces are highly concentrated in the region where the inner, fractured nanotube interacts with the outer nanotube.

Figure 39 is a TEM image of the fracture surface of Ni/CNT composite. At the fracture surface of the composites, fractured ends of nanotubes can be seen. From the element maps of carbon and nickel, we can see the carbon nanotube is covered by nickel.

A high-resolution TEM image of a protrusion is shown infigure 39(B). About ten layers of graphene can clearly be seen in the lower portion of the protrusion. The upper portion of the covered crystal material is nickel. The carbon map indicated in figure 39(C) shows clearly that the carbon distribution coincided with the distribution of MWCNTs (figure 39(B)). Figure 39(D) is a nickel map, which indicates that nickel atoms are not present on the exposed MWCNTs portion (figure 39(B)). Therefore, an MWCNT was pulled out partially from the nickel matrix. However, figure 39(D) does show a gradually changed nickel distribution on a MWCNT, the 'sticky' nature of nickel bonded on CNTs. These are different from what was reported for polymer-based composites, as well as metallic composites fabricated with powder metallurgy sintering, where a clearly separated boundary between the CNTs and the matrix was identified. Since a MWCNT has multiple layers of graphene and the inter-layer bonding is weak (van der Waals force), it is possible that the exterior layer may separate from the inner layers if the

exterior layers bind well with the nickel matrix. However, this is not the case for Ni/SWCNT. As a result, Ni/MWCNT behaves with a relatively low strength compared to that of Ni/SWCNT but with greater strain at fracture, due to the inter-layer deformation-induced resilience.

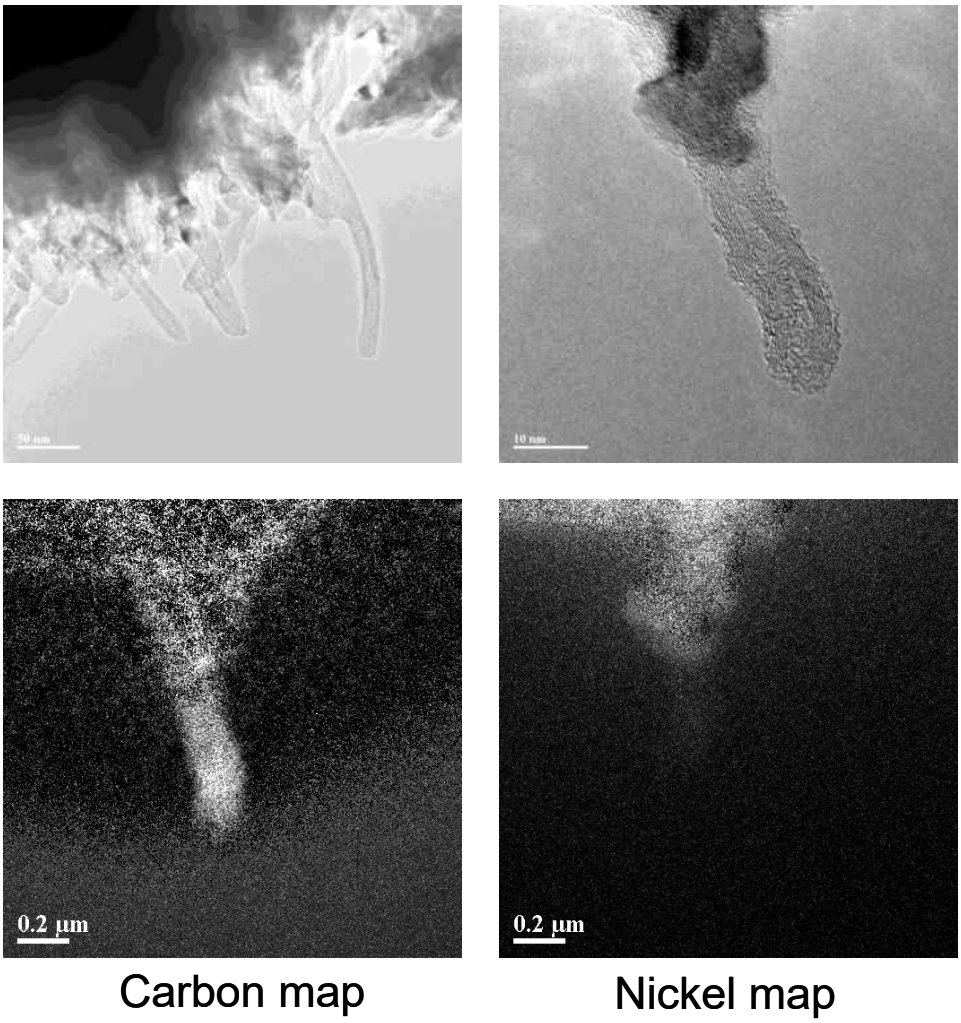

Figure 39. TEM images of the fracture surface of composite

5.3.1 Effect of Carbon Nanotube Concentration

A series of experiments have been done by adjusting the concentration of multi-walled carbon nanotube in the bath. The influence of CNT addition to Ni/CNTs nanocomposites was examined and the results are plotted in figure 40.

The concentration of nanotubes in the electrolyte bath is 30, 90, 150mg/L respectively. When the amount of carbon nanotubes is increased, the tensile stress of the composite increased at the same time. As the addition of CNTs in electrolyte increases, the resultant tensile strength is increased in a polynomial pattern. On the other hand, fracture strain versus CNT addition in the electrolyte behaves differently (Fig.40 B). This indicates that, for small CNT addition in electrolyte, the fracture strain decreases in comparison to that of pure nickel. When CNT addition is larger than 90mg/L, the fracture strain is similar or slightly greater than that of pure nickel. The average tensile stress is about 1,374 MPa when 150mg/L of nanotubes were added.

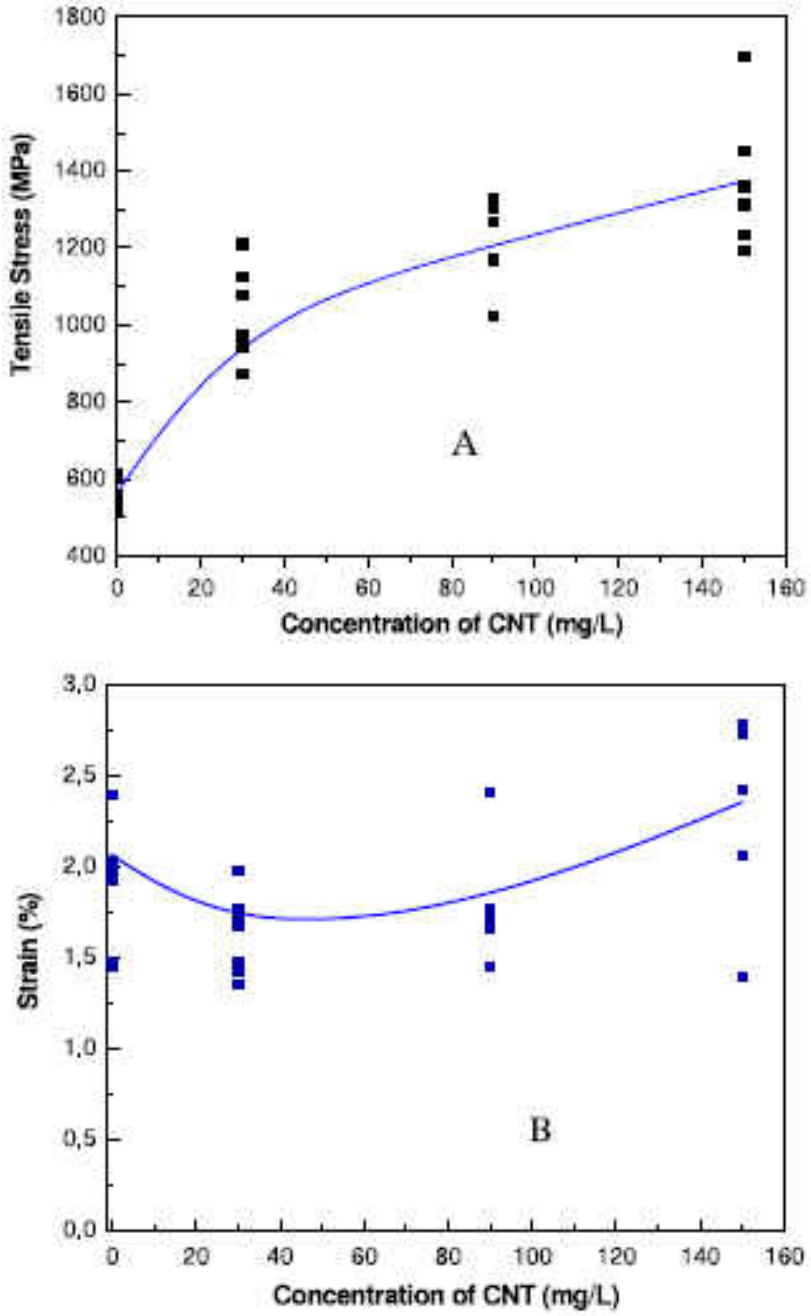

Figure 40. Experimental data of (A) tensile stress and (B) Fracture strain of composite vs. CNT addition

Various amounts of MWCNTs were also added into copper matrix using electro-chemical deposition and micro-tensile tests were conducted to determine the concentration influence on the copper/CNT nano-composites. The testing results were plotted in figure 41. It shows that as

the addition of the MWCNT in the electrolyte increases, the resultant tensile strength is increased in a polynomial pattern. This is due to the fact that more MWCNT added to the electrolyte would result in more trapped MWCNT in the deposited nano-composite. The more CNTs in the copper matrix, the greater the load bearing ability is.

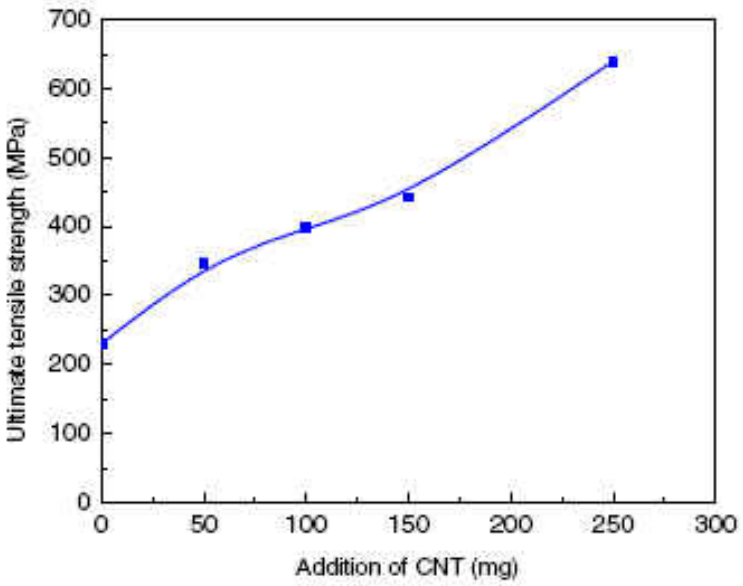

Figure 41. Tensile strength of the Cu/CNT nanocomposite versus CNT additions in a Cu electrolyte (mg/L)

5.3.2 Effect of Carbon Nanotube Dimension

According to Equation 13 derived in chapter 3, the dimension of nanotube is one of the main factors in determining the resultant mechanical strength of the nano-composites. Therefore, it is important to understand this issue. In this project, CNTs with different diameters were added into copper matrix to form CNT/Cu nanocomposites by electrochemical co-deposition.

Purified multi-walled carbon nanotubes were obtained commercially and CNTs with different diameters are shown as in Table 4. Figure 42 shows TEM images of MWCNTs that verify the

diameter range and the length. The surface morphology of these nanotubes shows some damages on the outmost layer but there are no obvious differences among them.

Table4. Different CNTs used in the experiments

	Outer Diameter	Length	Source
DWNT	1.5~3.0nm	~2 μm	Carbon Nanotechnologies Inc.
MWNT	<8nm	10~30 μm	Cheap Tubes Inc.
MWNT	8~15nm	10~50 μm	Cheap Tubes Inc.
MWNT	20~30nm	10~30 μm	Cheap Tubes Inc.
MWNT	30~50nm	10~20 μm	Cheap Tubes Inc.

The received Carbon nanotubes were treated with nitric acid first and then rinsed 3~5 times using de-ionized water. After this, carbon nanotubes will be dispersed in de-ionized water. Ultrasonic agitation (one hour) was used to break up potential nanotube aggregates. The dispersed CNT solutions were added into copper electrolyte (same electrolyte as shown in Table 2) and continue ultrasonic dispersion was applied again for one hour. During the ultrasonic bath, a great amount of heat will be produced which will increase the temperature of electrolyte. Higher temperature will aggravate the aggregation of carbon nanotubes. Ice will be put into the ultrasonic bath to cool down the electrolyte. Same amount (150mg/L) of different CNTs was added to the copper electrolyte for comparison purpose.

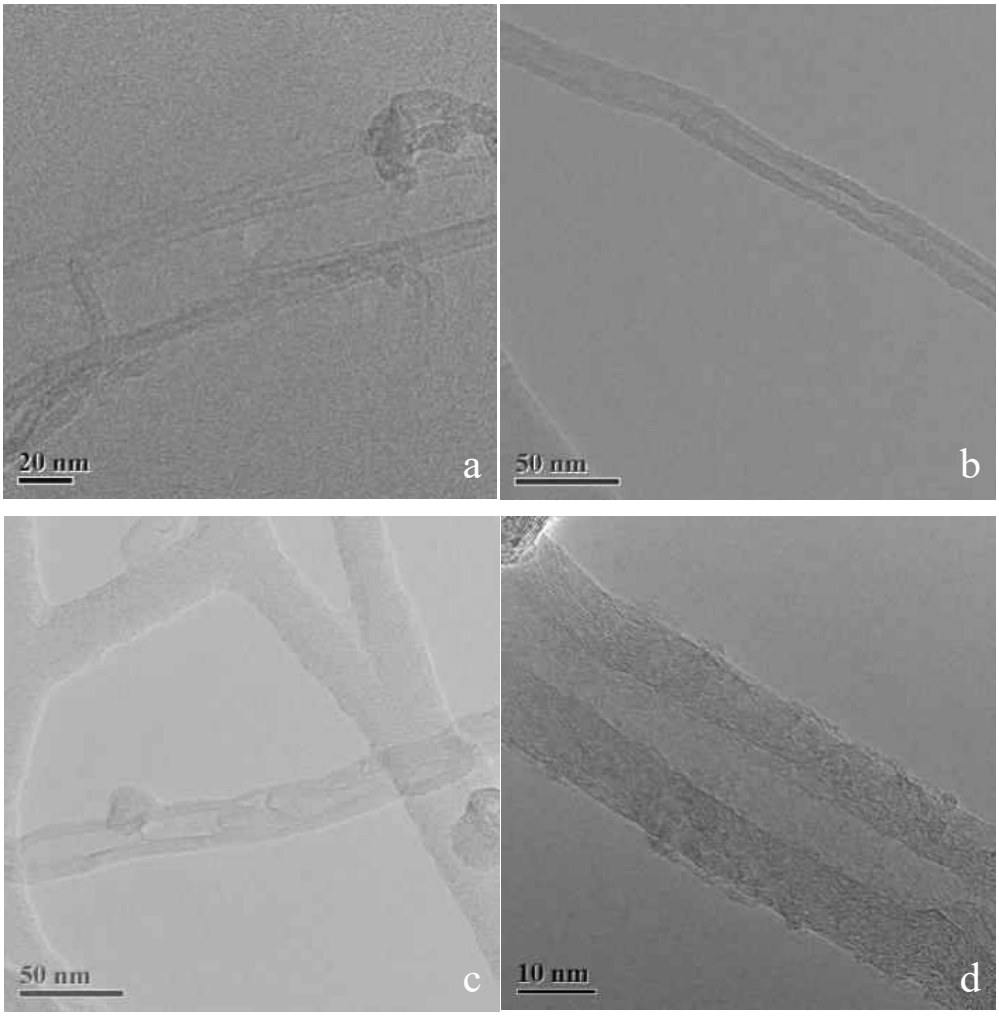

Figure 42. TEM results of MWNTs (a) CNT <8 nm, (b) CNT 8~15 nm, (c) CNT 20~30 nm and (d) CNT 30~50 nm

Pulse-reverse electrochemical deposition was carried out by using square pulse waveforms. A forward (deposition) time period of 5ms and a pulse of 1ms were used first, and then a reverse time of 1ms was applied for trimming purpose. A peak current density of 20mA/cm^2 was chosen for both forward and reverse waveform. For comparison purposes, both pure copper and CNT/Cu composite were deposited under the same condition.

Tensile test samples were prepared following the same procedure as described in previous section (4.2).

The thickness of the samples used in the present study was about 40 micrometers. The sample's actual thickness was determined by using scanning electron microscopy (SEM). Uniaxial tensile tests were performed on a MTS Tytron 250 Microforce Testing System and a force loading rate of 50mN/sec was used during the test. At least five samples of each group (pure Cu and Cu/CNT composites with different diameters) were tested. After test, both SEM (JOEL 6400F) and TEM were used to study the as deposited and the fractured surface morphology as well as texture of samples.

Figure 43 shows SEM images of surface morphologies of the as-deposited pure copper (Fig 43a) and Cu/CNTs composites (Fig 43b~Fig 43f). The surface morphology of the pure copper is smoother than that of the Cu/CNT composites fabricated with different diameters. For Cu/CNT composites, dispersed bulges can be seen on surfaces. It indicates that the addition of CNTs into copper introduces additional nucleation sites that cause the rougher surfaces. It shows also that when the outer diameter (OD) of carbon nanotubes increases the resultant surface roughness of Cu/CNT composites increases too.

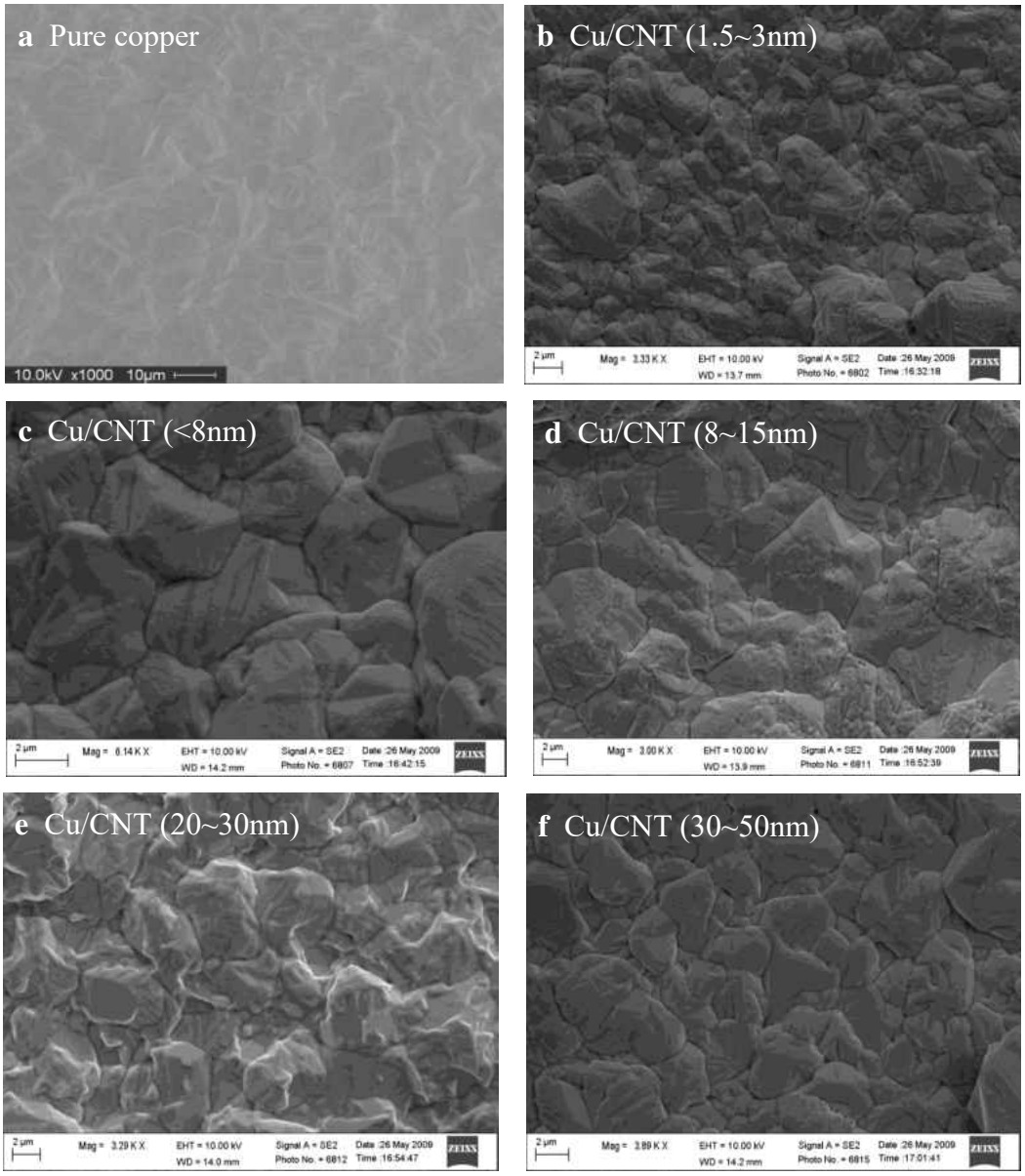

Figure 43. SEM images of the deposited pure copper (a) and Cu/CNT composite samples (after using alcohol to reveal grain boundaries) with different CNT diameters: (b) CNT 1.5~3 nm, (c)CNT <8 nm, (d)CNT 8~15 nm, (e) CNT 20~30 nm and (f) CNT 30~50 nm

Figure 44a shows typical results of tensile stress-strain responses of the fabricated pure Cu and Cu/CNT composites with different CNT diameters.

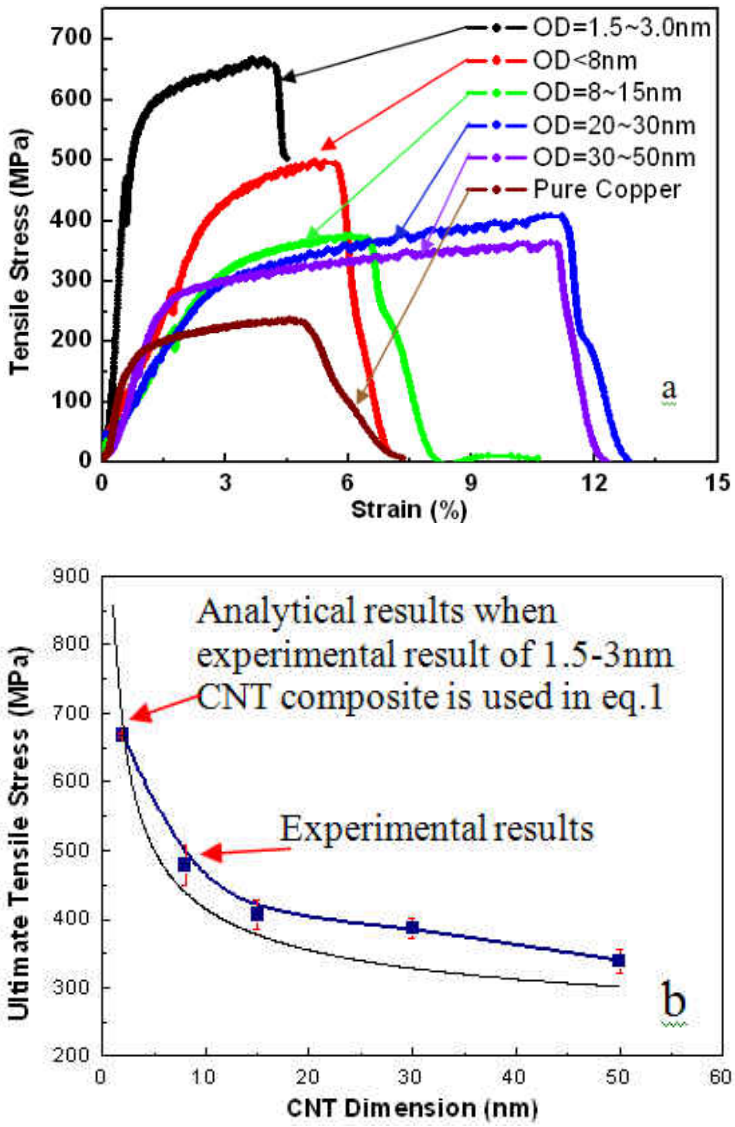

Figure 44. Tensile stress-strain curve of pure Cu and Cu/CNT composites with different diameters (a) and averaged tensile strengths versus CNT diameters of Cu/CNT composites (b)

The ultimate strength of pure copper is about 230MPa, which is the similar as published data[110]. When CNTs with diameter of 30nm-50nm was added to form Cu/CNT composite, the resultant tensile strength is increased to about 350MPa, or about 52% greater than that of pure copper in tensile strength. Under the same condition, if the same CNTs smaller diameters (20nm~30nm)

were used, the resultant tensile strength is increased to about 400MPa, or about 74% greater than that of pure copper. When CNT diameter of <8nm was used the resultant tensile strength is increased to about 500MPa, or about 117% higher than that of pure copper. Similarly, if Cu/CNT nanocomposites were fabricated with diameter of 1.5nm~3nm the resultant tensile strength is increased to about 670MPa (Cu/DWNT, Figure 44a). This value is about 191% greater than that of pure copper, or almost about three times of that of the pure copper fabricated under the same condition. These data show that the smaller the CNT diameters the greater tensile strength will be resulted (thicker line, Figure 44b). However, Cu/CNT composites with larger CNT diameters produce greater ductility than that of CNTs with smaller diameter (Figure 44).

In order to understand if other effects such as grain size and density are issues to the resultant strength, during this study following characterizations were made. First, alcohol was used as etchant to reveal grain boundaries on the composites' surfaces (Fig. 43). SEM results show that the grain size of all composites are similar, in a range of 2~5 microns. This makes sense since copper's grain size is dependent on the deposition condition including the electrolyte composition, the deposition temperature and the current density used for deposition. Since these conditions were all kept the same during the deposition of composites, the resultant grain size should be similar. For example, the grain size and of smallest CNT (1.5nm~3nm, Fig. 43b) used and the largest CNT (Fig. 43f) used are similar but the resultant strengths are about 2 times different. Therefore, effects of grain size on the resultant strength among all composites tested are considered negligible. As for the density effects, since a deliberated purse-reverse deposition waveform was developed to trim the front surface that as Figure 43 shows that the as deposited composites are dense. Therefore, no dependence of resultant strength on density can be identified.

SEM images of fractured morphologies are shown in Figure 34.

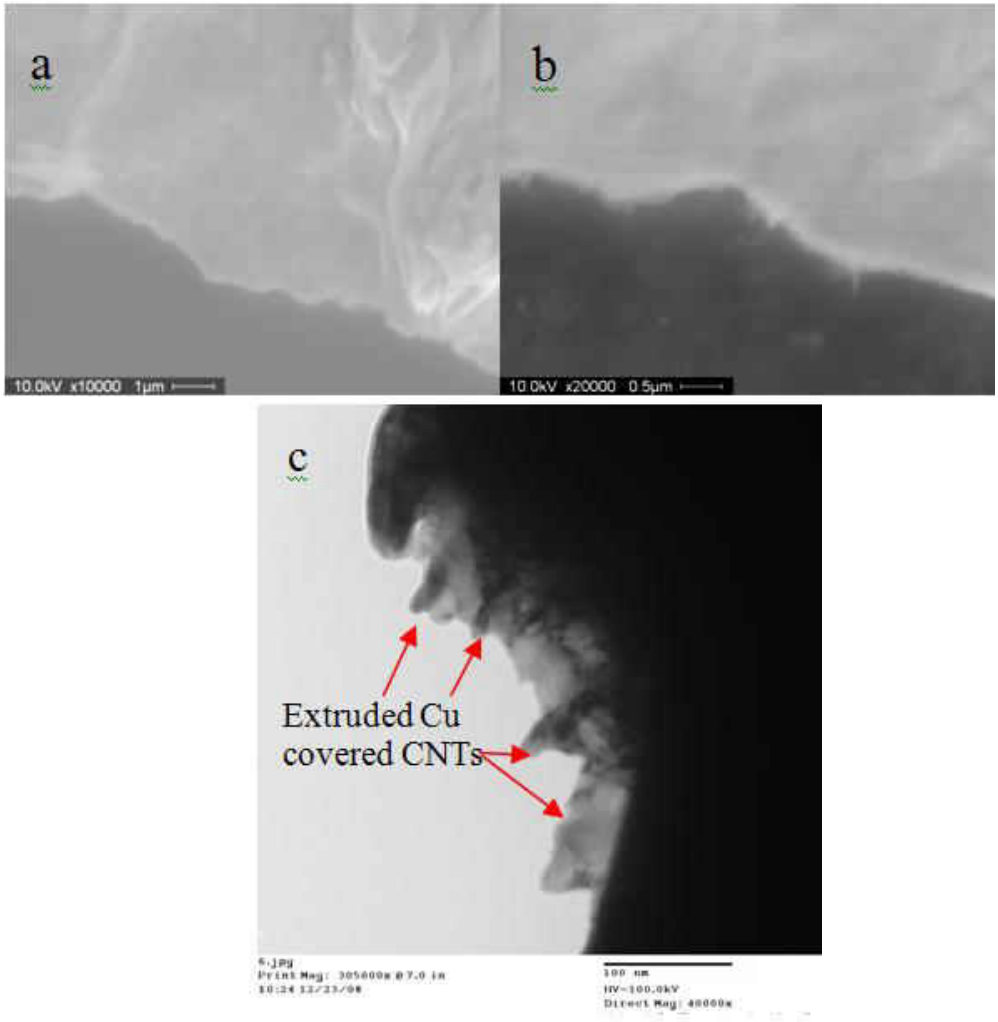

Figure 45. SEM images of fractured morphologies of pure copper (a) and Cu/CNT (20-30nm) composite (b). A TEM image of the fractured Cu/CNT (c) shows trapped CNTs in Cu matrix.

The image indicates that for pure copper (Fig. 45a), the fractured surface is relatively flat. However, the fractured surface of Cu/CNT composite (Fig. 45b) shows textured feature. A TEM image is shown in Fig. 45c that individual CNTs are clearly seen trapped in the copper matrix. Fig. 45c shows that CNTs are well dispersed and are still trapped in the Cu matrix after the

fracture test. No CNTs are pulled out from the Cu. Therefore, good interfacial bonding between CNTs and copper is formed.

$$\sigma^2 = \frac{A}{d_{CNT}} \text{ here } A \text{ is a constant.} \qquad (15)$$

Experimental results of tensile strength versus CNT diameters (thicker line, Fig. 44b) show a parabolic relationship. If we assume this parabolic relationship as denoted in eq.15, where σ is the tensile strength, d_{CNT} stands for CNT's diameter, and A is a constant that needs to be determined. If tensile strength data of Cu/CNT with diameter of 1.5nm~3nm is used in eq.15, the analytical results tensile strength of Cu/CNT composites versus CNT diameters as denoted in eq.15 can be plotted (thinner line, Fig. 44b). Fig. 44b indicates that the experimental results agree well (<5%) with the predications made by eq.15. The parabolic relationship between the resultant strength and CNT diameters can be attributed to the interfaces between CNT and the matrix. Smaller CNTs result in large total interfacial bonding areas if CNTs are well dispersed in the matrix. Analytical results have shown that the resultant tensile strength of CNT reinforced nano-composite has a parabolic relationship with the CNT diameter[111] that is similar as shown in the Fig. 44b.

5.4 Summary and Conclusions

Carbon nanotubes have been considered as ideal fillers to develop advanced nanocomposites with enhanced material properties resemble to that of CNTs. In our study, CNT was incorporated into metal (copper and nickel) matrix in order to get improvement on mechanical properties of resulting nanocomposites. An innovative electrochemical co-deposition method has been developed for fabricating uniform and dense CNT/metal nanocomposites. A test method that

combines a micro-fabrication process and a micro-force test frame has been developed for characterizing the mechanical strength of CNT/metal nanocomposites. Our promising results showed that in both copper and nickel matrix, the addition of a small amount of CNT (single walled or multi walled) can increase the ultimate tensile stress up to three times compared with that of pure metals. The good reinforcement of CNTs in metal matrices is attributed to the good interfacial bonding as well as to the stiffer nature of the matrices.

A theoretic equation had been derived to investigate several main parameters in determining the strength of carbon nanotube reinforced nanocomposites. According to the equation, the effect of nanotube concentration and dimension was investigated in detail using experimental results.

The strength of CNT/Cu and CNT/Ni nanocomposites are proportional to the CNT addition. When the addition of CNTs in electrolyte increases, the resultant tensile strength is increased as well.

Various CNTs have been tried so far. Experimental results of CNT/Cu and CNT Ni composites have both shown that the resultant tensile strength of nanocomposites is CNT diameter dependent. The smaller the CNT diameters the greater the resultant strengths of Cu/CNT composites will result. A parabolic relationship between CNT diameters and the resultant tensile strength has been established which has been verified by the experimental results. The largely increased strength is attributed to the good CNT dispersion in the electrolyte and the good CNT dispersion in Cu after deposition as well as to the good interfacial bonding formed by the electrochemical deposition process.

CHAPTER 6. STUDY THE BONDING BETWEEN CARBON NANOTUBES AND COPPER MATRIX USING ELECTRICAL PROPERTY

6.1 Introduction

Besides the amazing mechanical property of carbon nanotubes we discussed in the previous chapters, carbon nanotubes (CNTs) are excellent multifunctional materials in terms of electrical and thermal conductivity. Due to the perfect atomic arrangement and strong sp^{2-} bonding between the carbon atoms, CNTs have also demonstrated amazing thermal properties. The thermal conductivity (K) of a SWCNT at room temperature is predicted to be about 6,600 W/m-K[112] to 11,000 W/m-K[113]. The measured thermal conductivity at room temperature is about 7,000 W/m-K[114] for a SWCNT and about 3000 W/m-k for a MWCNT[115]. These thermal conductivity values are essentially higher than that of diamond, largely due to the large mean free path which is about 140 nm for SWCNT. Therefore, these remarkable thermal properties of carbon nanotubes make them excellent candidates for developing advanced materials for heat dissipation applications in high dense thermal generation devices.

Copper has received broad attention as an electrode material due to its high (second only to silver) electric conductivity at room temperature and abundant nature. Recently, the interconnecting material in integrated circuits (ICs) has shifted from aluminum to copper mainly due to its lower electric resistivity. However, the continuous down scaling of CMOS devices puts key challenges on interconnecting and packing materials. For example, the down scaling of supply voltage requires an accelerated shrink of the gate length in order to keep up with the demands for drive currents and speeds. The scaling of the gate length in turn results in an increase of the gate resistance thus novel low resistive metal gates is needed. Another result of

down scaling is the thickness reduction of the source/drain region that results in high series resistance. Since interconnects have replaced transistors as the dominant determiner of chip performance in last decade and the total interconnect length with active wiring excluding globe levels amounts up to more than 10,000m/cm^2 of an advanced chip, the continuous down scaling of CMOS (complementary metal-oxide semiconductor) device produces key challenges on interconnects and copper maybe no longer acceptable for future giga-scale interconnects. For example, for a 35 nm device, the RC (resistor-capacitor) response time of a 1 mm benchmark length of copper interconnect is about 100 times greater than that of the MOSFET's (metal–oxide–semiconductor field-effect transistor) switching delay time; and this difference will exceed 1,000 times greater for a 10 nm device. On the other hand, copper's resistance is enlarged when the dimension shrinks to less than the free electron's mean free path (about 40 nm at room temperature), due to the effects of surface scattering as well as grain boundary scattering. For example, the resistivity of copper's bulk material is about 1.7×10^{-6} ohm-cm at room temperature. However, the resistivity will be increased to between 2×10^{-6} ohm-cm to 3×10^{-6} ohm-cm for a film thickness of less than 45 nm. The enlarged resistivity and the longer response time as well as the increased density of the MOSFET on the chip will inevitably cause large energy consumption and heat dissipation will be a severe problem. Therefore, the International Technology Roadmap for Semiconductors (ITRS) has pointed out that, on the longer term, the key challenge for interconnects will be the limited conductivity of the present conductor material, copper. Unfortunately, there is no better material available (silver is the only other material with marginally better electric conductivity).

The resistance of metallic materials can be expressed as $R = R_l + R_i$, in which R_l stands for the lattice resistance and R_i is for the impurity induced resistance. Lattice resistance (R_l) depends

mainly on temperature and inter-atomic bonding. It will become zero when the temperature reaches absolute zero. On the other hand, the impurity induced resistance (R_i) is caused by impurity atom inclusions or defects formed within the crystal lattice. Since copper is one of the best electric conductive metals, it is not possible to achieve largely improved electric conductivity by alloying copper with other elements. For example, CuMo has a resistivity of $2.16x10^{-6}$ ohm-cm, which is larger than copper's ($1.72x10^{-6}$ ohm-cm at room temperature) since the addition of Mo atoms into copper behaves as inclusions and thus increases R_i.

The focus of increasing copper's conductivity is now shifted to how to reduce the resistivity from lattice scattering, or how to reduce phonon (lattice)-electron scattering under an electrical potential. Reducing the working temperature is not practical and is not applicable for room temperature applications. The question arises that if less scattered conduction tunnels can be established within the copper matrix, can electrons bypass through them thus undergoing less electron-lattice scattering?

Carbon nanotubes (CNTs), including single walled carbon nanotubes (SWCNTs) and multi-walled carbon nanotubes (MWCNTs), are tiny single atomic layered cylinders with diameters as small as 0.4nm to tens of nanometers. SWCNTs have proven either metallic or semiconductor (with small energy gap) type based on the charity. Armchair (n, n) nanotubes are metallic since they have a zero energy gap in axial directions. Those zigzag nanotubes (n, m) with n-m a multiple of 3 are tiny-gap semiconductors. Other SWCNTs are belonged to semiconductor type with an energy gap predicted to be Eg=0.9eV/d, where d is the diameter of the nanotube in nanometers[116]. The Fermi velocity of metallic carbon nanotube is about $8x10^5$m/s; this is comparable to copper's Fermi velocity ($15.7x10^5$m/s). The electrical conductance of SWCNT

has been proven a ballistic nature with a multiple of e^2/h, or $G=Ne^2/h$, where e is the electron charge and h is the Plank's constant and N is the number of conductional channel. It has demonstrated that N=4 has been found for short tubes[86, 117, 118, 119]. The resultant resistivity of carbon nanotube is in an order of 10^{-4} to 10^{-6} ohm-cm at room temperature, which is close to copper's resistivity ($1.7\text{x}10^{-6}$ohm-cm at room temperature). The mean free path of carbon nanotubes at room temperature is about 1μm to 30μm[120-121], which is much larger than copper's (about 40 nm at room temperature[122]). The large mean free path of carbon nanotube is attributed to its 1D character and phonon electron scattering is very small at room temperature, since the acoustic phonons have much less momentum than electrons at the Fermi energy. However, in a metal such as copper, electrons with large momentum is allowed to travel in 3D. Even though the phonon-electron scattering is small, the series small angled scattering eventually reverse the motion direction. That is the main reason of reducing the mean free path of copper at room temperature. This is not the case in carbon nanotubes, since only forward and backward motion is allowed in the axial direction. However, much large mean free path of carbon nanotube does not turn into greater electrical conductivity (worse than copper's).

From free electron gas theory, the electrical conductivity of metals is described as[123]:

$$\sigma = \frac{ne^2\tau}{m} \qquad (16)$$

where n is the electron density of state, τ is the mean free path related traveling time, m is the electron's mass.

From this equation it is clear that both large effective electron density and large mean free path are necessary to achieve high electrical conductivity. For metals such as copper have much

higher effective density of stats than that of carbon nanotubes. In order to increase carbon nanotube's density of states, efforts have been made on doping SWCNT. It has been proven that doping SWCNT can increase its electrical conductivity, since electron-donor reagents (K, Rb) transfer electrons to intinerant electron π^* states in the SWCNTs[124, 125]. However, the doped CNT's electrical conductivity is still not as good as copper's.

6.2 Object and Experimental Detail

Our object is to develop a novel approach that combines copper's high density of states together with carbon nanotubes' large mean free path nature to achieve electrical conductivity better than both carbon nanotube and copper at room temperature. Electrochemical deposition has been utilized to build connections between carbon nanotube and copper. In our study, different carbon nanotubes will be used similar as describe in our previous study.

Carbon nanotube was first purified with acid, and then rinsed and well dispersed with DI water. After that, the carbon nanotube solution will be mixed with copper electrolyte. The electrochemical deposition was carried out at room temperature. The advantages of electrochemical deposition of Cu/CNT, in comparing to other fabrication methods of metallic composite including power metallurgy are: 1) the deposition is at room temperature that there will be no diffusion between Cu and CNT. The diffusion occurred at elevated temperature (powder metallurgy, e.g.) may introduce additional phonon electron scattering that will increase the resistance of *Ri*. 2) There is no alloying reaction occurred between CNT and copper, thus the nature of copper and CNT is conserved; 3) Good electron transfer between copper and CNT is achieved, since the electrochemical deposition is a redox in which electrons transfer to copper ions through CNT (copper deposits on CNT surface).

The same copper electrolyte will be used here as described before (table 2, chapter 4). Carbon nanotubes were dispersed in the copper electrolyte. Ultrasonic stirring was employed to break up nanotubes aggregates. Uniform dispersed solutions were obtained after 2 hours of enforced dispersion. The solutions can keep for several hours without visible aggregation.

The electrochemical co-deposited Cu/SWCNT nanocomposites were characterized with SEM, TEM and Raman scattering spectra.

SEM results show that attention need to be paid to ensure the distribution and concentration of SWCNT buried within the copper matrix. Long SWCNTs are easily aggregated and thus form clusters.

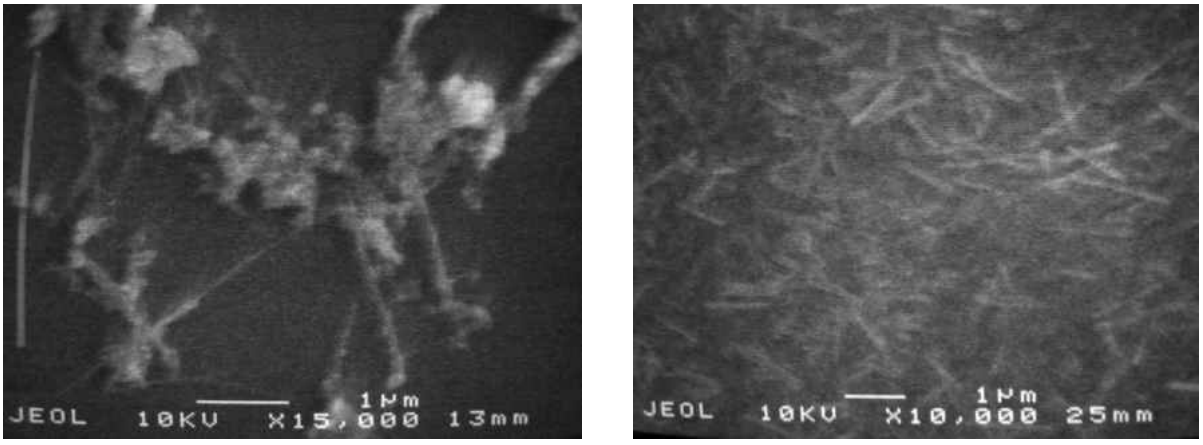

Figure 46. SEM picture of Cu/SWCNT where long SWCNT appears aggregated and form clusters. (b) shorter SWCNT forms uniform distribution within the copper matrix

The fabricated composite with long SWCNTs does not have the desired uniformity (Figure 46a). Uniform distribution of SWCNTs can be achieved if shorter SWCNT is used (Figure 46b). Therefore, the length of SWCNT is important in achieving the uniformity of the Cu/SWCNT composite.

6.3 Electrical Property Test and Discuss

Electrical resistivity was measured with Magnetron four points probe. Both electrochemical deposited pure copper and SWCNT/Cu composite were characterized under same conditions. Test results shown that the pure copper's electrical conductivity measured was $1.7x10^{-6}$ohm-cm, which is similar to the published data. However, the measured electrical resistivity on Cu/SWCNT was 1.0~1.2 $x10^{-6}$ohm-cm, which is about 40% less than pure copper. The Cu/SWCNT nanocomposites will have great potential for future interconnects and packaging due to its lower electrical resistivity.

The reason of such better electrical conductivity of Cu/SWCNT can be analyzed in the following. First, there is not much to do with the copper matrix, since pure copper fabricated under the same condition has similar electrical resistivity as bulk copper. On the other hand, copper does not alloy with carbon during the fabrication process and there is no diffusion of carbon atoms into copper matrix either since the fabrication was accomplished at room temperature. As the result, the influence on copper matrix from impurities during fabrication is negligible. Second, the Cu/SWCNT has the similar electron density as pure copper since the volume fraction of SWCNT is very small. From quantum mechanics point of view, the electron conductivity is proportional to the electron density and the mean free path. Based on electrical conductivity value, the equivalent mean free path is about 66nm, which is larger than pure copper's (about 40nm at room temperature). The enlarged mean free path implies that less lattice electron scattering existed in this material. Therefore, there should be some easy passes formed for electron transportation under electrical potential during resistivity measurement. There are two possible electrons easy passes: 1) along SWCNT sheet and 2) the interface between copper

and SWCNT. Since SWCNT has large mean free path (up to 30 um, comparing to copper's 40nm), electrons will experience less scattering along the carbon atomic sheet.

In order to identify if SWCNT sheet is important for the electric conductivity, a series research have been conducted on Cu/MWCNT fabricated with the similar fabrication condition to that of Cu/SWCNT.

6.3.1 Effect of Carbon Nanotube Dimension

Different type of carbon nanotube was used in our study to investigate the electron transportation in this nano-composite.

Carbon nanotube used here is similar as we used in previous study. (Shown in table 4)

Table5. Nanotube used to investigate the dimension effect

	Outer Diameter	Length	Source
SWNT	~1nm	500nm	Carbon Nanotechnologies Inc.
DWNT	1.5~3.0nm	~2 μm	Carbon Nanotechnologies Inc.
MWNT	<8nm	10~30 μm	Cheap Tubes Inc.
MWNT	8~15nm	10~50 μm	Cheap Tubes Inc.
MWNT	20~30nm	10~30 μm	Cheap Tubes Inc.
MWNT	30~50nm	10~20 μm	Cheap Tubes Inc.

For each type of carbon nanotubes, 150mg nanotube was purified, rinsed and then dispersed in 1000ml copper electrolyte. Electro-deposition process was carried under the same condition. In order to get smooth surface finishing, we use pulse-reverse current and the waveform setup was

same as in our previous study (chapter 4). The surface morphology and thickness of the samples were observed using SEM.

Figure 47 show the surface and thickness of DWCNT/Cu composite. Using the SEM picture, the thickness of the samples can be precisely measured.

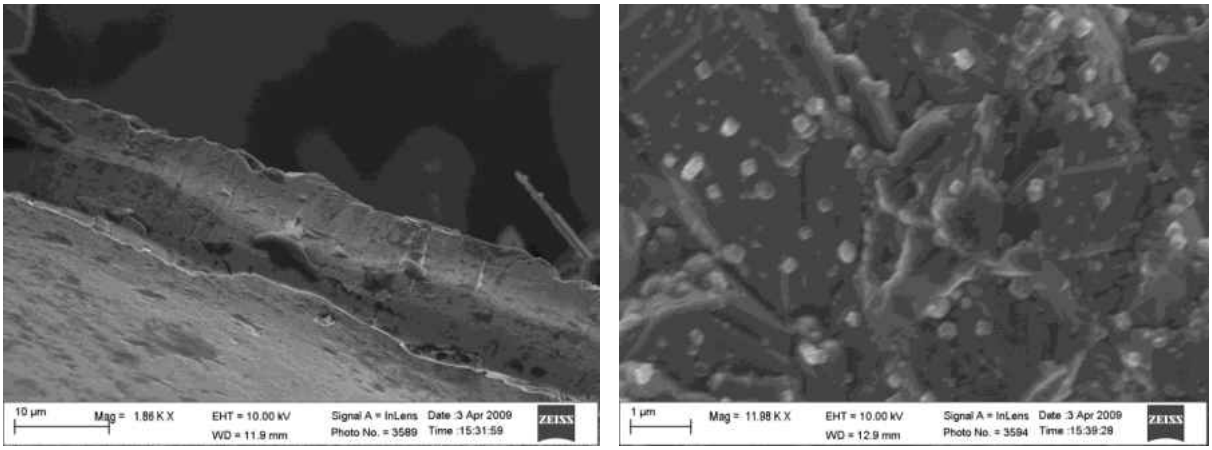

Figure 47. Surface and thickness of DWCNT/Cu composite

Electrical resistivity of the samples was tested using 4-point probe. For each type of carbon nanotubes, at least 5 samples are tested and the results are shown in table 6 and figure 48.

From the data in table 6, we can see that the data are very stable. Plotting these data into figure 48 and we can see the trend much more clearly. Under the same deposition condition, when the dimension of the carbon nanotube increased, the corresponding resistivity of composite increased too. For single-walled carbon nanotube with a diameter less than 1nm, the resistivity of the composite can be as low as less than 1×10^{-8} Ω-m. But by using the largest multi-walled carbon nanotube (OD=30~50nm), the resulting resistivity is around 1.7×10^{-8} Ω-m, which is similar to that of pure copper.

Table6. Testing results of CNT/Cu composite using 4-point probe

OD of CNT (nm)	Sheet Resistance (Ω)					Thickness (um)	Resistivity (Ω-m)
~1	0.001	0.0011	0.00114	0.00112	0.00118	9.24	1.016×10^{-8}
1.5~3	0.00094	0.00097	0.00098	0.00101	0.00099	11.5	1.124×10^{-8}
< 8	0.00123	0.00136	0.00119	0.00112	0.00118	9.23	1.1178×10^{-8}
8~15	0.00076	0.000786	0.000749	0.00075	0.000757	18.47	1.4079×10^{-8}
20~30	0.00144	0.00147	0.0015	0.00166	0.00177	9.24	1.4483×10^{-8}
30~50	0.00163	0.00162	0.00155	0.00166	0.00167	10.39	1.6902×10^{-8}

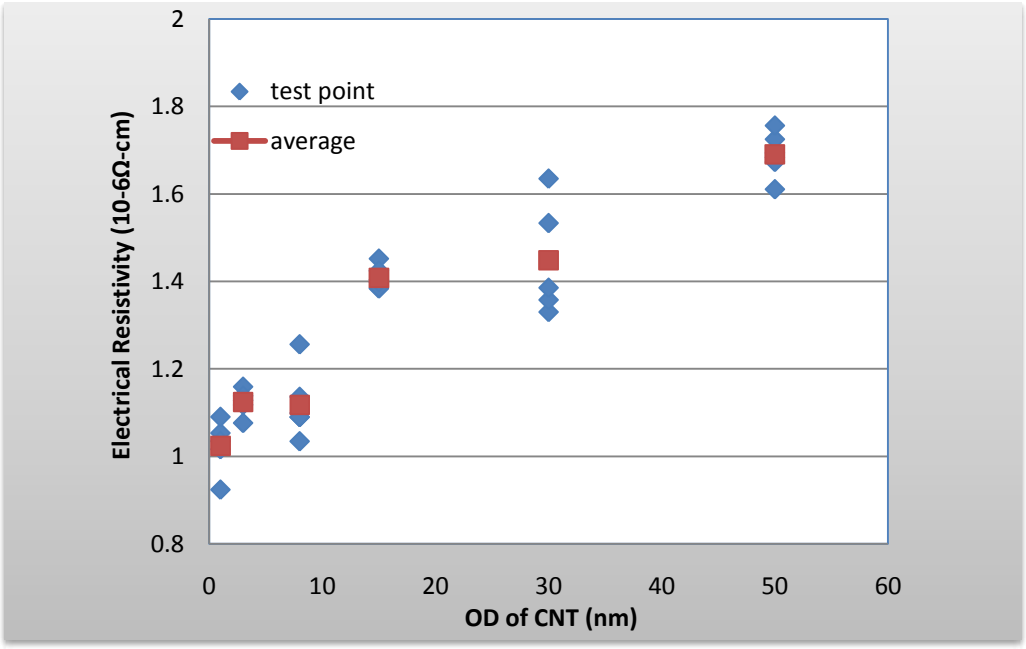

Figure 48. Electrical resistivity of CNT/Cu composite versus the dimension of CNT

Compare to MWCNT/Cu composites, the resistivity of Cu/SWCNT/Cu is much lower (1.0-1.2x10^{-6}ohm-cm). If all the carbon nanotube used were short and with opened end, electroplated copper would contact each layer of MWCNT. Therefore, electrons from copper would be able to

pass through each layer of grapheme sheet in MWCNT and the electrical resistivity of Cu/MWCNT should be at least similar to that of Cu/SWCNT.

In this case, there are three possible reasons. First, the multi-walled carbon nanotubes are much longer than single-walled carbon nanotubes. They will tangle together easily and consequently reduce the free pass of CNT. Second, the end caps of carbon nanotubes always exist. Third, it is the interface that owns copper's large electron density and SWCNT's large mean free path that causes the lower resistivity of the Cu/SWCNT. The interface is conductive since the electrochemical deposition of copper on SWCNT is a redox during which electron exchange is realized between SWCNT and copper deposited.

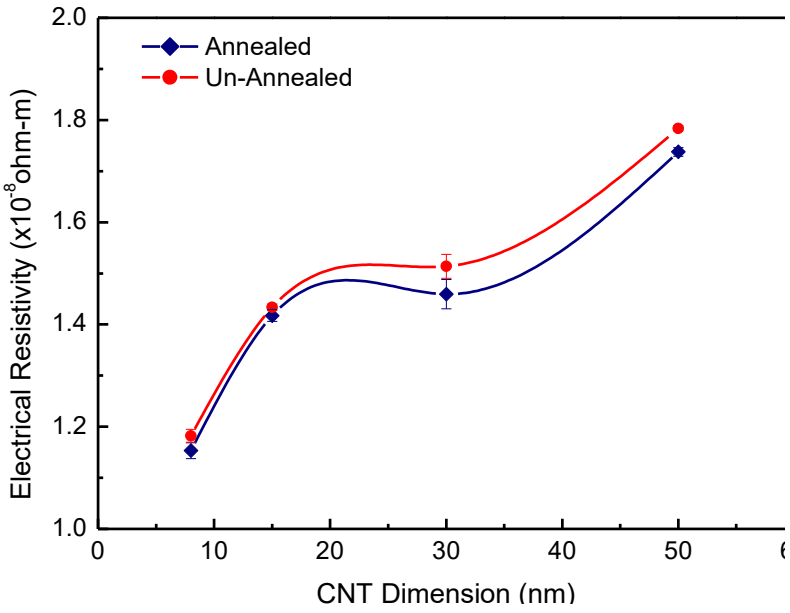

Figure 49. Effect of annealing process to composite's resistivity

Low temperature annealing process can help increase the interfacial bonding between carbon nanotube and copper matrix. Also annealing is a profitable process to release the residual stress created during electro-chemical co-deposition. The samples here are annealed at 600F under the

protection of hydrogen flow. Tube furnace was used. All samples showed a slightly decrease on their electrical resistivity. The result was shown in figure 49.

6.3.2 Effect of Carbon Nanotube Concentration

Besides dimension, the effect of carbon nanotubes' concentration was also been studied. MWCNT only was used in this study. The MWCNT used here has 5-10 layers of grapheme sheet. The measured electrical resistivity using the same four point probe is shown in Figure 41. When the 5 mg of MWCNT was added into 150 ml electrolyte, the resulted resistivity is decreased by a very small extent. When the addition of MWCNT was increased to 10 mg, the resistivity is reduced to 1.58×10^{-6} ohm-cm. As the addition of MWCNT increased to 20 mg, the electrical resistivity is reduced further to 1.4×10^{-6} ohm-cm. This is the similar amount that CNT was used in previous study (150mg/L). According to the above discussion, the more MWCNT added, the large portion of Cu and graphene interface formed, and the lower resistivity resulted (Figure 50).

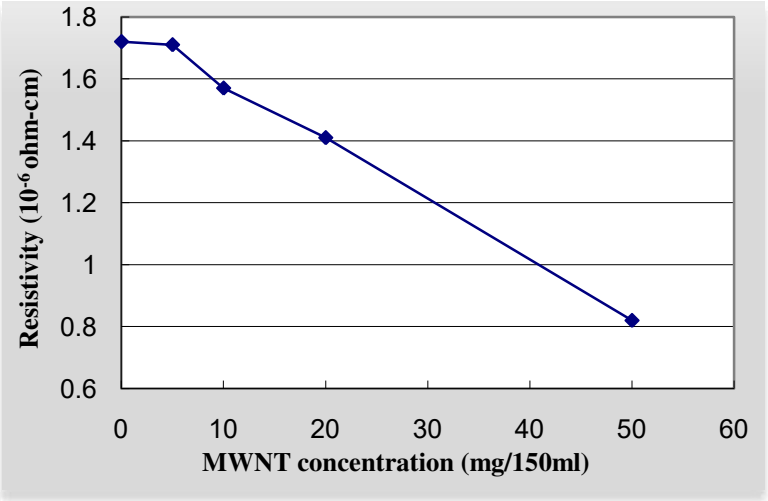

Figure 50. Resistivity versus carbon nanotube concentration

6.4 Theoretical analysis

Carbon nanotubes' multifunctional properties make it promising candidates as reinforcements to develop robust multifunctional nanocomposites. However, although extensive efforts have been made, especially on developing polymer matrices composites, the scientific community has still been suffered with reinforcement efficiency problems. The main reason has been attributed to the poor interfacial bonding between CNT and polymer matrix materials, in addition to other factors associated with polymer based matrices, such as the soft nature. On the other hand, metals are naturally more robust and multifunctional than polymer matrices, in terms of mechanical strength, electric and thermal conductivities, etc. In other word, metallic matrices may match better with CNT in forming CNT reinforced composites.

More important, although three electrons of a carbon atom in CNTs form three strong inplane sp^2 bonds, the fourth electron in the Pz orbit forms a weaker π bond (Fig. 51), which is responsible for the electrical conductivity of CNT as well as other graphene material such as graphite.

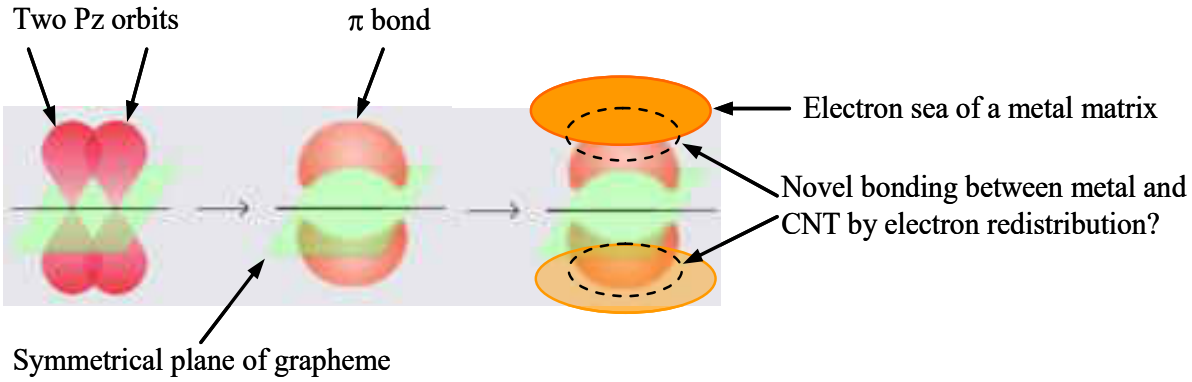

Figure 51. Sketch of bond in graphene and a conceptual sketch of bonding formed between CNT and a metal matrix

These electrons receive less restriction and it is possible for electrons to be redistributed. The interaction of electrons in π bond of CNT and metallic sea in metals may form an ad hoc metallic bonding between CNT and metal matrix via electron redistribution (Fig. 51). This theory agreed with the increase of electrical conductivity in carbon nanotube/copper composites as we got from previous electrical resistivity tests. In other words, CNT reinforced metal matrix composites can achieve better interfacial bonding between carbon nanotubes and matrix compared with polymer nanocomposites which was promising to form robust and multifunctional composites.

Raman scattering has proven to be an efficient method in characterizing carbon nanotubes[126-127] as well as CNT/polymer composites. The Raman scattering technique was used to characterize the Cu/SWCNT nanocomposites. Also, pure SWCNTs were prepared on a copper seed layer and underwent a Raman scattering analysis as well. Ethanol dispersed SWCNTs were dispensed on a copper-seed/silicon wafer and dried. The Raman scattering for both samples was done with LabRam made by Jobin Yuon. The laser excitation wave length used was 532 nm. Raman scattering spectra showed that a clear radial breathing mode (RBM) resonance peak existed at wave numbers between 150 to 212 cm^{-1} on the pure SWCNT wafer (Figure 52a). Contrastingly, the Raman spectra on the Cu/SWCNT's did not have a visible RBM peak (Fig. 53a) in the frequency tested. This is not the same results found in the SWCNT/polymer composite where a visible RBM peak had been identified at the similar frequency of pure SWCNT. It has been proven that a RBM peak happens in SWCNTs but not in MWCNTs. The reason for this is that the radial vibration is confined by adjacent carbon layers in MWCNT where the inter layer gap is only 0.34nm. The RBM peak did appear in the SWCNT/polymer composite since there is no such tight confinement on vibration in the radial direction due to the poor interfacial bonding and the soft nature of the matrix[128-129].

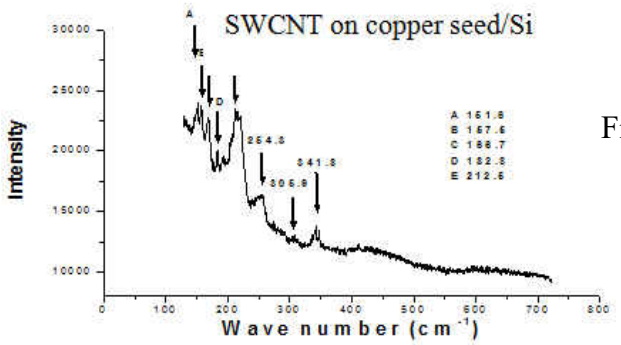

Fig. 52a

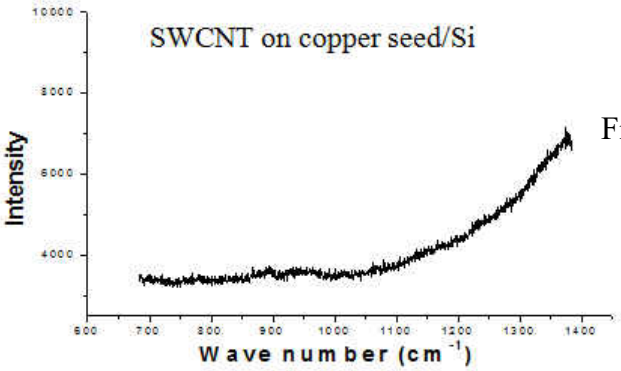

Fig. 52b

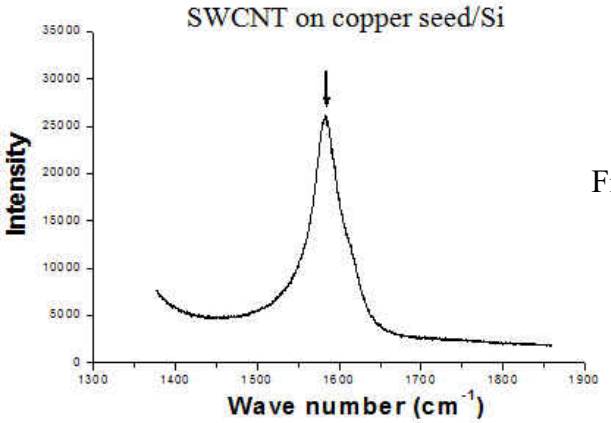

Fig. 52c

Figure 52. Raman scattering spectra of pure SWCNT coated on copper seed layer

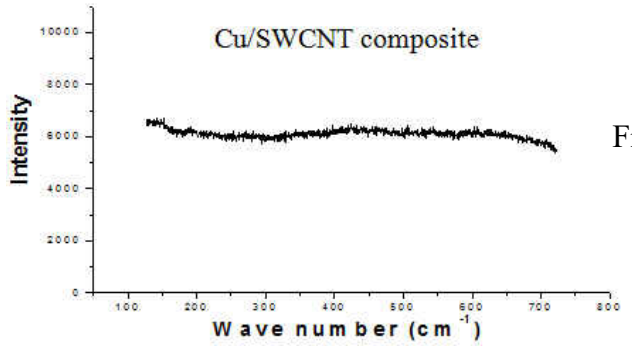

Fig. 53a

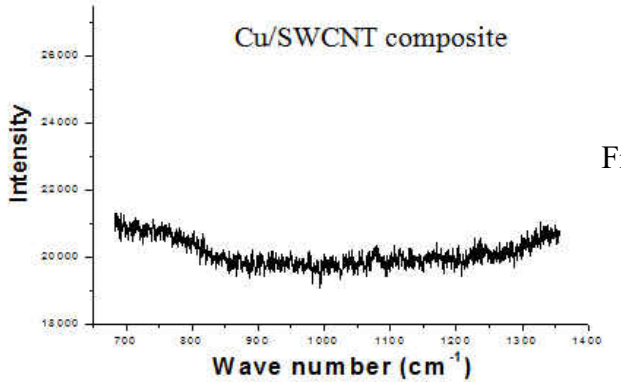

Fig. 53b

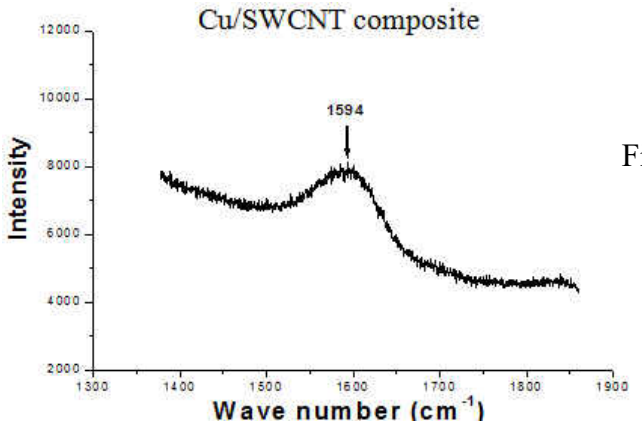

Fig. 53c

Figure 53. Raman scattering spectra of Cu/SWCNT nanocomposites. Disappeared RBM and shifted and widened G-band is clearly visible

Therefore, the disappearance of the RBM peak in the Cu/SWCNT nano-composite indicates that a strong interfacial bonding must have occurred, providing a tight confinement on vibration in the radial directions.

The tangential mode or G-band of the pure SWCNT spectra is clear and peaked at a wave number of 1578 cm^{-1} (Figure 52c). The G-band also appeared on the spectra from the Cu/SWCNT nanocomposites (Figure 53c). However, the peak of the G-band was shifted to 1684 cm^{-1} from 1578 cm^{-1} seen in the pure SWCNT spectra. Moreover, the G-band from the Cu/SWCNT nanocomposites was also widened (Fig. 53c).

It has been pointed out that doping SWCNTs increases their conductivity thus creating a more metallic nature characterized by the Raman spectra G-band peak being shifted and overall widening of the G-band[130]. The shifted and widened G-band on Cu/SWCNT spectra implies that the electrochemical co-deposited Cu/SWCNT nanocomposites should have enhanced energy transport properties, better than other composites made with CNTs. Raman spectra tested in the frequencies between the RBM and the G-band, on both pure SWCNTs (Fig. 52b) and Cu/SWCNTs (Fig. 53b), were similar.

6.5 Summary

Carbon nanotubes are excellent multifunctional materials in terms of mechanical, thermal and electrical conduction. These multifunctional properties plus the tiny size nature make CNTs ideal building block as reinforcement element in developing nanocomposites. Metallic materials such as copper are good matrix material in developing multifunctional composites since these materials have higher intrinsic conductivities.

Electrochemical co-deposition Cu/CNT composites has been proven in our study a better approach to achieve good interfacial bonding between SWCNT and copper matrix, thus lower resistivity has been achieved. The good interfacial bonding is realized by the electrochemical

deposition - a redox process in which electron exchange occurs between graphene and copper ions.

The good interfacial bonding has been proven by changed Raman scattering spectra in which RBM is disappeared and the G-band is shifted and widened. The increased electric conductivity is attributed to the facts that interface between Cu and graphene possesses copper's high electron density and SWCNT's large mean free path.

CHAPTER 7. CONCLUSION AND FUTURE WORK

7.1 Summary and Conclusions

Carbon nanotubes (CNTs), including single walled CNT (SWCNT) and multi-walled CNT (MWCNT), are fibers with diameters ranging from 1 nm to about 100 nm and a large aspect ratio (>1,000). CNTs have been regarded as the stiffest and strongest material ever developed, mainly owing to their perfect atomic arrangement and intrinsic strong in-plane sp^2—sp^2 covalent bonds between carbon atoms. For example, the Young's modulus is about 1.0~1.8Tpa and the ultimate tensile strength is about 30 to 200 GPa, together with an elongation at break of about 10-30%. In addition, CNTs are chemically stable and have remarkable properties in electrical and thermal conduction. All these attributes make CNTs ideal candidates as reinforcement fillers in the development of advanced nanocomposites. So far various efforts have been made to develop nanotube/nanofiber reinforced composites with different matrices.

In our study, carbon nanotubes (both SWNTs and MWNTs) are added into copper and nickel matrices using pulse-reverse electro-chemical co-deposition method. Because of the "atomic level" mixing in the electrolyte, relatively uniform composites have been achieved. Uniaxial tensile test results showed that the ultimate tensile strength of Ni/CNTs composites reach as high as 1997 MPa in Ni/SWNT. This value is 3 times larger than that of pure nickel. Similar results were obtained from Ni/MWNT and copper/CNT composites.

In order to better understand this improvement of mechanical strength in carbon nanotube composite, a theoretical equation was developed to describe the relationship between the mechanical properties of the composites and several parameters.

The dimension of carbon nanotubes is a very important parameter in determining the resultant strength of composites. Therefore, it is important to understand issues regarding the effect of CNT diameter on the resultant strength of composites. CNTs with different diameters were added into a copper matrix to form CNT/Cu nanocomposites using an electrochemical co-deposition method. Resultant tensile strength was measured which shows a good relationship between CNT diameter and the resultant strength.

Besides the amazing mechanical properties, carbon nanotubes are excellent multifunctional materials in terms of electrical and thermal conductivity. The electrical resistivity of carbon nanotube/copper composites were also studied in this project. Both electrochemically deposited pure copper and SWCNT/Cu composite were characterized under the same conditions. Test results show that the electrical conductivity of pure copper was measured at $1.7x10^{-6}$ohm-cm, which is similar to the published data. However, the measured electrical resistivity on Cu/SWCNT was 1.0~1.2 $x10^{-6}$ohm-cm, which is about 40% less than pure copper. This improvement showed that the good interfacial bonding provided a better electron transportation pass. Raman scattering spectra also indicates that a strong interfacial bond must have occurred in the Cu/SWCNT nano-composite.

Particle size is a very important parameter in determining the properties of metals and composites, especially mechanical properties. In our project, nano-crystallized copper was produced using electro-chemical co-deposition. Samples showed increased tensile strength according to the decrease of particle size. When the particle size of copper samples was reduced to about 100 nm, their tensile strength increased to ~500MPa. This value is more than two times larger than that of coarse grain pure copper samples (~230MPa).

7.2 Future Work

Recent studies have already shown that nanocrystalline copper possesses better mechanical properties than ordinary coarse grain copper. In order to further improve the mechanical properties of this material, we are trying to reduce the particle size of the copper sample and add carbon nanotubes (both single-walled and multi-walled) into the copper matrix. From our preliminary results, the crystal size has been reduced to around 100 nm and the tensile strength of pure copper had been increased to near 500 MPa.

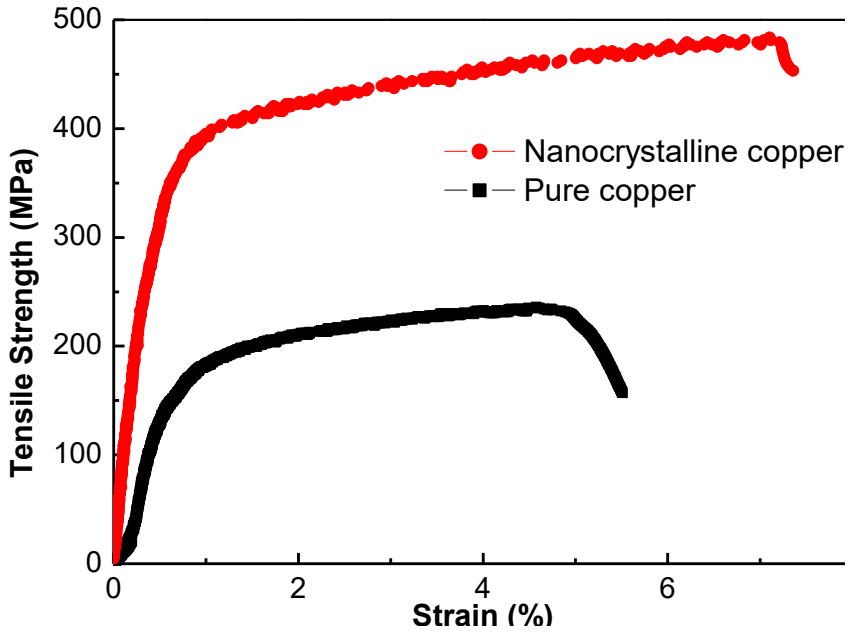

Figure 54. Tensile strength of nanocrystalline copper with grain size less than 100nm. As comparison, strength of normal coarse grain pure copper was also drawn

So far, carbon nanotube behavior in this new electroplating system has not been clearly investigated. The presence of complex former complicated the status of carbon nanotubes. Further investigations are necessary.

Twin boundary is a special kind of micro-structure which can block the motion of dislocation, and in the mean time, minimize the scattering of conducting electrons. This characteristic can benefit both mechanical and electrical properties of pure copper. Our studies also show that the addition of carbon nanotubes in copper metal could increase the mechanical strength, and in the mean time, decrease the electrical resistivity of copper. Combining these two options is the goal of our future research.

LIST OF REFERENCES

[1] S. Iijima. Helical microtubules of graphite carbon. Nature 1991; 354: 56-58

[2] A. V. Desai, and M. A. Haque. Mechanics of the interface for carbon nanotube-polymer composites, Thin-Walled Structures 2005; 43: 1787-1803

[3] K-T Lau, and D Hui. The revolutionary creation of new advanced materials-carbon nanotube composite. Compos Part B Eng 2002; 33; 263-77

[4] D. Qian, G. J. Wagner, W. K. Liu, M-F Yu, and R. S. Ruoff. Mechanics of carbon nanotubes. Appl Mech Rev 2002; 55: 495-532.

[5] H. Dai. Carbon nanotubes: opportunities and challenges. Surface Science 2002; 500: 218-41.

[6] C. A. Cooper, D. Ravich, D. Lips, J. Mayer, and H. D. Wagner. Distribution and alignment of carbon nanotubes and nanofibers in a polymer matrix, Composites Science and Technology, 2002; 330: 1105-12.

[7] A. Allaoui, et al. Mechanical and electrical properties of a MWNT/epoxy composite, Composites Science and Technology, 2002; 62: 1993-98.

[8] K-T. Lau, et al., Composites Science and Technology, 2003; 63: 1161-64.

[9] X. T. Wang, N. P. Padture, and H. Tanaka. Contact-damage-resistant ceramic/single-wall carbon nanotubes and ceramic/graphite composites. Nature Materials, 2004; 3: 539-44.

[10] G. D. Zhan, J. D. Kuntz, J. Wan, and A. K. Mukherjee. Single-Wall carbon nanotubes as attractive toughening agents in alumina-based nanocomposites. Nature Materials, 2002; 2; 38-42

[11] A. Esawi and K. Morsi, Composites, Part A, Applied science and manufacturing, 38A (2006), 646-650

[12] Z. Bian, R. J. Wang, H. Wei, T. Zhang and A. Inoue, Advanced functional materials, 14 (2004), 55-63

[13] Thostenson, E. T., Z. Ren, et al. (2001). "Advances in the science and technology of carbon nanotubes and their composites: a review." Composites Science and Technology **61**(13): 1899-1912.

[14] Harris, P. J. F. (2004). "carbon nanotube composites." International materials Reviews **49**(1): 31-43.

[15] Nardelli M.B., Yakobson B.I., Bernholc J., Brittle and ductile behavior in carbon nanotubes. Physical review letters 1998; 81(21):4656-9.

[16] Thostenson, E. T., Z. Ren, et al. (2001). "Advances in the science and technology of carbon nanotubes and their composites: a review." Composites Science and Technology **61**(13): 1899-1912.

[17] M. F. Yu, O. Lourie, M. J. Dyer, K. Moloni, T. F. Kelly and R. S. Ruoff: Science, 2000, 287, 637-640

[18] E. W. Wong, P. E. Sheehan and C. M. Lieber: Science, 1997, 277, 1971-1975

[19] Collins PG, Avouris P., Nanotubes for electronics. Scientific American 2000; 283 (6):62-9

[20] W. Zhang, Z. Zhu, F. Wang, T. Wang, L. Sun and Z. Wang, Nanotechnology, 15 (2004), 936-939

[21] M. Osman and D. Srivastava, Nanotechnology, 12 (2001), 21-24

[22] S. Berber, Y. K. Kwon and D. Tomanek, Physical Review Letters, 84 (2000): 4613

[23] J. Hone, M. Whitney, C. Piskoti and A. Zettl, Physical Review Letters, 59 (1999): 2514

[24] W. Wei, Y. Liu, Y.Wei, K. Jiang, L. Peng and S. Fan, *Nano Lett.,* **7** (1), 64 -68, 2007.

[25] Ji-Eun Kim, June-Ki Park and Chang-Soo Han, *Nanotechnology,* **17** (2006) 2937-2941

[26] Xiaobo Fu, Hao Yu, Feng Peng, Hongjuan Wang and Yu Qian, Applied Catalysis A: General, 321(2007):190-197

[27] Eunjoo Yoo, Taichi Habe and Junji Nakamura, Science and Technology of Advanced Materials 6 (2005): 615-619

[28] M. S. P. Shaffer, X. Fan and A. H. Windle: Carbon, 1998, 36, 1603-1612

[29] M. S. P. Shaffer and A. H. Windle: Adv. Mater., 1999, 11, 937-941

[30] M. Cadek, J. N. Coleman, V. Barron, K. Hedicke and W. J. Blau: Appl. Phys. Lett., 2002, 81, 5123-5125.

[31] D. E. Hill, Y. Lin, A. M. Rao, L. F. Allard and Y. P. Sun: Macromolecules, 2002, 35, 9466-9471

[32] D. Qian, E. C. Dickey, R. Andrews and T. Rantell: Appl. Phys. Lett., 2000, 76, 2868-2870

[33] Liao, Kin and Li, Sean, Applied Physics Letters, 79 (2001): 4225-4227

[34] H. Xia, Q. Wang, K. Li and G. Hu, Journal of Applied Polymer Science, 93(2004): 378-386.

[35] R. Andrews, D. Jacques, D. Qian and T. Rantell: Acc. Chem. Res., 2002, 35, 1008-1017

[36] R. Haggenmueller, H. H. Gommans, A. G. Rinzle, J. E. Fischer and K. I. Winey: Chem. Phys. Lett., 2000, 330, 219-225

[37] M. Sennett, E. Welsh, J. B. Wright, W. Z. Li, J. G. Wen and Z. F. Ren: Appl. Phys. A, 2003, 76, 111-113

[38] L. S. Schadler, S. C. Giannaris and P. M. Ajayan: Appl. Phys. Lett., 1998, 73, 3842-3844.

[39] X. Xu, M. M. Thwe, C. Shearwood and K. Liao: Appl. Phys. Lett., 2002, 81, 2833-2835

[40] M. J. Biercuk, M. C. Llaguno, M. Radosavljevic, J. K. Hyun, A. T. Johnson and J. E. Fischer: Appl. Phys. Lett., 2002, 80, 2767-2769

[41] M. Cochet, W. K. Maser, A. M. Benito, M. A. Callejas, M. T. Martinez, J. M. Benoit, J. Schreiber and O. Chauvet: Chem. Commun., 2001, 1450-1451

[42] M. S. P. Shaffer and K. Koziol: Chem. Commun., 2002, 2074-2075

[43] C. Park, Z. Ounaies, K. A. Watson, R. E. Crooks, J. Smith, S. E. Lowther, J. W. Connell, E. J. Siochi, J. S. Harrison and T. L. St Clair: Chem. Phys. Lett., 2002, 364, 303-308

[44] K. Jurewicz, S. Delpeux, V. Bertagna, F. Beguin and E. Frackowiak: Chem. Phys. Lett., 2001, 347, 36-40

[45] M. Hughes, G. Z. Chen, M. S. P. Shaffer, D. J. Fray and A. H. Windle: Chem. Mater., 2002, 14, 1610-1613

[46] Harris, P. J. F. (2004). "carbon nanotube composites." International materials Reviews **49**(1): 31-43.

[47] Vigolo B, Penicaud A, Coulon C, Sauder C, Pailler R, Journet C et al. Macroscopic fibers and ribbons of oriented carbon nanotubes. Science 2000, 290, 1331-1334

[48] R. Z. Ma, J. Wu, B. Q. Wei, J. Liang and D. H. Wu: J. Mater. Sci., 1998, 33, 5243-5246

[49] A. Peigney, E. Flahaut, C. Laurent, F. Chastel and A. Rousset : Chem. Phys. Lett., 2002, 352, 20-25

[50] G. D. Zhan, J. D. Kuntz, J. E. Garay and A. K. Mukherjee: Appl. Phys. Lett., 2003, 83, 1228-1230

[51] T. Seeger, G. De La Fuente, W. K. Maser, A. M. Benito, M. A. Callejas and M. T. Martinez : Nanotechnology, 2003, 14, 184-187

[52] P. Vincent, A. Brioude, C. Journet, S. Rabaste, S. T. Purcell, J. Le Brusq and J. C. Plenet : J. Non-Cryst. Sol., 2002, 311, 130-137

[53] J. S. Sakamoto and B. Dunn: J. Electrochem. Soc., 2002, 149, A26-A30

[54] George, R., K. T. Kashyap, et al. (2005). "Strengthening in carbon nanotube/aluminium (CNT/Al) composites." Scripta Materialia **53**(10): 1159-1163.

[55] Kuzumaki, T., K. Miyazawa, et al. (1998). "Processing of carbon nanotube reinforced aluminum composite." Journal of Materials Research **13**(9): 2445-2449.

[56] T. Kuzumaki, O. Ujiie, H. Ichinose and K. Ito: Adv. Eng. Mater., 2000, 2, 416-418

[57] Seung I. Cha, Kyung T Kim, et al. (2005). "Extraordinary Strengthening Effect of Carbon Nanotubes in Metal-Matrix Nanocomposites Processed by Molecular-Level Mixing." Advanced Materials **17**(11): 1377-1381.

[58] Laha, T., A. Agarwal, et al. (2004). "Synthesis and characterization of plasma spray formed carbon nanotube reinforced aluminum composite." Materials Science and Engineering A **381**(1-2): 249-258.

[59] W. X. Chen, J. P. Tu, L. Y. Wang, H. Y. Gan, Z. D. Xu and X. B. Zhang: Carbon, 2003, 41, 215-222

[60] Li, Z. H., X. Q. Wang, et al. (2006). "Preparation and tribological properties of the carbon nanotubes-Ni-P composite coating." Tribology International **39**(9): 953-957.

[61] Curtin, W. A. and B. W. Sheldon (2004). "CNT-reinforced ceramics and metals." Materials Today **7**(11): 44-49.

[62] Xu, C., G. Wu, et al. (2004). "Preparation of copper nanoparticles on carbon nanotubes by electroless plating method." Materials Research Bulletin **39**(10): 1499-1505.

[63] Lee, K. Y., M. Kim, et al. (2007). "Fabrication of metal nanoparticles-carbon nanotubes composite materials in solution." Chemical Physics Letters **440**(4-6): 249-252.

[64] Hu, X., T. Wang, et al. (2007). "A General Route to Prepare One- and Three-Dimensional Carbon Nanotube/Metal Nanoparticle Composite Nanostructures." Langmuir **23**(11): 6352-6357.

[65] Tan, J., T. Yu, et al. (2006). "Microstructure and wear resistance of nickel–carbon nanotube composite coating from brush plating technique." Tribology Letters **21**(2): 107-111.

[66] Mo, C. B., S. I. Cha, et al. (2005). "Fabrication of carbon nanotube reinforced alumina matrix nanocomposite by sol-gel process." Materials Science and Engineering A **395**(1-2): 124-128.

[67] Chen, X. H., F. Q. Cheng, et al. (2002). "Electrodeposited nickel composites containing carbon nanotubes." Surface and Coatings Technology **155**(2-3): 274-278.

[68] Y. Cho, G. Choi and D. Kim, Electrochem. (2006) Solid-State Lett., 9 (3): G107-G110

[69] S. Arai and M. Endo, Carbon nanofiber-copper composite powder prepared by electrodeposition. Electrochem. Commun., 2003, 5, 797-799

[70] Arai, S., M. Endo, et al. (2004). "Ni-deposited multi-walled carbon nanotubes by electrodeposition." Carbon **42**(3): 641-644.

[71] Shi, L., C. F. Sun, et al. (2006). "Electrodeposition and characterization of Ni-Co-carbon nanotubes composite coatings." Surface and Coatings Technology **200**(16-17): 4870-4875.

[72] M. M. J. Treacy, T. W. Ebbesen, and J. M. Gibson. Exceptionally high young's modulus observed for individual carbon nanotubes. Nature 1996; 381: 678.

[73] J-P. Salvetat-Delmotte, and A. Rubio. Mechanical properties of carbon nanotubes: a fiber digests for beginners. Carbon 2002; 40: 1729-34.

[74] P. Poncharal, Z. L. Wang, D. Ugarte, and W. A. De. Electrostatic deflections and lectromechanical resonances of carbon nanotubes. Science 1999; 283: 1513-6

[75] K.K. Chawla, Composite Materials – Science and Engineering, Springer 1998

[76] V. C. Moore, M. S. Strano, E. H. Haroz, R. H. Hauge, R. E. Smalley, J. Schmidt, and Y. Talmon, Nano Lett. 3, 1379 (2003).

[77] D. Tasis, N. Tagmatarchis, A. Bianco, and M. Prato, Chem. Rev. 106, 1105 (2006).

[78] Regev O, ElKati PNB, Loos J, Koning CE. Adv. Mater. (2004) 16:248–51.

[79] Liu J, Casavant MJ, Cox M, Walters DA, Boul P, Lu W, et al., Chem. Phys. Lett. (1999) 303:125–9.

[80] Grossiord N, Loos J, Meuldijk J, Regev O, Miltner HE, van Mele B, et al., Comp Sci Technol in press.

[81] Izard N, Riehl D, Anglaret E. Phys. Rev. B (2005) 71:195417-1–7.

[82] Vigolo B, Pe′nicaud A, Coulon C, Sauder C, Pailler R, Journet C,et al., Science (2000), 290, 1331–4.

[83] Grossiord N, Regev O, Loos J, Meuldijk J, Koning CE. Timedependent, Anal. Chem. (2005), 77,5135–9.

[84] J. Yu, N. Grossiord, C. E. Koning and J. Loos, Carbon 45 (2007) 618-623

[85] Thess A, Lee R, Nikolaev P, Dai H, Petit P, Robert J, et al. Science (1996) 273:483–7.

[86] Girifalco LA, Hodak M, Lee RS. Phys Rev B (2000) 62:13104–10.

[87] Jiang LQ, Gao L, Sun J. J Colloid Interface Sci (2003) 260:89–94.

[88] Guan LH, Shi ZJ, Gu ZN. Carbon (2005);43:1101–3

[89] Sabba Y, Thomas EL. Macromolecules (2004) 37:4815–20.

[90] Xiao KQ, Zhang LC. J Mater Sci (2005) 40:6513–6.

[91] Safadi B, Andrews R, Grulke EA. J. Appl. Polym. Sci. (2002) 84:2660–9.

[92] Islam MF, Rojas E, Bergey DM, Johnson AT, Yodh AG. Nano Lett. (2003) 3:269–73.

[93] O'Connell MJ, Bachilo SM, Huffman CB, Moore VC, Strano MS, Haroz EH, et al. Science (2002) 297:593–6.

[94] Strano MS, Moore VC, Miller MK, Allen MJ, Haroz EH, Kittrell C, et al. J. Nanosci. Nanotechnol. (2003) 3:81–6.

[95] H. Kuzmany, A. Kukovecz, F. Simon, M. Holzweber, Ch. Kramberger and T. Pichler, Functionalization of carbon nanotubes, Synth Metals **141** (2004) (1–2), 113–122.

[96] Z.H. Yu and L.E. Brus, Reversible oxidation effect in Raman scattering from metallic single-wall carbon nanotubes, J Phys Chem **A104** (2000), 10995–10999

[97] A. Kuznetsova, I. Popova, J.T. Yates, M.J. Bronikowski, C.B. Huffman and J. Liu et al., Oxygen-containing functional groups on single-wall carbon nanotubes: NEXAFS and vibrational spectroscopic studies, J Am Chem Soc **123** (2001), 10699–10704

[98] A. Kukovecz, C. Kramberger, M. Holzinger, H. Kuzmany, J. Schalko and M. Mannsberger et al., On the stacking behavior of functionalized single-wall carbon nanotubes, J Phys Chem **B106** (2002), 6374–6380

[99] D.B. Mawhinney, V. Naumenko, A. Kuznetsova, J.T. Yates, J. Liu and R.E. Smalley, Surface defect site density on single walled carbon nanotubes by titration, Chem Phys Lett **324** (2000), 213–216

[100] H. Hu, P. Bhowmik, B. Zhao, M.A. Hamon, M.E. Itkis and R.C. Haddon, Determination of the acidic sites of purified single-walled carbon nanotubes by acid–base titration, Chem Phys Lett **345** (2001), 25–28.

[101] D. Osmola, E. Renaud, U. Erb, L. Wong, G. Palumbo and K. T. Aust, Mat. Res. Soc. Symp. Proc., 1983, 286, 191

[102] U. Erb, A. M. El-Sherik, G. Palumbo and K.T. Aust, Nanostruct. Mater., 1993, 2, 383

[103] H. Natter, T. Krajewski and R. Hempelmann, Ber. Bunsen- Ges. Phys. Chem., 1996, 100, 55

[104] L. E. Candlish, B. H. Kear and B. H. Kim, Nanostruct. Mater., 1992, 1, 119

[105] R. Rofagha, R. Langer, A. M. El-Sherik, G. Palumbo and K. T. Aust., Scr. Matall. Mater., 1991, 25, 2867

[106] M.F. Yu, B.S. Files, S. Arepalli, R.S. Ruoff, Tensile loading of ropes of single wall carbon nanotubes and their mechanical properties, Phys. Rev. Lett. 84 (2000) 5552–5555.

[107] M.B. Nardelli, B.I. Yakobson, J. Bernholc, Brittle and ductile behavior in carbon nanotubes, Phys. Rev. Lett. 81 (1998) 4656–4659.

[108] S. Akita, And Y. Nakayama, ‚Jpn. J. Appl. Phys. (2003) 42, 3933

[109] Z. Xia and W. A. Curtin, Phys. Rev. B (2004) 69 (23), 233408

[110] G. Chai, Y. Sun, J. Sun, and Q. Chen, *J. Micromech. Microeng.* 18**,** 035013(2008).

[111] Q. Chen, unpublished.

[112] S. Berber, Y-K. Kwon, and D. Tomanek, Unusually high thermal conductivity of carbon nanotubes, Physical Review Letters 84 No. 20 (2000) 4613-4616.

[113] S.Y. Mensah, F.K.A. Allotey, G. Nkrumah, N.G. Mensah, High electron thermal conductivity of chiral carbon nanotubes, Physica E 23 (2004) 152-158

[114] P. Kim, L. Shi, A. Majumdar, and P.L. McEuen, Thermal transport measurements of individual multi-walled nanotubes, Physical Review Letters, 87 (2001) 215502,1-4

[115] C. Yu, L. Shi, Z. Yao, D. Li, and A. Majumdar, Thermal conductance and thermopower of an individual single-walled carbon nanotube, Nano Letters, vol.5 (2005), 1842-1846

[116] R. Haggenmueller, H.H. Gommans, A.G. Rinzler, J.E. Fischer, Aligned single-wall carbon nanotubes in composites by melt processing methods, Chemical Physics Letters 330 (2000) 219-225.

[117] M. S. Dresselhaus, G. Dresselhaus and P. Avouris, Carbon Nanotubes, Synthesis, Structure, Properties, and Applications, Springer 2000.

[118] J.-P. Salvetat, et al, Mechanical properties of carbon nanotubes, Applied Physics A 69 (1999) 255-260.

[119] S.Y. Mensah, F.K.A. Allotey, G. Nkrumah, N.G. Mensah, High electron thermal conductivity of chiral carbon nanotubes, Physica E 23 (2004) 152-158

[120] C. A. Cooper, D. Ravich, D. Lips, J. Mayer, H. D. Wagner, Distribution and alignment of carbon nanotubes and nanofibrils in a polymer matrix, Composites Science and technology 62 (2002) 1105-1112.

[121] A. Allaoui, et al, Mechanical and electrical properties of a MWNT/epoxy composite, *Composites Science and Technology* 62 (2002) 1993-1998

[122] R. Krupke, F. Hennrich, H. V. Lohneysen, M. M. Kappes, Separation of metallic from semiconductor single-walled carbon nanotubes, *Science* 301(2003) 344-347

[123] K.-T., Lau, et al, Micro-mechanical properties and morphological observation on fracture surface of carbon nanotube composites pre-treated at different temperatures, *Composite Science and technology* 63 (2003) 1161-1164

[124] K-T. Lau and D. Hui, The revolutionary creation of new advanced materials-carbon nanotube composite, Composites: Part B 33 (2002) 263-277.

[125] K-T. Lau and D. Hui, Effectiveness of using carbon nanotubes as nano-reinforcements for advanced composite structures, Carbon 40 (2002) 1605-1606.

[126] H. Dai, Carbon nanotubes: opportunities and challenges, Surface Science 500 (2002) 218-241.

[127] M. S. Dresselhaus, G. Dresselhaus and P. Avouris, Carbon Nanotubes, Synthesis, Structure, Properties, and Applications, Springer 2000.

[128] L. Valentini, D. Puglia, E. Frulloni, I. Armentano, J. M. Kenny and S. Santucci, Dielectric behavior of epoxy matrix/single-walled carbon nanotube composites, *Composites Science and Technology, Volume 64, Issue 1, January 2004, Pages 23-33*

[129] C. Stéphan, T. P. Nguyen, M. Lamy de la Chapelle, S. Lefrant, C. Journet and P. Bernier, Characterization of single walled carbon nanotubes-PMMA composites, *Synthetic Metals, Volume 108, Issue 2, 17 January 2000, Pages 139-149*

[130] A.M. Rao, P.C. Eklund, Shunji Bandow, A. Thess and R.E. Smallley, Nature 388, 257-279 (17 July 1997); 10.1038/40827